

New York Science Journal

ISSN 1554-0200

Volume 2 - Number 2 (Cumulated No. 6), February 1, 2009



Marsland Press

<http://www.sciencepub.net>

sciencepub@gmail.com

New York Science Journal

纽约科学杂志

ISSN 1554-0200

New York Science Journal is published bi-linguistically with Chinese and English for the scientists and Engineers. The journal aims to present experimental and theoretical findings of science and engineering and to report on advances in technologies of multidisciplinary subjects. The journal was founded in 2008 by Marsland Press. The Editor-in-Chief, Deputy Editor and editors have backgrounds in Philosophy, Science, Technology and Engineering, etc. This interdisciplinary team is ultimately suited for facilitating the publication of the best of your research work. The journal welcomes manuscripts from all fields in science and engineering research. Papers submitted could be reviews, objective descriptions, research reports, opinions/debates, news, letters, and other types of writings that are nature and science related. Manuscripts submitted will be peer reviewed and the valuable papers will be considered for the publication after the peer review. Authors are responsible to the contents of their articles.

Editor-in-Chief:Ma Hongbao, Brooklyn, New York, USA, editor@sciencepub.net**Associate Editors-in-Chief:**Cherng Shen, Niaocong, Taiwan, China, cherngs@csu.edu.twJingjing Z Edmondson, Hangzhou, Zhejiang, China, jjze@zju.edu.cnMark Hansen, Lansing, Michigan, USA, mark20082009@gmail.com**Editors:**Ajimotokan HA, Ilorin, Nigeria, hajims@unilorin.edu.ngAvinash Mundhra, Kolkata, India, mundhra.avi@gmail.comCasmir IC, Ekpoma, Edo State, Nigeria, elyonlab@yahoo.comDjamel Boubetra, Berlin, Germany, boubetra@gmail.comGeeta Kharkwal, Uttaranchal, India, geetakh@gmail.comGeorge Chen, East Lansing, Michigan, USA, chengu@msu.eduHamza HD, Zaria, Nigeria, Usmandhamza@yahoo.comJenny Young, New York, USA, jennyyoung123@gmail.comKlarizze Anne M. Puzon, Toulouse, France, klarizze@gmail.com, kmpuzon@gmail.comMargaret Ma, Boston, Massachusetts, USA, margaretgreat@gmail.comMark Lindley, Boston, Massachusetts, USA, mirabene@yahoo.comMary Smith, Washington DC, USA, smithsmith1234567@gmail.comMike Ma, Lansing, Michigan, USA, mikemausa@yahoo.comMohammad Shafie, Kuala Terengganu, Malaysia, msshafie@yahoo.com.myOnyema IC, Lagos, Akoka, Nigeria, iconyema@gmail.comOuyang Da, Okemos, Michigan, USA, ouyangda@msu.eduTracy X Qiao, Ann Arbor, Michigan, USA, xiaotan@umich.eduUsman MA, Ago-Iwoye, Nigeria, usmanma@yahoo.comWillie J McDonald, Houston, Texas, USA, Williemcdonald2007@yahoo.comZhang Meimei, Beijing, China, meimei20082008@gmail.comZhu Yi, Shanghai, China, zhuyi@msu.edu**Web Design:**Jenny Young, New York, jennyyoung123@gmail.com

Information for Authors**Manuscripts Submission**

- (1) **Submission Methods:** Electronic submission through email, on line submission and regular mail with formatted computer diskette would be accepted.
- (2) **Software:** The Microsoft Word file is preferred.
- (3) **Font:** Normal, Times New Roman, 10 pt, single space.
- (4) **Indent:** Type 4 spaces in the beginning of each new paragraph.
- (5) **Manuscript:** Don't use "Footnote" or "Header and Footer".
- (6) **Cover Page:** Put detail information of authors and a short running title in the cover page.
- (7) **Title:** Use Title Case in the title and subtitles, e.g. "**Debt and Agency Costs**".
- (8) **Figures and Tables:** Use full word of figure and table, e.g. "**Figure 1. Annual Income of Different Groups**", "**Table 1. List Data**".
- (9) **References:** Cite references by "last name, year", e.g. "(Smith, 2003)". References should include all the authors' last names and initials, title, journal, year, volume, issue, and pages etc. **Reference Examples: Journal Article:** Hacker J, Hentschel U, Dobrindt U. Prokaryotic chromosomes and disease. *Science* 2003;301(34):790-3; **Book:** Berkowitz BA, Katzung BG. Basic and clinical evaluation of new drugs. In: Katzung BG, ed. *Basic and clinical pharmacology*. Appleton & Lance Publisher. Norwalk, Connecticut, USA. 1995:60-9.
- (10) **Submission Address:** Marsland Press, 525 Rockaway PKWY, #B44, Brooklyn, New York 11212, USA; Telephone: (347) 321-7172; Emails: sciencepub@gmail.com; editor@sciencepub.net.
- (11) **Reviewers:** Authors should suggest 2-8 competent reviewers with their name and email.

2. Manuscript Preparation

Each manuscript should be formatted to include the following components:

- (1) **Title page:** including the complete article title; each author's full name; institution(s) with which each author is affiliated, with city, state/province, zip code, and country; and the name, complete mailing address, telephone number, facsimile number (if available), and e-mail address for all correspondence.
- (2) **Abstract:** including Background, Materials and Methods, Results, and Discussions.
- (3) **Key Words.**
- (4) **Introduction.**
- (5) **Materials and Methods.**
- (6) **Results.**
- (7) **Discussions.**
- (8) **References.**
- (9) **Acknowledgments.**

Journal Address:

Marsland Press
525 Rockaway PKWY, #B44
Brooklyn, New York 11212
The United States
Telephone: (347) 321-7172
E-mail: editor@sciencepub.net; sciencepub@gmail.com;
Websites: <http://www.sciencepub.net>

New York Science Journal

Volume 2 - Number 2 (Cumulated No. 6), February 1, 2009; ISSN 1554-0200

[Cover Page](#), [Introduction](#), [Contents](#), [Call for Papers](#), [All papers in one file](#)

Contents

| No. / Titles / Authors | page |
|---|-------|
| <u>1. Urinary Schistosomiasis And Concomitant Bacteriuria In The Federal Capital Territory Abuja Nigeria</u> Casmir I.C.Ifeanyi, Benard M. Matur and Nkiruka F. Ikeneche | 1-8 |
| <u>2. A Procedural Schedule For Groundwater Flow In Porous Media</u> Odunaike R. K. Usman M. A. Hammed F. A. Adeosun T. A. and Olayiwola, M.O. | 9-19 |
| <u>3. RAPD-PCR for DNA-Fingerprinting of Egyptian tilapia</u> Soufy. H ¹ , Laila A.M. ² , Iman M.K.A. | 20-25 |
| <u>4. 相对绝对论</u> 李学生 | 26-30 |
| <u>5. Subsurface Stratigraphic mapping using Geophysics and Its Impact on the Urbanization Development in Arepo Area, Ogun State, Nigeria</u> Oyedele, K. F. and Bankole, O. O. | 31-45 |
| <u>6. 论核场</u> 陈果仁 | 46-50 |
| <u>7. An Incidence of Substratum Discolouration in a Tropical West African Lagoon</u> Onyema, I.C. and Nwankwo, D.I. | 51-60 |
| <u>8. Enhancement Of Thermal Capabilities Of A Solar Concentrator</u> I. O. Ohijeagbon ¹ , A. S. Adekunle ² , and O.D. Awolaran | 61-68 |
| <u>9. 对黑洞的新观念和新的完整论证：黑洞内部根本没有奇点（上篇）^{***}====所有黑洞之最后命运就是由于发射霍金辐射而收缩成为宇宙中的最小引力黑洞 ($M_{\text{bm}} \approx 10^{-5} \text{g}$) 在爆炸中消亡于普朗克领域 Planck Era, 而不是塌缩成为奇点 =====</u> 张洞生 | 69-93 |

Marsland Press, 525 Rockaway PKWY, Brooklyn, New York 11212, The United States; (347) 321-7172;
<http://www.sciencepub.net> sciencepub@gmail.com

Urinary Schistosomiasis And Concomitant Bacteriuria In The Federal Capital Territory Abuja Nigeria

Casmir I.C.Ifeanyi, Benard M. Matur and Nkiruka F. Ikeneche

¹Department of Medical Laboratory Sciences, Faculty of Basic Medical Sciences, Ambrose Alli
University Ekpoma, Edo State; elyonlab@yahoo.com

²Department of Biological Science, Faculty of Science University of Abuja;

³Department of Medical Laboratory Sciences, Faculty of Health Sciences and Technology,
College of Medicine, University of Nigeria, Enugu Campus Nigeria

ABSTRACT: Urinary schistosomiasis and concomitant bacteriuria was investigated in the Federal Capital Territory (FCT) Abuja. Single urine samples collected from subjects aged 5 years and above between 1000 hours and 1400hours were examined for the presence of *S.haematobium* eggs using centrifugation technique and for bacteriuria by standard bacteriological methods. A total of 1,150 subjects comprised of 667 males and 483 females were studied from the 6 Area Councils of the FCT. Overall, 360 (31.3%) had the eggs of *S. haematobium* in their urine while 289 (80.3%) of the 360 who had eggs of *S. haematobium* in their urine, had bacterial growth. Prevalence of bacteriuria in urinary schistosomiasis ranged from 74-86% with no significant difference in the distribution of the prevalence of the co-infection in the 6 area councils surveyed ($P=0.125$). The distribution of bacteria colony count in relation to different ova intensity was significantly different ($P<0.001$) and assumed a weak positive linear relationship ($r=0.2$). There was no significant difference in the results of the methods used to investigate for bacteriuria ($P=0.05$). The bacteria isolated included: *klebsiella species*, *Escherichia coli*, *Enterococci species*, *Staphylococcus aureus*, *Staphylococcus saprophyticus*, *Salmonella species*, *Proteus species*, and *Pseudomonas species*. *Eshericha coli* occurred more frequently (70%) than the rest of the bacteria species isolated. The antimicrobial susceptibility pattern of isolates revealed varying percentage susceptibilities by all isolates. This study clearly suggests that bacteriuria is a potent complication in the management of urinary schistosomiasis. Therefore the complimentary incorporation of antibacterial therapy appear essential. [New York Science Journal. 2009;2(2):1-8]. (ISSN: 1554-0200).

Keywords: Schistosomiasis, Concomitant Bacteriuria, Prevalence, Susceptibility

INTRODUCTION

Urinary tract disease is a specific trait of infection with *Schistosoma haematobium* which affects in a diffuse manner the entire genitourinary tract (King, 2001; Pereira *et al.*, 1997). Bacteria infections are often recurrent and important complications of the inactive stage of urinary schistosomiasis which may be instrumental in precipitating renal failure (Farid, 1993). In schistosomiasis of the urinary bladder, secondary bacterial infections are common and in men can involve the seminal vesicles, spermatic cord, and to a lesser extent, the prostate. In women, infection can involve the cervix and fallopian tubes and can cause infertility. Mostafa *et al.*, (1999) opined that it seems possible that agricultural workers and others who are regularly exposed to contaminated water are occasionally simultaneously infected with both the schistosome parasite and pathogenic bacteria. The risk factor of agricultural practices the major occupation of indigenous residents of the Federal Capital Territory (FCT) Abuja, Nigeria is capable of breeding urinary schistosomiasis and concomitant bacteriuria. In the light of the relative high level of schistosomal and bacteria infection, active assessment and reporting of bacteriuria in urinary schistosomiasis and the complementary incorporation of antibacterial therapy to the integrated morbidity control approach to urinary schistosomiasis deserves emphasis. This study examined the terminal urine sample of individuals with or without signs of urinary disturbance and infection for

evidence of urinary schistosomiasis as well as evaluated associated bacteriological burden and susceptibility pattern of bacteria isolated.

MATERIALS AND METHODS

The study included 1,150 subjects both males and females between the ages of 5-50 years recruited directly through surveillance out-reaches to district/village schools and health related institutions. Informed consent of adult subjects was obtained, while consent to obtain specimen from 'minors'/pupils was obtained through parents/guardian and the Education department of the Ministry of the Federation Capital Territory (MFCT) Abuja.

The urine samples were collected between 1000 hours and 1400 hours and were examined for colour, naked eye haematuria, turbidity and these observations were noted. Ten millilitres of urine were transferred aseptically into centrifuge tube and centrifuged for 5 minutes at 5000 rpm (Anosike *et al.*, 2001). After discarding the supernatant the entire sediment was transferred to a slide covered with cover glass examined for red blood cells, pus cells (pyuria) and counting of eggs of *S. haematobium*. Using the 10x objective with the condenser iris closed sufficiently to give good contrast, the entire sediment preparation was examined systematically and ova count reported per 10ml of urine (Chessbrough, 1981; Richards *et al.*, 1984).

The remainder of urine samples positive for *S. haematobium* ova were homogenized by inverting the container severally and 0.002 ml of the urine inoculated and spread on Cysteine lactose electrolyte deficient medium (CLED-BIOTEC, UK) and blood agar (Blood agar base-BIOTEC, UK). Afterwards 10ul of the homogenized uncentrifuged urine were applied unto a glass slide allowed to dry without spreading at ambient temperature and stained by Grams method. Using 100x objective the slide was examined for bacteria per oil immersion field (Celso *et al.*, 1998).

The uncentrifuged urine samples were diluted 1:20 (20 ul of urine + 380 ul of Turks solution - 2% Acetic acid tinged with gentian violet). This is to destroy the red blood cells and stain the white blood cell nuclei. The dilutions were transferred to Neubauer haemocytometer chamber. The chamber was examined using 10x objective and 4 squares counted applying the margin rule for including and excluding cell lying on the peripheral lines to quantify pyuria (Campbell *et al.*, 2002). Reagent strip urinalysis was performed using L-Combur reagent strip (Boehringer Mannheim).

The culture plates were examined after 24 hours of incubation for bacterial growth and colony count. Bacteria growth less than 10^5 organisms per ml produced less than 30 colony forming units per ml of urine (Chessbrough, 2000). Bacteria isolates were identified and characterized using methods prescribed by Cowan and Steel, 1974; Chessbrough, 2000 and Graham and Galloway, 2001. Susceptibility testing of all pathogenic bacteria were performed using the standard disc diffusion method according to British Society for Antimicrobial Chemotherapy (Andrew, 2001).

Statistically Analysis

The data analysis was done using X^2 (chi-square) test to determine significant relationships between variable and coefficient of correlation for test of linearity of relationship.

RESULTS

The overall prevalence of urinary schistosomiasis was 31.1% (95% CI 26.2 – 36.4) in the Federal Capital Territory Abuja and ranged between 25 – 36.3% in the six area councils surveyed. Prevalence followed the typical age group pattern for urinary schistosomiasis attaining a peak 78.4% in subjects 10 – 14 years age, decreasing to 47.6% in subjects \geq 50 years and lower in subjects within 20 – 39 year. Prevalence of urinary schistosomiasis was higher at all ages in males ranging between 0 – 42.1% and in females 0 – 36.3% (Table1). *S. haematobium* infection

prevalence had a statistical significant difference between males and females at different age groups ($\chi^2=48$; $P<0.001$).

In all, of the 360 subjects that had ova in their urine, 275 was positive for uncentrifuged gram microscopy, 305 was positive for pyuria (WBC) count, 330 was positive for leucocytes esterase, 350 was positive for protein, 336 was positive for erythrocytes (urinary blood), 240 was positive for nitrite (Table 2). Overall, 289 samples from subjects had bacteria growth of varying count. 261 (90.3%) samples had overt significant bacteriuria ($\geq 10^5$ cfu/ml) in both males and females. Between males and females, there was a statistical significant difference in bacteria colony count in urinary schistosomiasis ($\chi^2=9.9$; $P=0.025$).

Bacteriuria in urinary schistosomiasis in F.C.T. had a prevalence of 80.3% ranging between 74 to 86% in the six area councils of F.C.T. surveyed. Bacteriuria and urinary schistosomiasis co-infection had no statistical significant difference ($\chi^2=9.8$; $P=0.125$). The distribution of bacteria colony count (cfu/ml) according to different ova intensity i.e. egg/10 ml of urine (Table 2); had a weak positive linear relationship ($r=0.2$). Albeit, there was a significant difference between bacteria colony count and different ova intensity in urinary schistosomiasis ($\chi^2=39.0$; $P<0.001$). The statistical analysis of results from culture and non – culture methods (enhanced microscopic urinalysis and reagent strip tests) for investigating bacteriuria are shown in Table 4. There is no significant difference in percentage positive results of culture and a combination of the non-culture methods for investigating bacteriuria ($\chi^2=5.9$; $P=0.05$). Various bacteria species were isolated with *Escherichia coli* occurring more frequent than the rest in males (Table 4). Notwithstanding, there was no significant difference in the bacterial isolates between males and females ($\chi^2=7.5$; $P=0.65$).

Antimicrobial susceptibility pattern of bacteria isolates are shown in Table 8. All the isolates had susceptibility in varying percentage to Ofloxacin Ciprofloxacin, Gentamicin and Cefuroxime in order of percentage effectiveness respectively. However all the isolates except 3 were susceptible to Nitofuranton, 2 species of the isolates (*Proteus species* and *Pseudomonas species*) were not susceptible to Co-trimoxazole while 1 species was not susceptible to Co-amoxiclav.

Table 1: Distribution of the prevalence of *S. haematobium* infection in FCT according to age and sex; statistical test of significance between make and female

| AGE GROUP (YEARS) | FEMALE | | | | MALE | | |
|----------------------|--------------------------|--------------------|--------------------|----------------|--------------------|--------|---------------|
| | TOTAL EXAMINED NUMBER | EXAMINED NUMBER | INFECTED NUMBER | INFECTED % | EXAMINED NUMBER | NUMBER | INFECTED % |
| 5 – 9 | 213 | 93 | 30 | 32.3 | 120 | 21 | 16.7 |
| 10 – 14 | 557 | 378 | 159 | 42.1 | 179 | 65 | 36.3 |
| 15 – 19 | 200 | 90 | 30 | 33.3 | 110 | 27 | 24.5 |
| 20 – 24 | 50 | 38 | 5 | 13.2 | 12 | 2 | 16.7 |
| 25 – 29 | 29 | 19 | 3 | 15.8 | 10 | 1 | 10 |
| 30 – 34 | 34 | 13 | 2 | 15.8 | 21 | 3 | 14.3 |
| 35 – 39 | 22 | 12 | 1 | 8.3 | 10 | 2 | 20 |
| 40 – 44 | 20 | 8 | 3 | 37.5 | 12 | 1 | 8.3 |
| 45 – 49 | 15 | 9 | 2 | 22.2 | 6 | 1 | 16.7 |
| >50 | 10 | 7 | 1 | 14.3 | 3 | 1 | 33.3 |
| TOTAL | | 1150 | | | 667 | | 236 |
| | | 483 | | 124 | 25.7 | | 35.4 |
| χ^2_{cal} | | 42 | | χ^2_{tab} | 18.25 | | |

Table 2: Analysis and statistical test of significance of percentage positively for culture and non culture tests for urinary schistosomiasis and bacteriuria.

| NON-CULTURE TESTS | | | | URINE |
|---|------------------------------|---|----------------|----------------------|
| CULTURE | | | | |
| + VE | % | NUMBER + VE OF 360 NUMBER . -VE % EXAMINED/METHOD PER METHOD | % | NUMBER PER |
| UNCENTRIFUGED URINE GRAM MICROSCOPY > 1 | 87.3 | 275 35 | 76.4 12.7 | 240 |
| ORGANISM/OIL IMMERSION FIELD | | | | |
| PYURIA (WBC) COUNT >1.0X10 ⁹ | 93.4 | 305 20 | 85 6.6 | 285 |
| LEUCOCYTES ESTERASE > 25 LEU/UL | 86 | 330 46 | 91.6 14 | 284 |
| PROTEIN > 30 MG/DL | 77.1 | 350 80 | 97.2 22.9 | 270 |
| ERYTHROCYTES URINARY BLOOD | 86.5 | 336 49 | 93.3 14.5 | 287 |
| > 10ERY/UL NITRITE POSITIVE | 84.2 | 240 38 | 66.7 15.8 | 202 |
| TOTAL | 510.20% | | 514.50% | |
| | X^2_{cal} <i>Pvalue</i> | 0.05 | 5.5 | X^2_{tab} 11.03 |

Table 3: Distribution of bacteria colony count (cfu/ml) according to different ova intensity (egg/10ml urine); Statistical test of significance and coefficient of correlation in urinary schistosomiasis.

| BACTERIA COUNT cfu/ml | NUMBER OF SUBJECTS | | | | |
|--------------------------|-----------------------------|------------------------------|------------------------------|----------------------------|------------|
| | 0-20 (egg/10ml urine) | 21-40 (egg/10ml urine) | 41-50 (egg/10ml urine) | >50 (egg/10ml urine) | TOTAL |
| $\geq 10^5$ | 13 | 20 | 10 | 218 | 261 |
| 10^4 | 0 | 3 | 4 | 5 | 12 |
| 10^3 | 3 | 2 | 2 | 3 | 10 |
| 10^2 | 0 | 0 | 2 | 4 | 6 |
| TOTAL | 16 | 25 | 18 | 230 | 289 |

X^2_{cal} **39**
 X^2_{tab} **16.92**
Pvalue **<0.001**
r **0.2**

Table 4: Bacteria pathogens associated with *S.haematobium* infection and their antimicrobial susceptibility pattern.

| ANTIMICROBIAL AGENT | PERCENTAGE SUSCEPTIBILITY | | | | | | | |
|------------------------|-------------------------------|-----------------------------|--------------------------------|----------------------------------|---|-------------------------------|---------------------------|--------------------------------|
| | Klebsiella Species n=30 | schiericha coli n=101 | Enterococci Species n=27 | Staphylococcus aureus n=78 | Staphylococcus saprophyticus n=19 | Salmonella Species n=11 | Proteus Species n=9 | Pseudomonas Species n=14 |
| <i>Ciprofloxacin</i> | 98 | 89.6 | 67.5 | 74 | 78 | 68.7 | 95 | 61.7 |
| <i>Cephalexin</i> | 25 | 38.5 | 39.2 | 25 | 30 | 16.9 | 25.4 | 0 |
| <i>Cefuroxime</i> | 65 | 70 | 67 | 63 | 50 | 46.3 | 72.5 | 45 |
| <i>Oxfloxacin</i> | 80.4 | 90 | 85 | 82.1 | 80 | 78 | 95 | 8.6 |
| <i>Gentamycin</i> | 76 | 82 | 47 | 45.9 | 49.6 | 85.2 | 58 | 70.5 |
| <i>Co-trimoxazole</i> | 26.4 | 56 | 61 | 68 | 54 | 25 | 0 | 0 |
| <i>Nitrofurantion</i> | 38.4 | 85 | 65.1 | 70 | 64.3 | 0 | 0 | 0 |
| <i>Co-amoxiclav</i> | 32.8 | 25 | 41 | 33.5 | 40.2 | 20.4 | 63.2 | 0 |

DISCUSSION AND CONCLUSION

The findings in this study demonstrates that the overall estimated prevalence of urinary schistosomiasis as determined by ova in the urine was high (31.3%; 95% CI 26.2-36.4%). Recent researchers estimate prevalence of 29.4% in the Eastern Nigeria (Anosike *et al.*, 2001) and 57.4% in the West (Adeyaba and Ojeaga, 2002). The result of this study is agreeable with these reports.

This study evaluated bacteriuria in urinary schistosomiasis revealing that of the 360 subjects (31.3%) who had Ova of *S. haematobium* from 1,150 examined; 289 (80.3%) had bacteriuria by culture characterization. The percentage positive results of culture and a combination of non-culture had insignificant difference ($P > 0.05$). Though King (2001) noted that urinary tract disease is a specific trait of infection with *S. haematobium*; The 80.3% prevalence of bacteriuria in urinary schistosomiasis need further categorization since by the definition of Gallagher and Hemphil (2004) it may simply be taken as referring to the presence of bacteria in the urine of individuals infected with *S. haematobium* and not necessarily implying infection. This is cogent as bacteriuria and urinary schistosomiasis co-infection assessed in the study had no significant difference ($P > 0.05$). Gallagher and Hemphil (2004) and Franz and Horl (1999) had equally noted that in general terms urinary tract infection (UTI) is infection by Pathogen along the urinary tract causing inflammation depicted by pyuria indicating significant inflammatory response to bacteriuria such as occur with infection even in asymptomatic setting. These views mentioned above explicitly suggests that bacteriuria may be significant or non- significant depending on the quantity of bacteria in the urine which imply infection and is traditionally urine culture containing $\geq 10^5$ cfu/ml. The result of our assessment of bacteriuria in urinary schistosomiasis agreeably categorized 261 (90.3%) subjects by urine culture as having significant bacteriuria ($\geq 10^5$ cfu/ml) with their sex distribution being significantly different ($P < 0.05$) . This finding in consonance to that by Rushton (1997) which suggest that it may be possible to eliminate the urine culture when enhanced microscopic urinalysis and reagent strip urinalysis are negative and clinical suspicion is low. Nonetheless, isolation of significant number of single organism on culture remains the definitive diagnosis.

The finding of lower threshold of bacteria counts (10^2 - 10^4 cfu/ml) and the distribution of bacteria colony count according to different ova intensity which had a weak positive linear relationship ($r = 0.2$) deserves critical scrutiny because bacteria colony count and different ova intensity in urinary schistosomiasis was significantly different ($P < 0.05$). This is pertinent to obtaining the best combination of sensitivity and specificity in the diagnosis of urinary tract infection. Franz and Horl (1999) reported that the utility and consistency of the criterion $\geq 10^5$ cfu/ml of clean-catch urine for the diagnosis of UTI has been validated repeatedly. Thus, Stamm and Hooton (1993) noted that in dysuric patients, an appropriate threshold value for defining significant bacteriuria is 10^2 cfu/ml of a known pathogen. Considering the foregoing and that dysuria is common in both early and late urinary schistosomiasis where ova count correlate with morbidity, it might be prudent to consider these thresholds significant for the diagnosis of UTI. More so, community –based epidemiological survey of bacterial count in Egypt (Mostafa *et al.*, 1999) of subjects with *S. haematobium* infection had similar low bacteria counts (10^3 cfu/ml). However, interpretation of low threshold counts as significant for diagnosis must be in the absence of mixed bacteria growth with a predominant organism typical of contamination.

Infection of the 289 (80.3%) subjects with one bacteria or the other was the trend in our study and had no significant difference ($P > 0.05$) in bacteria isolates between males and females. The isolation of *Escherichia coli* more frequently than the rest conforms to reports of many researchers (Farid, 1993; Mostafa *et al.*, 1999) about it's association with schistosome infection.

The antimicrobial susceptibility pattern of the bacteria isolates to routinely tested first line antimicrobial agents were quite diminished. There were notable pockets of resistance to all first line agents tested except for Ciprofloxacin and Cefuroxime (Table 4). This antimicrobial susceptibility results would be an invaluable premise for empirical therapy where suspicion exists but cultures are impracticable whereas enhanced microscopic urinalysis and reagent strip are

positive since comparative analysis of these methods had no significant difference ($P>0.05$). The main goal of most initiatives to control schistosomiasis is morbidity control. The reported complications of bacteria infections in urinary schistosomiasis are odious. Clinical and pathological conditions arising there from had been enunciated (Farid, 1993; Ganem *et al.*, 1998). Hence, this research further documents and authenticate the importance of a database for continued valuation and evolution of control programmes. The complementary incorporation of antibacterial therapy to the integrated morbidity control approach of diagnosis, drugs treatment, snail control, provision of safe, adequate water supply, sanitation and health education is advocated. More over, our results infer that urinary schistosomiasis is endemic in FCT Abuja Nigeria and deserves urgent intervention.

Corresponding author:

Casmir I.C. Ifeanyi
Department of Medical Laboratory Sciences,
Faculty of Basic Medical Sciences,
Ambrose Alli University
Ekpoma, Edo State
Email: elyonlab@yahoo.com

REFERENCES

1. **Adeyeba, O. A. and Ojeaga S. G. T.** (2002). Urinary schistosomiasis and concomitant urinary tract pathogens among school children in metropolitan Ibadan, Nigeria. *Afri. J. Biomed. Res.* Vol., 5:103-107.
2. **Andrews, J. M.** (2001). BSAC standardized disc susceptibility testing method. *J. Antimicrob Chemother.* 48 (suppl): 43-57.
3. **Anosike, J. C., Nwoke B.E. B. and Njoku, A. J.** (2001). The validity of haematuria in the community diagnosis of urinary schistosomiasis infection *Journal Of Helminthology* 75:223-225.
4. **Campbell, M. F.** (2002). Infection of urinary tract, In: Campbell M. F., Walsh, P. C. and Alan B. (eds). *Campbell's urology*, 8th ed. Elsevier Science.
5. **Celso, L. C., Carla, B. M., Vera Lucia, D. S. and Marcio, G.** (1998). Simplified technique for detection of significant bacteriuria by microscopic examination of rine. *Journal Of Clinical Microbiology* 36 No. 3: 830-823.
6. **Chessbrough, M.** (1981). *Medical laboratory manual for tropical countries volume I* 2nd edition University Press Cambridge pp 328 – 330.
7. **Chessbrough, M.** (2000). *District laboratory practice in tropical countries part II* Cambridge University Press.
8. **Ganem, J. P., Maire-Claire, M. and Charlotte, N. C.** (1998). Schistosomiasis of the urinary bladder in an African Immigrant to North Carolina *Southern Medical Journal* vol. 91 No. 6: 580-583.
9. **Gallagher, S. A. and Hemphil. R. R.** (2004). Urinary tract infections: Epidemiology, detection, and evaluation. *Hot Topics in Healthcare*, Thomson American Health consultants, Inc. pp 1-9.
10. **Graham, J. C. and Galloway, A.** (2001). The laboratory diagnosis of urinary tract infection, Review, ACP Best practice No. 167 *J Clin Pathol* 54:911-919.
11. **Hooton. T. M. and Stamm, W. E.** (1997). Diagnosis and treatment of uncomplicated urinary tract infection. *Infect. Dis. Clin. North Am.*, 11:551-581.
12. **Mostafa, M. H., Shenita, S. A. and O'connur, P.J.,** (1999). Relationship between schistosomiasis and bladder Cancer. *Clinical Microbiology Reviews* 12(1): 978-11.

13. **Pereira Arias,J.G.,Ibarluzea Gonzalez,J.G.,Alvarez Martinez,J.A.,Marana Fernandez M.,Gallego Sanchez,J.A.,Larringa Simon,J.and Bernuy Malfa,C.**(1997). Mixed Urogenital schistosomiasis.*Acta Urologica* **2**(3).272-277.
14. **Richards, F. O., Hassani, P., Cline, B. L. and El Alamy, M. A.** (1984). An evaluation of quantitative techniques for *Schistosoma haematobium* egg in urine preserved with carbol fuchsin. *Am. J. Trop. Med. and Hyg.*, **33**: 857-61.
15. **Rushton, H. G.** (1997). Urinary tract infection in children: Epidemiology, evaluation, and management *Ped. Clin. North Am.*, **44**:1133-1169.
16. **Stamm, W. E. and Hooton, T. M.** (1993). Management of urinary tract infections, in adults. *N. Engl. J. Med.*, **329**:1328-1334.

Note: This article was primarily published in [New York Science Journal. 2009;2(1):22-28]. (ISSN: 1554-0200).

A Procedural Schedule For Groundwater Flow In Porous Media

Odunaike R. K. Usman M. A. Hammed F. A. Adeosun T. A. and Olayiwola, M.O.

¹Department of Mathematical Sciences,
Olabisi Onabanjo University, Ago-Iwoye, Nigeria.
2 Department of Mathematics, Yaba College of Technology
Lagos, Nigeria

Dr. Usman M A
Dept. of Mathematical Sciences
Olabisi Onabanjo University, Ago-Iwoye, Nigeria.
usmanma@yahoo.com

ABSTRACT: The classical Darcy's law is generalized by regarding groundwater flow as a function of the hydraulic head; which is a quantity of primary interest. This generalized law and the law of conservation of mass are then used to derive the generalized form of the groundwater flow equation. Analytical solution of this groundwater flow equation for which a fractal dimension for the flow is assumed. Equation of unsteady flow in a leaky aquifer is discussed. Prediction of groundwater flow with illustrations of contouring the water table map helps to predict the direction of flow. [New York Science Journal. 2009;2(2):9-19]. (ISSN: 1554-0200).

Keywords: Porous media, Darcy's law, Hydraulic Head Introduction

INTRODUCTION

A problem that arises naturally in groundwater investigation is to choose an appropriate geometry for the geological system in which the flow occurs. For example, one can use a model based on unsteady state radial flow to simulate the flow in porous media with a very large pore fluid density (Black *et al*, 1986). This is in particular the case with the delineation of freshwater aquifer in the Coastal area of Lagos State (Ikoyi, Lekki, Apapa and Victoria Island), characterized by the presence of boreholes drilled in these area that serve as the main drawdown in pumping wells. Attempts to fit in analytical solution of the groundwater flow equation with a one dimensional flow and fit a Conventional radial flow model to the observed drawdown at early times underestimates and later times over estimates^[1-4].

The derivation of a generalized groundwater flow equation from the law of mass Conservation and energy balance is usually an indication that the theory is not implemented correctly or does not fit the observations. To investigate the possibility on the Lagos coastal areas. A generalized equation of groundwater flow in three-dimensional equation is expressed as^[6-10]

$$\frac{\partial}{\partial x} \left(K \frac{\partial h}{\partial x} \right) + \frac{\partial}{\partial y} \left(K \frac{\partial h}{\partial y} \right) + \frac{\partial}{\partial z} \left(K \frac{\partial h}{\partial z} \right) = S_s \frac{\partial h}{\partial t} \quad (1)$$

A fractal one-dimensional groundwater flow equation is assumed as an hypothetical case of a closed aquifer for which the flow is essentially horizontal direction and independent of y and z- axis.

$$\frac{\partial}{\partial x} \left(K \frac{\partial h}{\partial x} \right) = S_s \frac{\partial h}{\partial t}$$

$$\nabla \cdot [k \nabla h] = S_s \partial_t h \quad (2)$$

Where S_s the specific storativity

Where K the hydraulic conductivity tensor of the aquifer

Where $h(x,t)$ the hydraulic head with x and t the usual spatial and time coordinate

Where ∇ the gradient operator

Where ∂_t the time derivative

The model showed that the dominant flow in these aquifers is essentially horizontal and linear and not vertical and radial as commonly assumed. However, more recent investigations (Clout and Botha, 2006) suggest that the flow is also influenced by the geometry of the bedding parallel fractures, a feature that Equation (3) cannot account for. It is therefore possible that equation may not be application flow in fractured rock other than a porous media^[11-15]

In an attempt to circumvent this problem, we introduced a conventional geometry of the aquifer, which assumed a fractal one dimensional flow. (see fig. I). Although this model has been applied with reasonable success in the analysis of the hydraulic head from borehole in the Lagos' Coastal Area^[16].

As a review of the derivation of Equation (2) will show [see Bear, 1972], Darcy's Law is used as a keystone in the derivation of Equation (2)^[5].

$$q(x,1) = -k \nabla h \quad \dots (3)$$

This law proposed by Darcy early in the 19th century, is relying on experimental results obtained from the flow of water through a one-dimensional sand column, the geometry of which differs completely from that of a fracture^[17]. There is therefore a possibility that the Darcy's law not be valid for flow in fractured rock formation but is only a very crude idealization of reality. Nevertheless, the relative success achieved by (Clout and Botha, 2006) to describe many of the properties of Karoo aquifer on the campus of the university of free State, suggests also that the basic principle underlying this law may be correct: the observed draw down is to be related to either a variation in the hydraulic conductivity of the aquifer or a change in the hydraulic head. Any new form of the law should therefore be reduced to the classical form under a more common condition. Because K is essentially determined by the permeability of the porous medium and not the flow pattern, the gradient term in Equation (3) is the most likely cause for the deviation between the observed and the theoretical drawdown observed in the Karoo formation. In this work, the possibility is further investigated for a flow symmetry form of Equation (2) by creating an artificial vertical fault that divides the aquifer into two compartments of length L , on the left and L_1 on the right. The fault gauge is sufficiently low in hydraulic conductivity that acts as a flow barrier. Thus, the left compartment is hydraulically isolated from the right compartment. Initially, the hydraulic head is h_1 in the left compartment and h_2 in the right compartment. Assume that at time $t = 0$, the fault is ruptured by an earthquake, so that the two compartments are now hydraulically connected. The earthquake would deform the aquifer causing changes in hydraulic head. The question we want to answer is, what happens to the hydraulic head distribution in the aquifer after the fault rupture?^[19]

Therefore, when the fault ruptures, we expect groundwater to flow from compartment with higher head to compartment with lower head, in other word, flow would occur essentially in horizontal x -direction. Analytically, if we set the original length of the x -axis at the left hand boundary, then the How domain is for one-dimensional flow in a homogenous aquifer, the governing in equation (4).

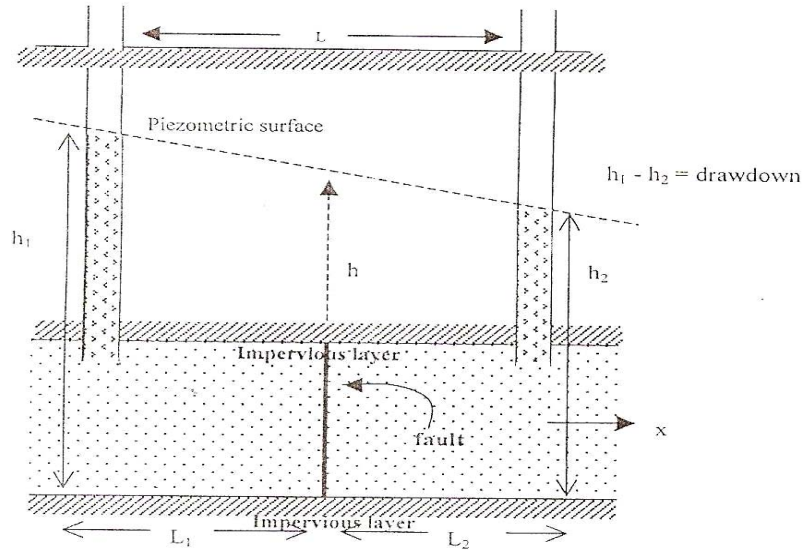


Fig.: Flow through a confined aquifer

The boundary condition are $\frac{\partial^2 h}{\partial x^2} = \frac{S_s}{K} \frac{\partial h}{\partial t}$ (4)

$$0 < x < L_1 + L_2$$

$$\frac{\partial h}{\partial x} = 0 \text{ at } x = 0$$

$$\frac{\partial h}{\partial x} = 0 \text{ at } x = L_1 + L_2$$

The initial conditions are

$$h(x,0) = h_1 \text{ for } 0 \leq x \leq L_1$$

$$h(x,0) = h_1 \text{ for } L_1 \leq x \leq L_1 + L_2$$

Separation of variables is employed and the solution is assumed as:

$$h(x,t) = f(x) \cdot g(t) \quad (5)$$

where:

$$a = \frac{S_s}{K} \text{ and } f(0) = 0 \text{ for } K_1 = \frac{n\pi}{L}$$

Using these in solution of (5), we have,

$$h(x,0) = A_0 + \text{Cos} \frac{n\pi}{L} x \lambda \frac{n^2 n^2 Kt}{S_s L^2}$$

Initial condition, we have,

$$h(x,0) = A_0 + \sum_{n=1}^{\infty} A_n \text{Cos} \frac{n\pi}{L} x \lambda \frac{n^2 n^2 Kt}{S_s L^2}$$

(6)

Substitute for A_0 and A_n from Fourier integral, we have

$$A_0 = \frac{1}{L} \int_0^L f(x) dx \quad \text{and}$$

$$A_0 = \frac{2}{L} \int_0^L f(x) \cos \frac{n\pi x}{L} dx$$

$$h(x,t) = \frac{1}{L} \int_0^L f(x) dx + \frac{2}{L} \sum_{n=1}^{\infty} \lambda \frac{n^2 n^2 K t}{S_s L^2} \cos \frac{n\pi x}{L} \int_0^L f(x) \cos \frac{n\pi x}{L} dx$$

(7)

Let x be a dummy variable of integration. To find the solution to the flow equation, we replace L in Equation (7) by L_1+L_2 and in addition, we replace $f(x)$ by $h(x,0)$ as defined. The integral inside the summation on the right hand side of equation (7) and substituting the preceding integral, we have.

$$h(x,t) = \frac{h_1 L_1 + h_2 L_2}{L_1 + L_2} + \frac{2}{L_1 + L_2} \sum_{n=1}^{\infty} \lambda \frac{n^2 n^2 K t}{S_s L_1 + L_2} \cos \frac{n\pi x}{L_1 + L_2} \frac{(h_1 - h_2)(L_1 + L_2)}{n\pi} \sin \frac{n\pi L_1}{L_2 + L_2}$$

$$h(x,t) = \frac{h_1 L_1 + h_2 L_2}{L_1 + L_2} + \frac{2(h_1 - h_2)}{\pi} \sum_{n=1}^{\infty} \frac{1}{n} \lambda \frac{n^2 n^2 K t}{S_s (L_1 + L_2)^2} \cos \frac{n\pi x}{L_1 + L_2} \sin \frac{n\pi L_1}{L_2 + L_2}$$

....(8)

This solution can be expressed in dimensionless form as:

$$h_D(x_D, t_D) = L_D + \frac{2}{\pi} \sum_{n=1}^{\infty} \frac{1}{n} \lambda^{-n^2 \pi^2 t_D} \cos(n\pi x_D) \sin(n\pi L_D) \dots$$

(9)

Where:

The dimensionless distance-

$$x_D = \frac{x}{L_1 + L_2}$$

The dimensionless time -

$$t_D = \frac{Kt}{(L_1 + L_2)^2 S_s}$$

The dimensionless -

$$L_D = \frac{L_1}{L_1 + L_2}$$

One advantage of a closed form analytical solution is that it allows us to examine the behaviour of the flow system. There are several interesting features in this solution. The first term on the right hand side is the steady state part of the solution. It gives the head in the aquifer when t is very large (see fig. 3). The second term on the right hand side is the transient part of the problem. Because t appears in the argument of the exponential function, the second term tends to zero as t becomes large. Furthermore, note that the second term goes to zero at a faster rate if K/S_s (hydraulic diffusivity) is large. Thus, the hydraulic diffusivity is a quantity that controls the rate of hydraulic head.

Unsteady Flow in a Leaky Aquifer

The generalized groundwater flow equation in a leaky aquifer is of the form,

$$S_s \frac{\partial h}{\partial t} = K \nabla^2 h - G$$

(10)

where $G = \frac{e}{T}$, and $e = K^1 \frac{h_0 - h}{b^1}$ can be determined from Darcy's law.

Under this condition, the above equation becomes a radial flow,

$$T \left(\frac{\partial^2 S}{\partial r^2} + \frac{1}{r} \frac{\partial S}{\partial r} \right) - S \frac{\partial}{\partial t} - q = 0$$

where

$$q = \frac{K^1}{b^1} S = \frac{S}{C}$$

(11)

Using the same approach as the solution for the confined (Theis) solution, we obtained the leaky partial differential equation:

$$u \left(\frac{\partial^2 S}{\partial u^2} + \frac{\partial S}{\partial u} \right) + \frac{\partial S}{\partial u} - \frac{r^2}{4uL^2} S = 0$$

...(12)

and from separation of variables, we obtain an appropriate solution

$$S = \frac{Q}{4\pi T} W \left(u, \frac{r}{B} \right)$$

...(13)

The quantity $\frac{r}{B}$ is given by $\frac{r}{\sqrt{T/(K^1/b^1)}}$

Which holds as long as $U < 0.01$

Where $W \left(u, \frac{r}{B} \right)$ is dimensionless form from a logarithm plot chart.

The plot of $S = h_i - h$; versus t at various observation wells, since drawdown is the hydraulic heads measured the level of the water table in wells relative to the piezometric surface (see fig. 4). The change in water table in the pumping well or in observation well nearby is referred to as drawdown (see fig. 5).

APPLICATION

Set of drawdown data was analyzed in order to validate the new method. The examples were obtained from borehole drilled along the coastal area of Lagos State. The boreholes belong to companies operating along the coastal area. The examples were to illustrate the application using equations developed in this case.

Example 1

A well is located in an aquifer with a conductivity of 15 meters per day and a storativity of 0.005. The aquifer is 20 meters thick and is pumped at a rate of 2725 cubic meters per day. What is the drawdown at a distance of 7 meters from the well after one day of pumping?

- Hydraulic conductivity = 15 metres per day
- Storativity = 0.005

- Aquifer thickness = 20 metres
 - Pumping rate = 2,725 cubic metres per day
 - Distance from the well = 7 metres
- $T=Kb = \text{m/day} \times 20\text{m} = 300 \text{ m}^2/\text{day}$

$$u = \frac{r^2 S}{4Tt} = \frac{(7\text{m})^2 \times 0.005}{4 \times 300\text{m}^2 / \text{day} \times 1\text{day}} = 0.0002$$

From the table of $W(u)$ and u , if $u = 2 \times 10^{-4}$, $w(u) = 7.94$:

$$h_1 - h_2 = \frac{Q}{4\pi T} W(u) = \frac{2727\text{m}^3 / \text{day} \times 7.94}{4 \times \pi \times 300\text{m}^2 / \text{day}} = 5.73\text{m}$$

The draw is 5.73 meters after one day.

Example 2

A well in a confined aquifer was pumped at a rate of 220 gallons per minute for about 8 hours. The aquifer was 18 feet thick. Time drawdown data for an observation well 824 feet away are given in table 2. Find T, K, and S.

$$W(u) = 1$$

$$l/u = 1$$

$$h_1 - h_2$$

$$t/r^2 = 6.06 \times 10^{-6}$$

Radial Diameter $d = 20\text{ft}$

Pumping Rate = 220 gallons per day for 8 hours

Aquifer thickness = 18 feet

Transmissivity:

$$T = \frac{114.6QW(u)}{h_0 - h} = \frac{114.6 \times 220 \times 1.0}{2.4} = 10,500 \text{ galonsgpd l ft}$$

Hydraulic Conductivity:

$$K = \frac{T}{b} = \frac{10,500}{18} = 580\text{gpd} / \text{ft}^2$$

Storativity

$$S = \frac{Tu}{2693} \times t / r^2 = \frac{10,500 \times 1}{2693} \times 6.06 \times 10^{-6} = 0.00002 \dots \quad (\text{Theis method})$$

$$S = \frac{Qr^{1-n}}{4\pi Td} = \frac{220}{4\pi(10,500)(20)} = 0.000018 \dots \quad (\text{Clout \& Botha method})$$

$$S = \frac{QW(u)}{4\pi Td} = \frac{220 \times 1.0}{4 \times \pi \times 10,500} = 0.0016 \dots \dots$$

(Observation)

(See fig 4 & 5)

Example 3

An aquifer 10 meters thick is penetrated by a well It is overlain by a semipervious layer I meter thick with a K of 10^{-5} centimeter per second. There is no storage in the leaky confining layer. The aquifer has a K of 10^{-2} centimeter per second and an S of 0.0005. If a well pumps at 500 cubic meters per day, compute values of drawdown at 1, 5, 10, 50, 100, 500, and 1000 meters. (see Table 2)

Aquifer Thickness = 10 metres
 Storativity = 0.0005
 Pumping rate = 500 cubic metres per day
 Various depths = 1, 5, 10, 50, 100, 500 & 1,000 metres

r = distance to the observation wells

t = time since pumping begin

$$K = 10^{-2} \text{ cm/sec} \times 60 \text{ sec/min} \times 1440 \text{ min/day} \times 10^{-2} \text{ m/cm} = 8.64 \text{ m/day}$$

$$K' = 10^{-5} \text{ cm/sec} \times 60 \text{ sec/min} \times 1440 \text{ min/day} \times 10^{-2} \text{ m/cm} = 8.64 \times 10^{-3} \text{ m/day}$$

$$b' = -1\text{m}$$

$$b' = 10\text{m}$$

$$T = Kb = 86.4 \text{ m}^2/\text{day}$$

$$B = (Tb'/K')^{1/2}$$

$$= (86.4 \text{ m}^2/\text{day} \times 1 \text{ m} / 8.64 \times 10^{-3} / \text{day})^{1/2}$$

$$(10^4)^{1/2}$$

$$B = 100$$

$$u = \frac{r^2 s}{4Tt} = \frac{r^2 \times 0.0005}{4 \times 86.4 \times 1} = 1.44 \times 10^{-6} r^2$$

$$\frac{r}{B} = \frac{r}{100} = 10^{-2} r$$

$$h_1 - h_2 = \frac{2.6Q}{4\pi T} W\left(u, \frac{r}{B}\right) = 1.06W\left(u, \frac{r}{B}\right) \quad (\text{our observation}) \text{ see fig. 5}$$

As $u = 1.44 \times 10^{-6} r^2$, we can find the value of u for each r-value

4.1 Discussion of Results:

All the three examples of drawdown data show that the new method underlying this law and the observed drawdown variations in hydraulic conductivity of the aquifer is correct. Each of the analytical solution describes the response to pumping in a very idealized representation of aquifer configurations. In the real world, aquifers are heterogeneous and isotropic: They usually vary in thickness; and they certainly do not extend to infinity. Where they are bounded, it is not by straight-line boundaries that provide perfect confinement. Aquifers are created by complex geologic processes that head to irregular stratigraphy and trendouts of both aquifers and aquitards. The Predictions that can be carried out with the analytical solution presented in this paper must be viewed as best estimates. In general, hydraulic head solutions are most applicable when the unit of study is a well.

They are less applicable on a large scale, where the unit of study is an entire aquifer.

The graphical method of solution starts with the construction of reversed type curve of $W(u)$ against $1/u$ on logarithm paper (see fig. 4). Data from observation well located at different distances from the pumping wells were used. If there is only one observation well, then it is sufficient to plot $h_1 - h_2$ as a function of t (table I).

Using "Contouring the Water Table Map", we noticed that the contours form V's with the river and its tributaries. That's because the river is a "gaining" river. It is receiving recharge from the aquifer. The contours show that ground water is moving down the sides of the valley and into the river channel. The opposite of a gaining stream is a "losing" stream. It arises when the water table at the stream channel is lower than the stream's elevation or stage, and stream water flows downward through the channel to the water table. This is very common in dryer regions of the Southwest. In the case of a losing stream, the V will point downstream, instead of upstream. (see fig. 6)

When making a water table map, it is important that your well and stream elevations are accurate. All elevations should be referenced to a standard datum, such as mean Sea level. This

means that all elevations are either above or below the standard datum (e.g., 50 feet above mean sea level datum). It's also very important to measure all of the water table elevations within a short period of time, such as one day, so that you have a "snapshot" of what's going on (Adeosun *et al* 2006). Because the water table rises and falls over time, you would be more accurate if readings are made before these changes occur.

Understanding how ground water flows is important when you want to know where to drill a well or a water supply, to estimate a well's recharge area, or to predict the direction of contamination is likely to take once it reaches the water table. Water table contouring can help groundwater developer to do all these things. Hence, groundwater flow through the subsurface is the whole essence of this paper and called for further investigation.

Table 1: Drawdown Table

| Time After Pumping Started (min) | T/r^2 | Drawdown (ft) |
|----------------------------------|-----------------------|---------------|
| 3 | 4.46×10^{-6} | 0.3 |
| 5 | 7.46×10^{-6} | 0.7 |
| 8 | 1.8×10^{-5} | 1.3 |
| 12 | 1.77×10^{-5} | 2.1 |
| 20 | 2.95×10^{-5} | 3.2 |
| 24 | 3.53×10^{-5} | 3.6 |
| 30 | 4.42×10^{-5} | 4.1 |
| 38 | 5.57×10^{-5} | 4.7 |
| 47 | 6.94×10^{-5} | 5.1 |
| 50 | 7.41×10^{-5} | 5.3 |
| 60 | 8.85×10^{-5} | 5.7 |
| 70 | 1.03×10^{-4} | 6.1 |
| 80 | 1.18×10^{-4} | 6.3 |
| 90 | 1.33×10^{-4} | 6.7 |
| 100 | 1.47×10^{-4} | 7.0 |
| 130 | 1.92×10^{-4} | 7.5 |
| 160 | 2.36×10^{-4} | 8.3 |
| 200 | 2.95×10^{-4} | 8.5 |
| 260 | 3.83×10^{-4} | 9.2 |
| 320 | 4.72×10^{-4} | 9.7 |
| 380 | 5.62×10^{-4} | 10.2 |
| 500 | 7.35×10^{-4} | 10.9 |

Table 2: Field Data

| R | U | | W |
|--------|-----------------------|------|-------|
| 1m | 1.44×10^{-6} | 0.01 | 9.44 |
| 5m | 3.6×10^{-5} | 0.05 | 6.23 |
| 10 m | 1.44×10^{-4} | 0.1 | 4.83 |
| 50 m | 3.6×10^{-3} | 0.5 | 1.85 |
| 100m | 1.44×10^{-2} | 1 | 0.824 |
| 500 m | 6×10^{-1} | 5 | 0.007 |
| 1000 m | 1.44 | 10 | 00001 |

From the computed values of $W(u, r/u)$ at each observation point, the drawdown can be computed from $h_0 - h = 1.06 W(u, r/b)$

Table 3

| R | h₁- h₂ |
|----------|-------------------------------------|
| 1m | 9.44m |
| 5m | 6.23m |
| 10 m | 4.83m |
| 50 m | 1.85m |
| 100m | 0.824m |
| 500 m | 0.007m |
| 1000 m | 00001m |

CONCLUSION

It has been clearly demonstrated that the study of flow in porous media was recognized in detailed through the physical behaviour of subsurface water and their interactions with the solid matrix (flow of groundwater was delineated through the presence of boreholes drilled along the coastal area of Lagos State for characterizing the flow in the subsurface aquifer. The classical Darcy's law governed the flow in porous media by regarding ground water flow as a function of the hydraulic head. A complete statement of this flow problem required specifying the extent of the flow domain, the governing equation, spatial distribution of properties, for example, hydraulic conductivity and specific storativity, boundary conditions and initial conditions. Analytical solution of this flow equation for which a fractal dimension was assumed to yield a closed form solution that could be written on paper and also be examined to understand the behaviour of the flow system in a typical limited homogeneous flow domain with relatively simple geometry.

The problem of solving fluid flow through porous media has proved analytically intractable and the problem of understanding flow and storage in aquifers is very complex. It was recognized that flow through such a medium is very significantly influenced by the porous media characteristics such as porosity and permeability. A limitation of this work is the estimation of permeability (hydraulic conductivity) of the medium which can not be examined and investigated without being to the field, even if examined, permeability estimation has proved to be complex and this concept has limited the free flow of fluid within the porous medium. Therefore, this work is hoped to complement the study of flow through porous media that might have been done in other parts of the world and contributes to the unveiling knowledge of the applicability of flow in porous media. Prediction of this flow shows several interesting qualitative features such as graphs and contouring of water table map, which held to predict change in drawdown in pumping well and the direction of flow. The method becomes more accurate and easy to handle with little or no variations in the observed drawdown and water table flow prediction.

NOMENCLATURE

S = Storativity
T = Transmissivity (L^2T^{-1})
 $h_1 - h_2$ = drawdown (L)
Q = pumping rate (L^3T^{-1})
t = time, (time since pumping began)
r = radial distance from pumped well (L)
e = leakage rate
B = leakage factor (Lb^{-1}) = **thickness of leaky layer (L)**
 b^1 = thickness of leaky layer (L)
 K^1 = vertical hydraulic conductivity of leaky layer (LT^{-1})
(X, y) = rectilinear coordinator
 S_s = specific storage

h = head (L)
 q = specific discharge (M^3d^{-1} per m^2)
 K = hydraulic conductivity of aquifer (md^{-1})
 h_2, h_1 = hydraulic heads measured along flow path
 L = distance between head measurements (m)
 W = width of cross - sectional flow (m)
 D = height of cross-sectional flow (m)
 $W(u)$ = dimensionless form from chart
 G = leakage factor
 U = flow velocity

Correspondence to:

Odunaike R. K. Usman M. A. Hammed F. A. Adeosun T. A. and Olayiwola, M.O.

¹Department of Mathematical Sciences,
Olabisi Onabanjo University, Ago-Iwoye, Nigeria.
² Department of Mathematics, Yaba College of Technology
Lagos, Nigeria

Dr. Usman M A
Dept. of Mathematical Sciences
Olabisi Onabanjo University, Ago-Iwoye, Nigeria.
usmanma@yahoo.com

REFERENCES

1. Adeosun T.A., Nwonwu, A.C. and Oladapo, M.I. (2006): Delineation of Freshwater Aquifers in the Coastal Area of Lagos State (Ikoyi, Victoria Island, Lekki, Apapa): conference paper presented at 29th Annual Conference of the Institute of Physics, held in the Department of Physics, University of Nigeria, Nsukka.
2. Allen, R. and Cherry, J.A. C200 I): Groundwater, Prentice - Hall, Inc, Englewood Cliffs. NJ.
3. Bear, J. (1972): Dynamics of fluids in porous media: Dover publication Inc., Mineola, New York. U. S. A.
4. Beltrami, E. (2004): Mathematics for Dynamic Modeling: Academic Press, Inc, N. Y. at Stony Brook, N. Y.
5. Cloot, A. and Botha J.F. (2006): A Generalised Groundwater Flow Equation Using The Concept of Non-Integer Order Derivatives, Institute of Groundwater Studies, Journal of Groundwater, SA Vol. 32 No.1. Department of Mathematics, University of the Free State, Bloemfontein, South Africa. www.wrc.org.za
6. Coat, J. and Smith, F. (2005): Reservoir Simulation, Dover Publication, New York.
7. Codinton, E.A. (1990): An Introduction to ordinary Differential Equation: Prentice-Hall, New Delhi.
8. Darton N. H. (1972): Preliminary Report on the Geology and Underground Water Resources of the Central Great Plains. U. S. A Geological Survey Professional Paper32, 433pp.
9. Douglas, J .F., Gasiorek, J. M. and Swaffield, J. A (1995): Fluid Mechanics: Longman Singapore Publishers, Third Edition, 1995.
10. Felter C. W. (1997): Applied Hydrogeology: Cambridge University Press, New York
11. Ferziger, J.R. and Milovon P. (2002): Computational Fluid Dynamics, 3rd edition, Springer- Verlag, New York
12. Fujita, K. (1997): Principle of Geophysics: Blackwell Science, Inc, U.S.A.

13. Harper, C. (1999): Introduction to Mathematical physics: Prentice- Hall, New Delhi,
14. Ogunleye L O. and Oni T.O. (2001): Simple Approach to Fluid Mechanics for Science and Engineering Students: Godliness Printing and Publishing Co. Vol. 1. University of Ado Ekiti, Ado Ekiti, Nigeria.
15. Oladapo M. 1. And Omosuyi O. (2000): Groundwater Geophysics: Lecture Note Series, Vol. I. Department of Applied Geophysics, Federal University of Technology, Akure.
16. Oteri A. U. (1988): Report on water pollution in the coastal area of Lagos State, Nigeria.
17. Wright, W.S. Wright, C.D. (1997): Differential Equations with Boundary Value Problems, Brooks and Cole Publishing Coy. N. Y.
18. Zhan, H. and Park, E. (2005): Modeling of Underground Water Flow, Department of Geophysics, Texas A & M, University College. Station, Tx 77843-3115, Corresponding Author (Zhan@hydrog.tamu.edu).

Note: This article was primarily published in [Academia Arena, 2009;1(1):4-12]. ISSN 1553-992X.

Wed, Aug 27, 2008 at 2:55 PM

RAPD-PCR for DNA-Fingerprinting of Egyptian tilapia

Soufy. H¹, Laila A.M.², Iman M.K.A.²

¹ Department of Paracitology, National Research Centre, Egypt.

² Department of Hydrobiology, National Research Centre, Egypt.

imankam_2@yahoo.com

Abstract: Evaluate of common patterns of genetic variations or similarities among three species of tillapine through the DNA fingerprinting analysis was performed in this study using RAPD-PCR (Random amplified polymerase chain reaction) using 10 arbitrary primers, out of 10 primers used, 7 primers gave strong sharp distinct bands. The 7 primers produced a total of 15 , 13 , 16 , 14 , 18, 14 and 17 bands respectively. Depending on the similarity coefficient through the used primers, the similarity between *Oreochromis niloticus* and *Oreochromis galilaius* was 95% and between *Oreochromis niloticus* and *Tilapia zilli* was 80% and between *Oreochromis galilaius* and *Tilapia zilli* was 75%. The values of the genetic distances obtained were utilized to generate a distance matrix to construct a dendrogram which linked the studied species. The results of DNA fingerprinting of the studied fishes can be taken into consideration as a joint patterns of similarity and probability of Hybridization between the very closed species to improve the genetic characters. [New York Science Journal. 2009;2(2):20-25]. (ISSN: 1554-0200).

Keywords: RAPD-PCR, DNA-Fingerprinting, Egyptian tilapia

Introduction

Morphological studies have been especially successful in defining species and in organizing these species into genera. These groupings have usually been confirmed when examined with molecular approaches. Molecular characters have revealed some cryptic species (**Awise, 1994**) and identified some incorrectly split groups (e.g., species inclinid klep fish genus *Gibbonisia* by **Stepien and Rosenblah, 1991**).

Although morphological studies have generally been successful in defining genera, it is rare to find studies which present a hypothesis of relationship above the level of species comprising a genus, primarily due to a lack of congruence of characters (**Stepien and Kocher, 1997**), fortunately this is one of the strengths of molecular data, and inter- and intrageneric relationships are now being rapidly tested and elucidated. Molecular data are also means used to assess the phylogenetic relationships among populations.

Development in RAPD-PCR technology is known as Random Amplified Polymorphic DNA-Polymerase Chain Reaction (RAPD-PCR). This approach of DNA polymorphism which based on PCR amplification of DNA segment using single primers of arbitrary nucleotide sequences has been developed by **Williams et al. (1990)** and **Welsh and McClelland (1990)**. This technique involves amplification of certain regions of the nuclear genome flanked by inverted sequences complementary to particular nucleotide 10-mer primer, provided that the primer anneals within a range of annealing temperatures (35- 40°C). The primer randomly anneals to an unknown segment on one of the DNA strands. When two species, strains, or individuals are compared, polymorphism between them will be revealed on agarose electrophoresis gels by presence or absence of an amplification product., this method has been applied to the discovery of genetic

markers for mapping studies (**Poslethwait et al., 1994**) and to elucidate the phylogenetic relationships between species (**Bardakci and Skibinski, 1992; Welsh and McClelland, 1990**). **In this investigation , RAPD-PCR was used to examine the DNA-fingerprint and the similarity among three tilapia fish in Egypt, *Oreochromis niloticus*, *Sarotherodon galilaeus* and *Tilapia zilli* .**

Materials and Methods

Fish samples:

Fish samples of three species *Oreochromis niloticus*, *Sarotherodon galilaeus* and *Tilapia zillii* were collected from El-Abbassa fish farm , from October to December 2005

DNA extraction :-

Genomic DNA was extracted using the phenol- chloroform extraction method (**dinesh et al., 1993**).

Polymerase chain reaction (PCR) amplification was carried out following the RAPD- fingerprinting protocol previously established for fish (**Dinesh et al . , 1993**) . Genomic DNA was amplified in reaction volume of 50 µl using a 10 –mer seven RAPD primers with G + C content 60 and 70 %.

the sequences of primers were : **GAAACGGGTG , AATCGGGCTG , GGGTAACGCC, CAGCACCCAC, GTGATCGCAG, CCGGGAATCG and AGTCAGCCAC**

The reaction mixture was prepared using 2.5 ml of 10 X PCR buffer , 2.5 ml 50 mM Mgcl2 , 1 ml 10 mM DNTPs , 1 – 7 ml primer , 2 ml DNA (100 - 200 ng) 0.5 ml Taq DNA polymerase enzyme and H 2O in a total volume of 50 ml. Amplification was carried out with the following cycle program: 4 min. of denaturation at 94°C; 37cycles of amplification at 94°C (1 min); 36°C-42 °c (2 min) and 72 °c (1 min). Soaking was carried out in 4°C.

Analysis of RAPD - PCR products:

The products of amplification were analyzed by electrophoresis on

1.4% agarose gels in 1X TBE buffer, visualized under UV trans-illuminator and photographed by a Polaroid camera.

(1)Genetic statistical analysis:-

The similarity coefficients between the three tilapia species were calculated based on pair wise comparison between them for primers using the formula:

$$\delta = 2 N_{xy} / (N_x + N_y)$$

Where N_x and N_y are the number of bands in individuals X and Y.

N_{xy} is the number of shared bands (**Nei and Li, 1979; Lynch and Milligan , 1994**) .

The average pair wise similarity (S) was then calculated as an average across primers. The similarity values were converted into genetic distance using the formula: $D = 1 - S$ (**Nei and Li, 1979**).

The data derived from this formula was plotted to establish a matrix of distance using computer program of unweighted pair- group Arithmetic average cluster analysis to construct a dendrogram for the three tilapia species.

Results

Out of 10 primers used, 7 primers gave strong sharp distinct bands. The RAPD fingerprints of three fish species are shown in fig.(1) the total bands generated by the primers A-G respectively are: 15 , 13 , 16 , 14 , 18, 14 and 17 bands respectively.

Figure1(A-G) have four lanes, from left to right are: the DNA marker, *Oreochromis niloticus*, *Sarotherodon galilaeus*, and *Tilapia zilli* PCR products.

Using primer A, the amplification products of *Oreochromis niloticus* DNA by application of RAPD technique showed five bands of molecular weights 207, 328, 569, 790 and 1145 bp. While *Sarotherodon galilaeus* produced 5 bands of molecular weights 207, 383, 472, 734 and 1003 bp. and *Tilapia zilli* showed five bands, 207, 362, 461, 764 and 1040 bp.

(Fig.1-A)

The RAPD-PCR products using primer B revealed six bands in *Oreochromis niloticus*, 253, 317, 412, 506, 758 and 1017 bp. And three bands only in *Sarotherodon galilaeus*, 506,758 and 1029 bp. But in *Tilapia zilli* it revealed four bands of molecular weights 390, 506, 1029 and 1425 bp.(Fig.1-B)

In primer C, *Oreochromis niloticus* produced five bands, 202,403, 581, 632 and 1403 bp., where in *Sarotherodon galilaeus* five bands were appeared as 217,418,571,632 and 1406 bp. and six bands appeared in the amplification of *Tilapia zilli* DNA, 92, 209,461,581,632 and 1403 bp. .(Fig.1-C).

Primer D revealed six bands of molecular weights 196, 270, 449, 578, 810 and 901 bp. in case of *Oreochromis niloticus*, but produced four bands of molecular weights 254, 449, 578 and 810 bp. in case of *Sarotherodon galilaeus* and four bands in *Tilapia zilli* of molecular weights 578, 710, 810 and 930 bp. .(Fig.1-D). The amplification products of RAPD-PCR using primer E produced eight bands utilizing *Oreochromis niloticus* DNA, there molecular weights were 67,123, 215, 278, 340, 461, 720and 903bp. and six bands in *Sarotherodon galilaeus* of molecular weights 59, 187, 270, 390, 607 and 840 bp. Also it revealed four bands in *Tilapia zilli*, 117,270, 390 and 607 bp. .(Fig.1-E). Primer F produced six bands in the amplification of *Oreochromis niloticus* DNA, there molecular weights were 168, 173, 288, 390, 582 and 783bp.; four bands of molecular weights 317, 405, 591 and 698 bp. in *Sarotherodon galilaeus*, while in *Tilapia zilli* it revealed four bands of molecular weights 317, 405, 591 and 677 bp. .(Fig.1-F). Finally using primer 7, six bands appeared in *Oreochromis niloticus*, there molecular weights were 170, 202, 460, 591, 632 and 1343 bp. ; five bands in case of *Sarotherodon galilaeus* of molecular weights 270, 431, 583, 620 and 1281 bp. and six bands of molecular weights 146, 270, 436, 583, 620 and 281 bp in *Tilapia zilli*. .(Fig.1-G)

Phylogenetic relationships:

Depending on the data produced from RAPD-PCR amplification and fish DNA fingerprinting, similarity coefficient was obtained from statistical analysis to assess the similarity between the three tilapia fish species. A

linkage map (dendrogram) is constructed among the three tilapia fish species of (Fig.2).

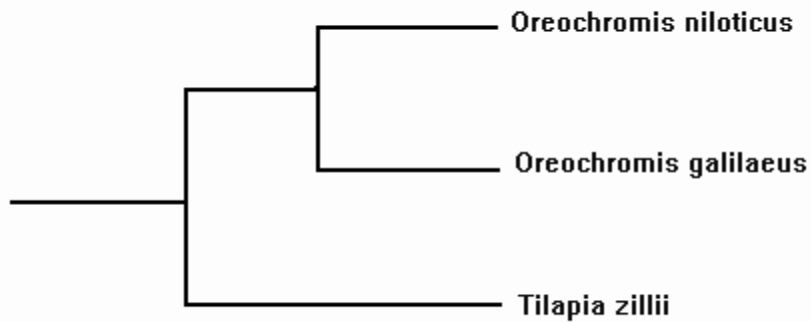
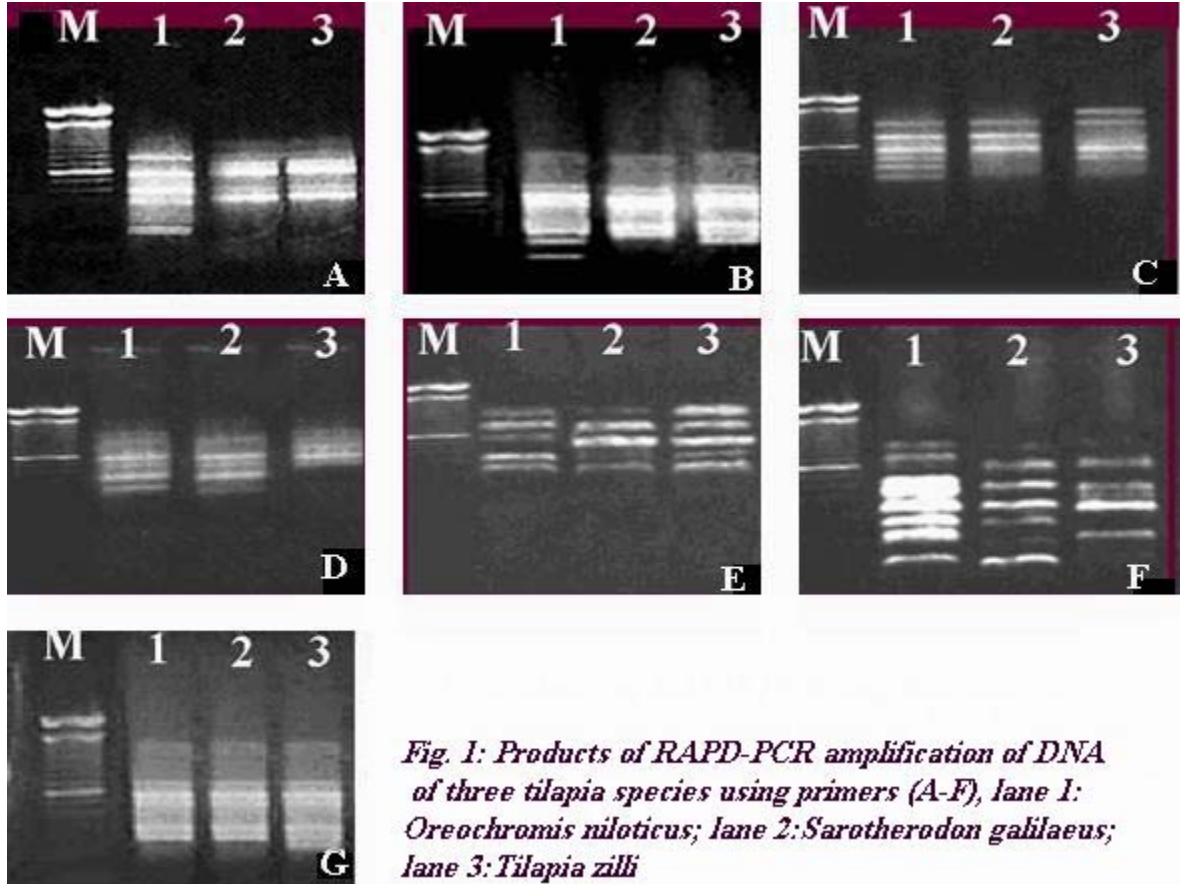


Fig.2: Dendrogram generated by clustering using Unweighted Pair-Group Arithmetic Average analysis of 1-s values (based on Nei and Li's index) computed from pairwise comparison between three tillapine fish speci

Discussion

RAPD bands in this study were always variant (i.e., strong, faint, fuzzy and sharp bands) generated with each primer because one or more copies of DNA may exist per genome or may be attributed to the varying of the annealing process between the primer and the DNA. This problem of mixed bands shows the well known sensitivity of PCRs (**Bielawski et al., 1995**). RAPD fragments generated by primer four produced low polymorphism among fishes studied. This primer sequences may have annealed to variable sequences, which might be of great utility at lower taxonomic levels, e.g. for the differentiation of very related species. However, in RAPD fragments generated by the other primers, there were high degree of polymorphism, their sequences may be considered as more conserved sequences, which are most useful in higher taxonomic levels and evolutionary relationships. These results are in agreement with **Bardkci and Skibinski (1994)** who stated that, patterns of similarities and differences between populations showed broad agreement across primers and the overall similarity level varied between primers. Thus, primer choosing is a very important for this technique.

RAPD fingerprinting has been used to construct a genetic linkage map (**Postlewait et al., 1994**). In this study, three species of tilapia fish were studied genetically through the RAPD technique to put a species fingerprint and to identify the similarity coefficient among the fishes under study. This coefficient represents a measure of the shared bands two or more different species within the same, and different, primers. These are important measurements that help to quantify the degree of relationships between different species.

The description of this similarity coefficients is not simple, especially when more than one character are involved in the same cluster. Thus, *O. niloticus* and *S. galilaeus* are found to have a similarity coefficient of 95%, where between *O. niloticus* and *T. zillii* is 80% and between *S. galilaeus* and *T. zillii* is 75%. The genetic similarity between *O. niloticus* and *S. galilaeus* was higher compared with that between *O. niloticus* and *T. zillii*. Also, between *S. galilaeus* and *T. zillii* there was low similarity compared with that of *O. niloticus*. The dendrogram (fig. 2) indicates the relationship among the three *tilapia* species which are of family *Cichlidae*, taking into consideration the close relationship between *O. niloticus* and *S. galilaeus*.

However, this study concluded that the very high similarity between *O. niloticus* and *S. galilaeus* leads to high probability of hybridization between them, but not between *O. niloticus* and *T. zillii*. These findings are an indication of the distinct character of *T. zillii* territoriality, in contrast to the other two species, in spite of the close morphology of body shape they all share.

It can be concluded also that, RAPD-PCR could prove to be a useful tool for estimating the genetic variability and degree of similarity among fish species.

References

- Avise, J.C. (1994): Molecular markers, National History, and evolution. Chapman and Hall, New York.
- Baradakci, F. and Skibinski, D.O.F. (1994): Application of the RAPD technique in tilapia fish species and subspecies identification. *Heredity*, 73: 117-123.
- Bielawski, J.P.; Noach, K. and Pumo, D.E. (1995): Reproducible amplification of RAPD markers from vertebrate DNA. *Biotechniques*, 12: 36-39.
- Dinesh, K.R.; Lim, T.M.; Chua, K.L.; Chan, W.K. and Phang, V.P.E. (1993): RAPD analysis: An efficient method of DNA fingerprinting in fishes. *Zool. Sci.*, 10: 849-854.
- Nei, M., and Li, W. S. (1979). Mathematical model for studying genetic variation in terms of restriction endonucleases. *Proc. Natl. Acad. Sci. U.S.A.*, 76: 5269-5273.

- Postlethwait, J.H.; Johnson, S.L.; Midson, C.N.; Talbot, W.S.; Gates, M.; Ballinger, E.W.; Africa, D.; Andrews, R.; Carl, T.; Eisen, J.S.; Horne, S.; Kimmel, C.B.; Hutchinson, M.; Johnson, M. and Rodriguez, A. (1994): A genetic linkage map for the Zebra fish. *Science* 264: 699-703.
- Stepien, C. A. and Kocher, t. d. (1997): Molecular systematics of fishes: molecules and morphology in studies of fish evolution, *mol. Phylogenetic. Evol.*, 1:1-11.
- Stepien, C. A. and Rosenblat, R.H.(1991): Patterns of gene flow and genetic divergence in the Northeastern Pacific Clinidae (Teleostei: Blennioidei), based on allozyme and morphological data. *Copeia*, 4: 873-896.
- Welsh, J. and McClelland, M. (1990): Fingerprinting genomes using PCR with arbitrary primers. *Nucleic acids Res.*, 18: 7213-7218.
- Williams, J.G.K.; Kubelik, A.R.; Livak, K.J.; Ratajski, J.A. and Tingey, S.V. (1990): DNA polymorphisms amplified by arbitrary primers are useful as genetic markers. *Nucleic acids Res.*, 18: 6531-6539.

10/23/2008

相对绝对论

李学生

山东大学副教授，中国管理科学院学术委员会特约研究员、北京相对论研究联谊会会员，中国民主同盟盟员

xiandaiwulixue@21cn.com

摘要：相对与绝对是指世界上一切事物都具有相对与绝对两种不同的属性，它们之间的关系可以用量子力学的互补原理（或者中国古典哲学中阴阳太极图）来表述——彼此互补的两种事物，不可能用任何方式把它们结合成一个无矛盾的统一体（统一图景），只有这些现象的总体才能将关于客体的可能性包罗尽。光的波粒二象性正是这一问题的表现形式之一。[New York Science Journal. 2009;2(2):26-30]. (ISSN: 1554-0200).

关键词：相对；绝对；量子力学；互补原理

（一）问题的提出

20世纪以来，以相对论与量子力学的创立为标志的现代物理学研究工作，从理论和实践两个方面，对人类认识和社会发展起到了难以估量的作用。物理学理论的发展，在三个层次上把人类对自然界的认识推进到了前所未有的深度和广度。在微观领域内，已经深入到基本粒子的亚核世界（ 10^{-15} 厘米），并建立起统一描述电磁、弱、强相互作用的标准模型，还引起了人们测量观、因果观的深刻变革。特别是量子力学的建立，为描述自然现象提供了一个全新的理论框架，并成为现代物理学乃至化学、生物学等学科的基础。在宇观领域内，研究的探针已达到 10^{28} 厘米的空间标度和 10^{17} 秒的宇宙纪元；广义相对论的理论预言，在巨大的时空尺度上得到了证实，引起了人们时空观、宇宙观的深刻变革。在宏观领域内，关于物质存在状态和运动形式的多样性、复杂性的探索，也取得了突破性的进展。凝聚态物理层出不穷、令人眼花缭乱的成果和混沌现象奇特规律的惊人发现，给人类原有的知识体系以巨大的冲击，在动力学系统长期行为的确定性与随机性，决定性描述与概率性描述等方面，引起了认识上的深刻变革。自20世纪以来，以相对论与量子理论为基础的现代物理学的显著特征是它的广泛性与深刻性。广泛性：在宏观上我们开始了对整个宇宙的严肃研究，而没有广义相对论的基础这是不可能的。古典哲学对整个宇宙的最好的认识也只是到康德的“先验”概念。微观上，基本粒子不再只是哲学思辩的产物，我们对物质结构有了真正的认识。深刻性：古典物理里面很多不同的概念我们突然发现原来是统一的。比如我们发现了时间和空间只是统一的时空的两个部分，宇宙和物质的基本结构可能与制约它们的基本规律是同一回事。现代物理学的一个重要目的，是为了获得一种对自然的深刻理解和洞察力，使我们能够以一种接近上帝的角度观察我们的宇宙。牛顿在他的《原理》中表达这样的观点：“我只写下这些自然规律的数学公式，至于为什么这些公式是这样，不是我需要关心的问题。”

在实践方面，现代物理学的发展导致了原子能的释放和应用，导致了半导体、光通讯等新兴工业的崛起，为激光技术、新材料研制、新能源开发开辟了新的技术途径，并推动了计算机革命的进展。现代物理学在推动能源科学、空间科学、材料科学、信息科学、环境科学、海洋科学的发展中起到了关键性的作用，成为20世纪下半叶以来蓬勃发展的现代科学技术革命的重要科学基础。现代物理学以新兴高技术群为中介向生产力的转化，极大地改变了人类的生产方式和生活方式，成为推动现代社会发展的重要杠杆。

50年代以来的当代物理学已经发展成为一个相当庞大的学科群，包括了高能物理（粒子物理）、原子核物理、等离子体物理、凝聚态物理、原子分子物理、光物理、声学、计算物理和理论物理等主体学科以及难以数计的分支学科。物理学内部各个分支学科的渗透和交叉，物理学和化学、生物学、材料科学、天文学等其他学科的渗透和交叉，又产生了许多新的、富有生命力的边缘学科，形成了众多极有发展前途的科学前沿。当代物理学还呈现出高速发展的趋势，现代物理学中90%的知识是1950年以后取得的。其发展之快，分支之多，变化之大，已使人们很难及时作出全面的概括。当代物理学研究的综合性、深入性、复杂性、创新性和可应用性，都呈现出鲜明的时代特点。物理学在21世纪发展的全景，人们无法作出全面的预测。只能根据我们目前的认识水平，根据当代物理

学发展的状况和特点,对 21 世纪最初几十年的发展趋势作“豹斑之窥”。大体说来,在科学技术整体发展的推动下,物理学仍将加速地发展和分化,同时又会出现更多的渠道,增强各个分支之间的交叉和非线性作用,导致更为广泛和深刻的综合,朝着各个分支学科不断深入而整体领域综合交叉的整体化方向进展。物理学作为精密科学的典范,并以其探索视野的广阔性、研究层次的广谱性、理论适用的广泛性,在今后很长时期内仍将发挥其中心科学和基础科学的作用。它也仍将不断地推出新思想、新原理和新方法,孕育出功能奇特、威力巨大的新技术,成为新技术和新兴产业部门的源泉和生长点。物理学与未来高新技术将更加紧密地发生融合,互相促进,协同发展,成为科学技术革命深入发展的主旋律;物理科学技术领域愈来愈频繁出现的突破性进展,将会更加吸引社会公众对物理学事业发展的热切关注。

Einstein 是本世纪初物理学革命的巨人, Einstein 说过:“常听人说,科学家是蹩脚的哲学家,这句话肯定不是没有道理的。那么,对于物理学家来说,让哲学家去做哲学推理,又有什么不对呢?当物理学家相信他有一个由一些基本定律和基本概念组成的严密体系可供他使用,而且这些概念和定律都确立的如此之好,以及怀疑的风浪不能波及它们,在那样的时候,上述说法固然可能是对的;但是象现在这样,当物理学的这些基础本身成为问题的时候,经验迫使我们去寻求更新更可靠的基础,物理学家就不可以简单地放弃对理论基础作批判性的思考,也最确切地感到鞋子究竟在哪里夹脚的。在寻求新的基础时,他必须在自己的思想上尽力弄清楚他所用的概念究竟有多少根据,有多大的必要性。整个科学不过是日常思维的一种提炼。正因为如此,物理学家批判性思考就不可能只限于检查他自己特殊领域里面的概念。如果他不批判地考查一个更加困难得多的问题,即分析日常思维的本性问题,他就不能前进一步。”【7】海森伯在谈到 Einstein 的贡献时说,他“有点像艺术领域中的达·芬奇或者贝多芬, Einstein 也站在科学的一个转折点上,而他的著作率先表达出这一变化的开端;因此,看来好像是他本人发动了我们在本世纪上半期所亲眼目睹的革命”。的确,从 1905 年的“幸运年”年到 1916 年广义相对论论文“标准版本”的发表, Einstein 在两个研究方向上奠定了 20 世纪物理学的基础。一是不变性原理的研究,最终创立了狭义相对论(1905 年)和广义相对论(1915 年)。二是统计理论的研究,其结果导致布朗运动理论(1905 年)、分子大小测定法、光量子假设(1905 年)、首次固体量子论(1907 年)、光的波粒二象性(1907 年)以及导致激光发现的 A、B 系数(1916 年)。最后,在 1925 年,他完成了另一主要创造性工作,即独立于德布罗意的关于物质波粒二象性的假设。指明不变原理和统计涨落这两个别出心裁的研究方向,乃是 Einstein “前不见古人,后不见来者”的杰作。在 1916 年之后,这两个方向合二而一,成为 Einstein 探索统一场论的指南。Einstein 认为:“我们关于物理实在的观念决不会是最终的。为了以逻辑上最完善的方式来正确地处理所感觉到的事实,我们必须经常准备改变这些观念——也就是说,准备改变物理学的公理基础”。Einstein 曾对他的相对论等理论作过交代:“我的工作中没有一个概念是站得住的,我不能肯定我所走过的道路一般是正确的……”。“然而为了科学,就必须反反复复地批判这些基本概念,以免我们会不自觉地受它们支配。在传统的基本概念的贯彻使用碰到难以解决的矛盾而引起了观念的发展的那些情况下,这就变得特别明显”。他曾多次表示,他的理论绝不是完美无缺的终极理论,它们将来一定会被其他更完善的理论来代替。

我们的科学被划分成了一个相对孤立的体系,并不断地进行继续的分化,看起来科学之树越来越枝繁叶茂,但同时也越来越繁琐,越来越孤立。划分这些体系的是一个开创新学科的大师们所进行的分析与简化。回顾科学大师们的足迹,我们不得不惊叹他们对于事物本质的把握能力,但他们把握的依然不是事物的完全真实本质,而只是相对正确。审视整个科学之树,我们看到,新的科学体系的诞生无不是在固有体系的基础上,根据当时所了解的知识,理想化出一系列基本理论,并在这些基本理论基础上发展出来整个体系。但没有人能保证这些基本理论始终有效。当我们学习这些科学体系时,对权威的崇拜,对这些科学体系魅力的迷恋,对整个科学体系坍塌的恐惧使得我们的自由意志与既有结论或权威对立时,我们的第一个反应就是逃避。而作为科学基本的态度和精神怀疑与批判,则早已被我们置之脑后。逐渐地,我们就把这些基本理论看成神圣不可侵犯的“公理”,即使它们已经不合时宜。

狭义相对论天空存在着“两朵乌云”,这是 Einstein 发现的:第一朵乌云——在狭义相对论中, Einstein 采用了“欧氏几何对于确定绝对刚体的空间位置是正确的”这个假设,并采用了惯性系和惯性定律,从而给出力学相对性原理。因此在力学相对原理的推论中起着基本作用的是绝对刚体的概念。1923 年, Einstein 提交哥德堡北欧自然科学家会议的报告中又意识到这种做法有着缺欠,而

且这个缺欠存在于整个相对论中。是的，把全部的物理学研究建立在绝对刚体的概念上，然后又用基本的物理定律在原子论上再重新建立刚体的概念，而基本的物理定律又是用刚体的概念建立起来的，这在逻辑上是不正确的。同时他也承认，“由于我们还没有充分认识大自然的基本规律，以致不能够提出一个更为完善的方法来解脱我们的困境”。可惜的是，一直到他去世也没有找到解脱这个困境的办法。这个问题就这样挂起来了，而且一挂就是近百年。第二朵乌云——在狭义相对论中，任何事物都随观察者的不同而不同。它还包含下面两层意思：一个是每个观察者都只承认自己的结论正确，其他观察者的结论不正确；另一个是所有观察者都对。想在两个观察者中决定谁是正确的，既没有经验上的方法，也没有理论上的方法。这就是相对论的相对性。很明显，这个观点与经典天体力学中的观念相矛盾。“Einstein 自从量子力学革新了物理学中的思想方法以后，到他逝世为止，一直想要保持经典天体力学中的观念，即一个系统的客观物理状态必须跟观察它的方式完全无关。虽然 Einstein 坦白地承认，他对这方面达成一个完整的解答的希望到目前为止尚远未满足，而且他还没有证明这一观点的可能性，他认为这是一个有待解决的问题。(W. 泡利的《相对论》补注 23)”不排除相对论与其它学科的认识存在严重矛盾的情况。也许在过去我们过多地在相对论中自言自语，缺乏与其它学科知识的比较研究。或者说相对论的革命并不彻底普遍，在相对论中推翻了的观念在其他学科中依然成立，这必然导致矛盾冲突。《Einstein 传》395 页：“Einstein 很快乐，并且还自己编了一个小幽默：‘对于那个 Einstein 来说，这是非常容易的事。每年他都取消上一年所做的工作。’”

在 Einstein 以前，物理学家从来没有认识到区分绝对物理量和相对物理量在理论上有多么得重要！Einstein 也在《相对论》中写道：如果相对于 K, K_1 是一个匀速运动而全无转动的坐标系，那么，自然现象在 K_1 中的发生过程，和 K 中的发生过程遵循完全一样的基本定律。这就是相对性原理 (Principle of Relativity)。回顾科学大师们的足迹，我们不得不惊叹他们对于事物本质的把握能力，但他们把握的依然不是事物的完全真实本质，而只是相对正确。

2005 年 6 月，英国的 J. Dunning-Davies 教授曾说过一段很有意思的话：“在 20 世纪末，许多人仍象对待圣物那样盲目相信由相对论推出的任何结果。他们忘记了所有理论都是人为的，而宇宙却不是人造的。任何理论或模型，只不过是微不足道的人类智力作出的某种解释。但许多人如此深信某个理论的正确，而知名权威们竟不惜代价地阻止任何人对这些理论提出任何问题。Dingle (对相对论) 的忧虑至今被隐藏起来，Thornhill 对狭义相对论 (SR) 的有效性的怀疑难见天日。……实际上，主流物理学并非如大多数人所以为的那样坚实与无懈可击。”在两次革命之间，有一个较长的所谓“常规科学”时期。在这个时期，新范式被发展、被应用。同时占统治地位的范式也逐渐暴露出无法使人满意的地方，不断产生“反常现象”。大量反常现象的涌现导致“危机”，危机是新理论诞生的一种适当的前奏，是科学革命的前兆。库恩的科学发展动态模式是：前科学→常规科学→危机→科学革命→新的常规科学……

早在 1908 年，在物理学急剧发展的浪潮中，列宁就一针见血地指出：“……一般自然科学家以及物理学这一专业部门中的自然科学家，极大多数都始终不渝地站在唯物主义方面。但也有少数新物理学家，在近年来伟大发现所引起的旧理论的崩溃的影响下，在特别明显地表明我们知识的相对性的新物理学危机的影响下，由于不懂得辩证法，就经过相对主义而陷入了唯心主义。……”【3】Rosenberg 在《科学哲学》一书中给科学哲学下的一个工作定义：“哲学处理两类问题：首先，科学——如物理科学、生物科学、社会科学和行为科学等——现在不能回答也许永远不能回答的问题。其次，有关为什么科学不能回答第一类类型的问题的问题。”科学哲学担负了区分科学与伪科学的一种持久的责任。霍金在《时间简史》中说：“迄今，大部分科学家太忙于发展描述宇宙为何物的理论，以至于没有工夫去过问为什么的问题。另一方面，以寻根究底为己任的哲学家不能跟得上科学理论的进步。在 18 世纪，哲学家将包括科学在内的整个人类知识当作他们的领域，并讨论诸如宇宙有无开初的问题。然而，在 19 世纪和 20 世纪，科学变得对哲学家，或除了少数专家以外的任何人而言，过于技术性和数学化了。哲学家如此地缩小他们的质疑范围，以至于连维特根斯坦这位本世纪最著名的哲学家都说道：‘哲学仅余下的任务是语言分析。’这是从亚里斯多德以来哲学的伟大传统的何等堕落！”

(二) 相对与绝对的辩证关系

物理学在一开始就与哲学紧紧地联系在一起。哲学的思维始终影响着物理学的发展，物理学的

新发现又影响着哲学的新认识。其中，尤以**相对性**与**绝对性**最为突出。相对性原理在不同的惯性系中找到了相同的部分，这些部分，无论是观察还是实验，都不可否认的是“这个”样子，它也就是我们的常识。绝对量和相对量的区分依据就是相对所有的惯性测量坐标系变换而言，凡是那些不变的物理量——即绝对量，只有这种绝对物理量才可以称之为基本物理量；也是所谓的不可测的物理量。也是永远不可测知的物理量。同时也是最核心的物理量。凡是那些可变的物理量——即相对量，这种相对物理量只有技术工程学的意义。当然，这是可测知的物理量。是核心物理量的外围物理量。是次基本物理量。绝对式和相对式的区分依据就是相对所有的惯性测量坐标系变换而言，凡是那些不变的物理式——即绝对式，只有这种绝对物理式才可以称之为基本物理定律；也是所谓的不可测分的物理式。同时也是最核心的物理定律。凡是那些可变的物理式——即相对式，这种相对物理式只有技术工程学的意义。当然，这是可测分的物理式。是核心物理式的外围物理式。是次基本物理式。绝对和相对区分，早在18世纪的数学大师就自觉地明确区分开来，并且深知只有那些绝对量和绝对式才有核心意义。

研究物理必须要有哲学观点作指导。把简单的哲学观点用数学表达出来，并进行逻辑验算，进而解释、预言实验现象，这就是物理。Einstein是这一方面的杰出代表。不管是狭义相对论，还是广义相对论，都是从基本假设开始，进行数学验算，继而形成物理理论。恩格斯说：“世界真正的统一性是它的物质性，而这种物质性并不是魔术师的三两句所能证明的，而是哲学和自然科学的长期的持续的发展来证明的。”自然科学的物质观在于研究物质的构造，是随着自然科学的进步而变化的，它总是具有近似的、相对的性质，而这些相对真理的总和，使我们日益接近于客观的、绝对的真理。从逻辑上来说，相对性原理，最小作用原理，守恒原理，不可逆原理不能认为是独立的。若是以要求世界线和测地线重合，即一般说来和以要求非欧氏空间的短程线重合这种形式提出相对性原理，那么相对性原理和变分原理的联系就变得十分明显了。守恒原理和变分原理的联系是如此紧密，以致拉格朗日也不再认为变分原理是独立的。热力学第二定律并不能归结到第一定律或力学原理上面去，然而在逻辑上却同这些原理密不可分。现在已逐渐形成的时间空间理论就是同相对性概念，守恒概念和不可逆概念联系在一起的。

绝对和相对的关系，是辩证的统一。没有绝对，就没有相对；没有相对，也就无所谓绝对。绝对存在于相对之中，并通过无数相对来体现；在相对中有绝对，离开绝对的相对是没有的。绝对和相对的区别既是绝对的，又是相对的，二者是相互渗透的，在一定条件下相互转化。【1】

黑格尔说：“无论这命题是如何的真，但它是否意味这它所包含的真理，却是有疑问的，因此至少这个命题的表达方式是不完美的。因为我们不能明确决定它所意味的是抽象的知性同一，亦即与本质的其他规定相对立的同一，还是本身具体的同一。而具体的同一，我们将会看到，最初[在本质阶段]是真正的根据，然后在较高的真理里[在概念阶段]，即是概念。——况且绝对一词除了常指抽象而言外，没有别的意思。譬如绝对空间、绝对时间，其实不过指抽象空间、抽象时间罢了。”【6】绝对空间和绝对时间，无非是抽象空间和抽象时间而已，换言之，与客观事物存在形式完全一致的“空间尺度”就是该客观事物的“绝对空间”，与客观事物运动过程完全一致的“时间尺度”就是该客观事物的“绝对时间”。正如黑格尔所说：“如果我们将同一与绝对联系起来，将绝对作为一个命题的主词，我们就得到：‘绝对是自身同一之物’这一命题”。也就是说，只要一种描述能够与自在之物完全一致，也就真正体现了这种描述本身的**绝对意义**。当然，这是从“形式逻辑”的意义上来说的。如果从“辩证逻辑”的意义上来看，则如同黑格尔所说：“无论这命题是如何的真，但它是否意味这它所包含的真理，却是有疑问的，因此至少这个命题的表达方式是不完美的。因为我们不能明确决定它所意味的是抽象的知性同一，亦即与本质的其他规定相对立的同一，还是本身具体的同一。而具体的同一，我们将会看到，最初[在本质阶段]是真正的根据，然后在较高的真理里[在概念阶段]，即是概念。——况且绝对一词除了常指抽象而言外，没有别的意思。譬如绝对空间、绝对时间，其实不过指抽象空间、抽象时间罢了。”【4】”。

物理学家普朗克曾说过，“一项重要的科学发明创造，很少是逐渐地争取和转变它的对手而获得成功的，扫罗变成保罗的事是罕见的。而一般的情况是，对手们逐渐死去，成长中的一代从一开始就熟悉这种观念。”【2】相对绝对论应当是唯物辩证法的一条基本原理，毛泽东讲：“相对绝对的道理，是关于矛盾问题的精髓”。相对与绝对是指世界上一切事物都具有相对与绝对两种不同的属性，笔者认为它们之间的关系可以用量子力学的**互补原理**（或者中国古典哲学中**阴阳太极图**）来

表述——彼此互补的两种事物，不可能用任何方式把它们结合成一个无矛盾的统一体（统一图景），只有这些现象的总体才能将关于客体的可能性包罗尽。光的波粒二象性正是这一问题的表现形式之一。正如 Bohr 所讲的：“在伟大的戏剧存在中，我们既是观众又是演员。”“原子客体和测量仪器之间的相互作用，构成原子现象中一个不可分割的整体。”从超对称到超引力，从量子理论到 M——理论，从全息论到对偶论，把 Einstein 的广义相对论和费因曼的多重历史思想结合成能描述发生在宇宙中的一切完备的统一理论，都说明了相对绝对论的正确。“当我们终于知道物理学的最终定律时，我们一定会感到意外，为什么它们一开始不是那么明显呢？假如是这样，我们要探索的就是：寻求一组简单的物理原理，它们可能具有最必然的意味，而且我们所知有关物理学的所有一切，原则上都可以从这些原理推导出来” 【5】

参考文献：

- 邢贲思 主编.《哲学小百科》 中国青年出版社 1984 年 10 月
转引自方励之《哲学是物理学的工具》长沙：湖南科学技术出版社，1988 年版，第 6 页。
《唯物主义与经验批判主义》，列宁 著，第 359—360 页
《小逻辑》第 247~248 页
理查德·费曼 S·温伯格. 从反粒子到最终定律 [M]. 湖南：湖南科学技术出版. 2003. 5
《小逻辑》第 247~248 页
《物理学与实在》原载《Einstein 文集》中文版第一卷第 341 页

Relative and Absolute Theory

Li Xuesheng

Shandong University, Qingdao, Shandong, China
xiandaiwulixue@21cn.com

Abstract: This article describes the relationship between relative and absolute and the absolute relative theory. [New York Science Journal. 2009;2(2):26-30]. (ISSN: 1554-0200).

Keywords: relative; absolute; theory; physics

1/10/2009

Subsurface Stratigraphic mapping using Geophysics and Its Impact on the Urbanization Development in Arepo Area, Ogun State, Nigeria

Oyedele, K. F. and Bankole, O. O.

Department of Physics (Geophysics Programme)
University of Lagos, Nigeria
kayodeunilag@yahoo.com

Abstract: This article presents the findings of geophysical investigations carried out at Arepo area, Ogun State, Nigeria. The main geophysical methods employed was resistivity sounding, induced polarization and borehole geophysics. The integrated geophysical techniques has demonstrated its ability to be a better approach to resolve the subsurface stratigraphical ambiguities than a single geophysical technique. The method was suitable to distinguish between sand and clay beds in a complex geologic zone. Based on the thickness of sand layer, the area investigated can probably support low to giant engineering structures. [New York Science Journal. 2009;2(2):31-45] (ISSN: 1554-0200).

Keywords: Stratigraphic mapping, lithologic beds, geoelectric sections, resistivity sounding

1. Introduction

Ogun State has witnessed an upsurge in infrastructural development and increased in human population in recent years particularly in those areas that shear borders with Lagos State. The study Area, Arepo falls within this category (Fig.1). On the basis of increasing economic activities and booming construction works coupled with the incidence of collapsed building structures in the country, this investigation was carried out to provide detailed information on the characteristics of the subsurface lithology and ground conditions prior to the commencement of construction works. Since nearly every civil engineering structures – building, bridge, highway, tunnel, wall, tower, canal, and dam – must be founded in or on the surface of the earth (Lambe and Whitman, (1979), it is expedient that detailed information on the strength and the fitness of the host earth materials must be ascertained via pre-construction investigation of the subsurface at the proposed site.

In a simplistic sense, drilled core can be used to map subsurface materials. However, geophysics can provide some of the required information to delineate those materials in subsurface space. Geophysical tools that are routinely used to image the subsurface of the earth in support of mining related geotechnical investigations, include Seismic methods, ground penetrating radar (GPR), Electrical resistivity (ER), Electromagnetic (EM), Induced polarization (IP) and Magnetic method (M) (Gowd 2004, Ward, 1990 and Neil and Ahmed, 2006). This survey, which could be carried out for less than the cost of a single cored drill hole, provides critical insight into the complex subsurface architecture and stratigraphic relationships of buried units (Susan, 2000). To this end, intergrated geographical techniques-via electrical resistivity induced polarization and borehole geophysics have been employed to delineate subsurface stratigraphic relationship or variation of Earth materials of Arepo, area Ogun state, Nigeria as an aid to civil engineer in charge of construction works.

2. Geology and Hydro geology

The geology of the area (fig.1) can be described broadly as a sedimentary basin, which thickens from north to south (down dip) and from East to West. The project area is underlain by the littoral and lagoon deposits of recent sediments. The coastal belt vary in width from about 8km near the republic of Benin boarder to about 24m toward the eastern end of Lagos lagoon (Jones and Hockey, 1964). The recent sediment can be divided into littoral and lagoon sediments of the

coastal belt and the alluvial sediments of the major river. The sediments consist of unconsolidated sands, clay and mud with a varying proportion of vegetation matter, along the coastal area while the alluvial deposits consist of coarse, clayey, unsorted sands with clay lenses and occasional beds. Hydro-geologically, Kampsax and Kruger (1987) subdivided the aquifer in the coastal terrain of Lagos and Ogun into four with the first aquifer representing the recent sediments and the second and third aquifers being within the coastal plain sands. The water table aquifer occurs in recent sediments along the coast and within alluvial plains of the river valleys. However the water table is shallow with results of chemical analysis of the water from recent sediments showing higher TDS and conductivity than water from the coastal plain sands aquifer (Oyedele, 2006).

3. Equipment and Field Procedure

Electrical resistivity and Induced polarization measurements were carried out using ABEM terrameter SAS 1000 system. This equipment is reliable and provides adequate spatial resolution and target definition. The data were acquired using the vertical electrical sounding method (VES). A total of thirteen (13) VES were carried out using the Schlumberger array with a maximum current electrode separation AB/2 of 120m. The essential idea behind the VES is that it assumes conductivity variation with depth only, such that as the distance between the current and potential electrode is increased, the current filament passing across the potential electrode carried a current fraction that has returned to the surface after reaching increasingly deeper depth (Telford *et al.*, 1976). To ensure that geophysical results can be interpreted in a way that is clear and meaningful to all project participants drilled borehole logs were used to correlate with the geophysical data (Fig. 3a to 3c).

4. Data Processing and Presentation

To minimize erroneous interpretation due to human error, the WinGlink software was utilized for the processing of the acquired data. The processed data were presented in the forms of 1-D models resistivity curves, geoelectric sections and maps.

5. Results and Discussion

1-D Models Resistivity Curves

The apparent resistivity values were plotted against the electrode separation (AB/2) in meter on a computer based log-log graph using the WinGlink software for a computer iterated interpretation. These iterations were presented as 1-D iteration models. Figure 2 shows the representative samples of these curves. Visual examination of the 1-D model curves shows a typical 4-layered case. This consists of topsoil (clayey sand), fine sand/medium sand, clay and coarse sand. Table 1 shows the detailed interpreted resistivity measurements of the subsurface sediments.

Geoelectric Sections

The geoelectric sections of the various VES stations in the study area were created to indicate the various geoelectric layers within the subsurface with their characteristic resistivity values and probable geologic connotations (Fig.3a to 3d).

The geoelectric section across A to A¹ is made up of data from VES 1, 2, 5, 7 and 8 correlated with drilled hole (D2) (Fig. 3a). The top geoelectric layer has resistivity values ranging from 74 to 118Ωm with a thickness that varies from 1.56 to 4.11m and is composed of predominantly clayey sand. The second geoelectric layer has resistivity values that vary from 96 to 265Ωm and thickness values that range from 7.64 to 19.87m. It is predominantly fine sand. The third geoelectric layer has resistivity values that vary from 34.7 to 62.5Ωm and thickness values of 19.3 to 25.6m and consists of clay. The fourth layer has resistivity values that vary from 318 to 403.6Ωm and with no thickness values because the current terminated in this zone.

The geoelectric section across B to B¹ is made up of data from VES 5, 6 and 10 (Fig. 3b). The first geoelectric layer has resistivity values that vary from 29.4 to 118.0Ωm and thickness values that range from 1.1 to 3.5m and is made up of clayey sand with decomposed organic and inorganic materials. The second geoelectric layer consists of fine sand with resistivity values that vary from 150 to 188Ωm and thickness values that vary from 11.5 to 14.3m. The third layer has resistivity values that vary from 26.3 to 152.3Ωm and thickness values that range from 17.3 to 21.8. This layer is predominantly clay. The last layer is made up of coarse sand with resistivity values that vary from 23.4 to 463.9Ωm with no thickness.

The geoelectric section across C to C¹ is made up of data from VES 7, 6, 11, 12 and 13. The first geoelectric layer is made up of clayey sand with resistivity values that vary from 32 to 118Ωm and thickness values that range from 0.7 to 3.5m. The second layer is made up of fine to medium sand and consists of resistivity values that range from 96.0 to 104.6Ωm and thickness of 1.7 to 6.4m. The third layer has resistivity value that vary from 26.3 to 202.0Ωm and thickness that range from 16.2 to 25.6m. The lithology is predominantly clay. The fourth layer is made up of coarse sand with resistivity values that vary from 26.4 to 464.0Ωm.

Across D to D¹ the geoelectric section is made up of VES 2,4,6 and 9. The first layer is composed of clayey sand with resistivity values that vary from 76 to 118Ωm and thickness values that range from 1.5 to 3.5m. The second layer has resistivity values that vary from 171 to 188.6Ωm and thickness values that vary from 2.5 to 19.5m. This is indicative of fine to medium sand. The third layer has resistivity values that vary from 26.3 to 44.6Ωm and thickness between 6.3 to 32.5m, which is indicative of clay material. The fourth layer has resistivity values that range from 292.2 to 540Ωm and consists of coarse sand.

Contoured Maps

Several maps were produced using SURFFER program to monitor the trend of lithological variations with a view to assessing the subsurface stratigraphic stratum suitable for low, medium and giant engineering structures.

Figure 4 shows the isopach map of thickness of sand layers that vary from 2 to over 18m. Based on the sand thickness, the northern, western southern and south-eastern sections of the area can probably support giant engineering structures while the north-eastern section show an indication of low to medium structures. The depth to sand layers range from 1.1 to 55.0m.

Figure 5 shows the isopach map of depth of clay layers. The depth to clay layers vary from 4 to over 24m. Both the northwestern and southeastern portions of the area investigated have depth to clay layers that range from 9 to over 24m. On the other hand, the northeastern portion has depth to clay layers that vary from 4 to 14m. Figure 6 shows the isopach map of thickness of clay layers and it varies from 6 to over 30m. Over ninety five percent (95%) of the area have thickness values that vary from 12 to over 30m with the exception of VES 9 that has clay thickness value of about 10.2m (Table 1).

The depth to groundwater table (GWT) in the area vary from 0.5 to over 8.5m (Fig.7). With the exception of VES 9, the depth to GWT at all the VES stations range from 2.5 to over 8.5m.

Figures 8,9,10,11 and 12 shows iso-resistivity depth-slice maps at 3m, 7m, 10m, 15m and 25m respectively. With the exception of iso-resistivity depth-slice map at 25m (Fig.2), in which the resistivity values vary from 200 to over 230Ωm, all the other iso-resistivity depth-slice maps have resistivity values that vary from 20 to over 230Ωm (Figs. 8 to 11).

6. Implication of Study Area on Engineering Structures

The results of the geophysical investigation carried out shows that the study area can accommodate probably low to high engineering structures based on the inferred thickness of the sand layers. In the northeastern portion however, low to medium structures are feasible except extensive pilling is done. This is because the sand layer in that area is thin (2.5 to 7.6m) and it is underlain by clay. Beneath all the VES stations, with the exception of VES 8 and 9, the thickness of the sand body ranges from 10.9 to 19.9m with resistivity values ranging from 109.6 – 118.0Ωm. These areas can probably support giant engineering structures.

However, it is important to note that underneath this sand layer is a thick clay body beneath all the VES stations. To ensure the safety of giant engineering structures in the area, adequate pilling is recommended.

7. Conclusion

The subsurface geotechnical investigation using the combination of electrical resistivity, induced polarization and borehole geophysics at Arepo area, Ogun State, Nigeria revealed that the stratigraphy consists basically of four layers which are representative of top soil (clayey sand), fine to medium sand, clay and coarse sand. Based on the qualitative and quantitative interpretation of VES data alongside with borehole data, it is deduced that low to high engineering structures are feasible. However, for massive constructions, structural foundation via pilling is recommended at depth not less than 32m because of the clay beds that directly underlain the sand bodies.

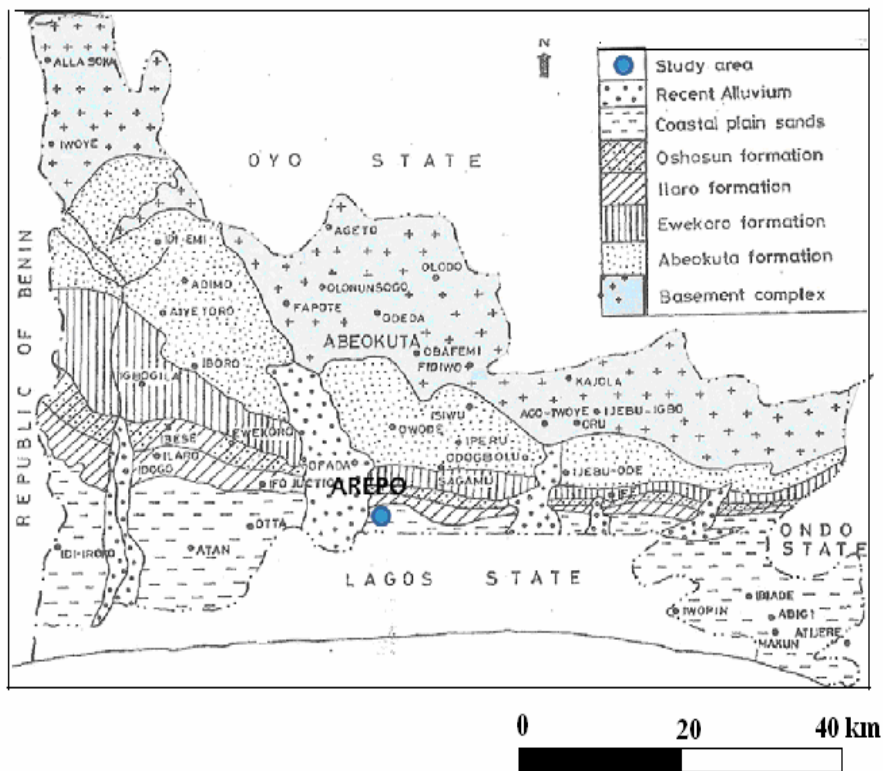


Fig 1: Geological map of Ogun State showing the study area.

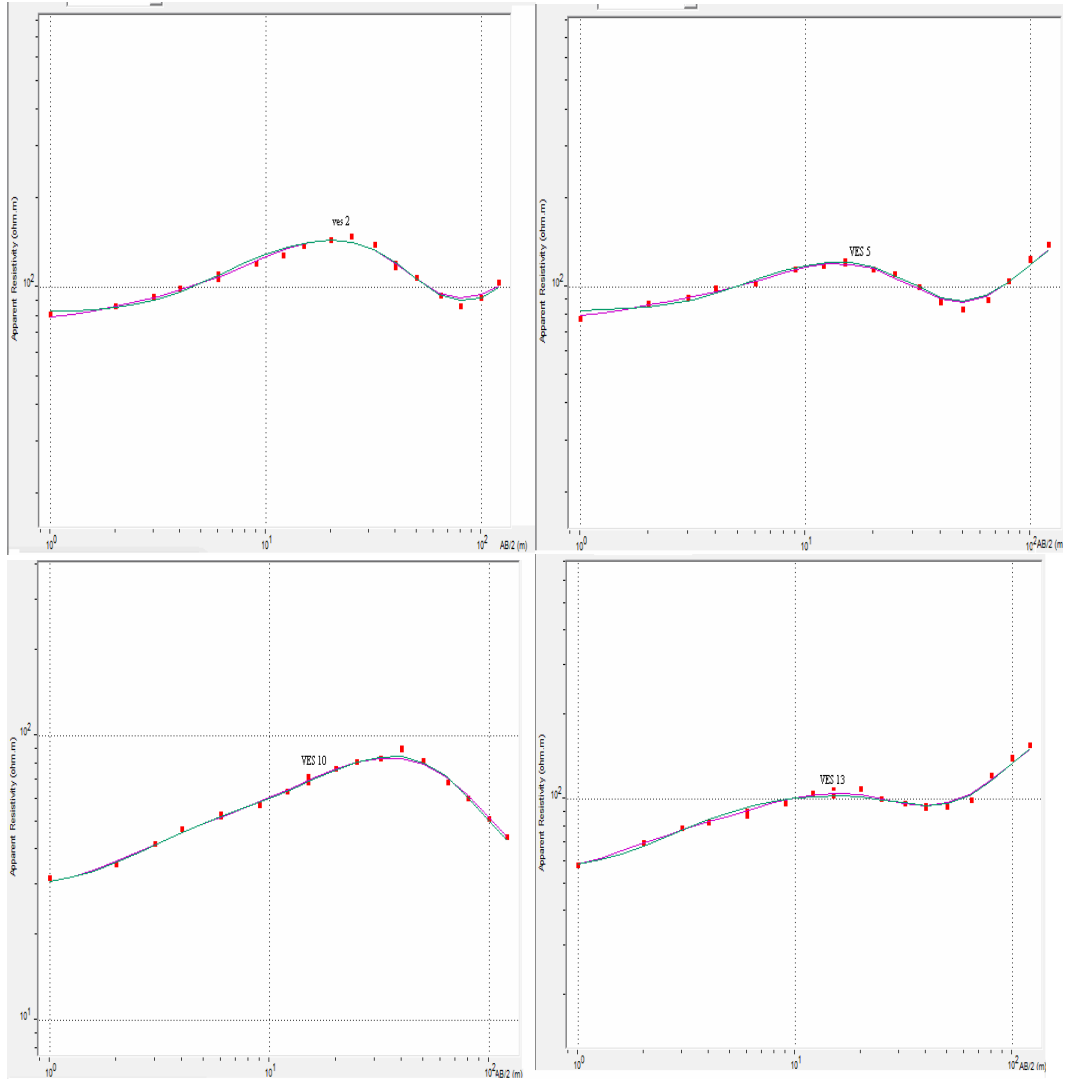


Fig 2: Representative sample of 1D model resistivity curves.

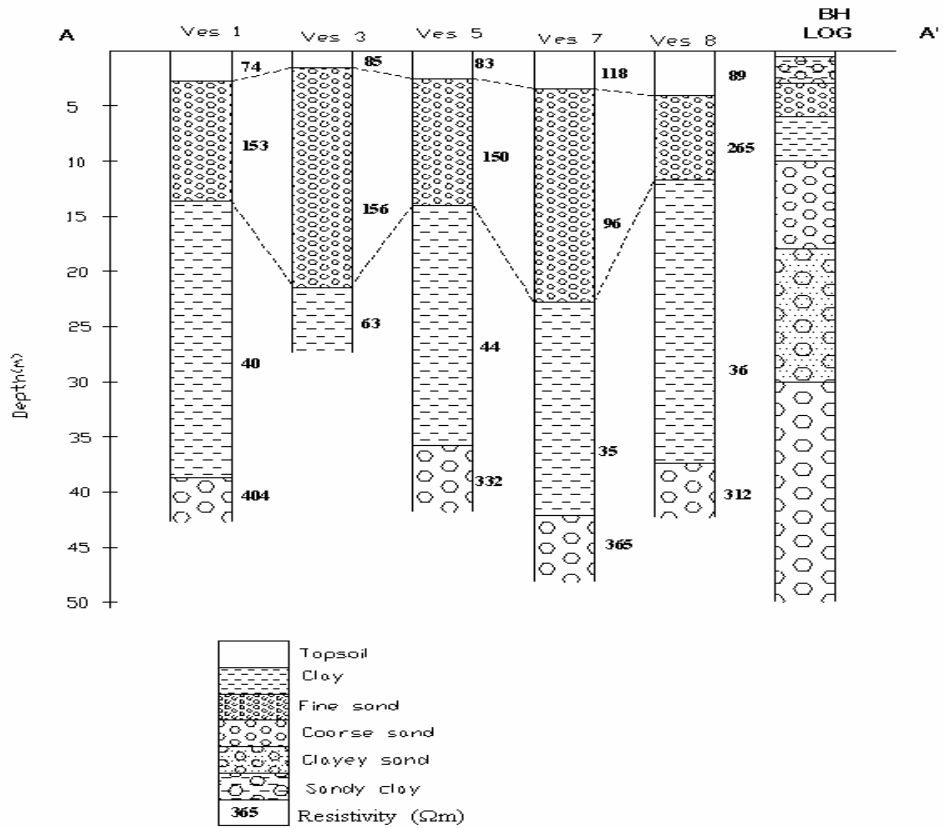


Fig 3a: Geoelectric section across A to A' beneath VES 1, 3, 5, 7 & 8 correlated with available borehole log.

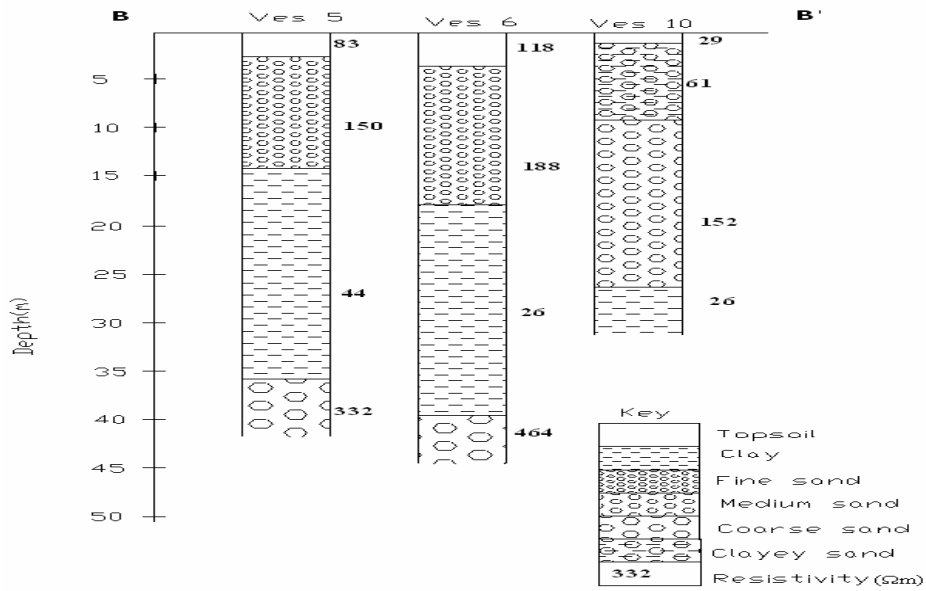


Fig 3b: Geoelectric section across B to B' beneath VES 5, 6 and 10.

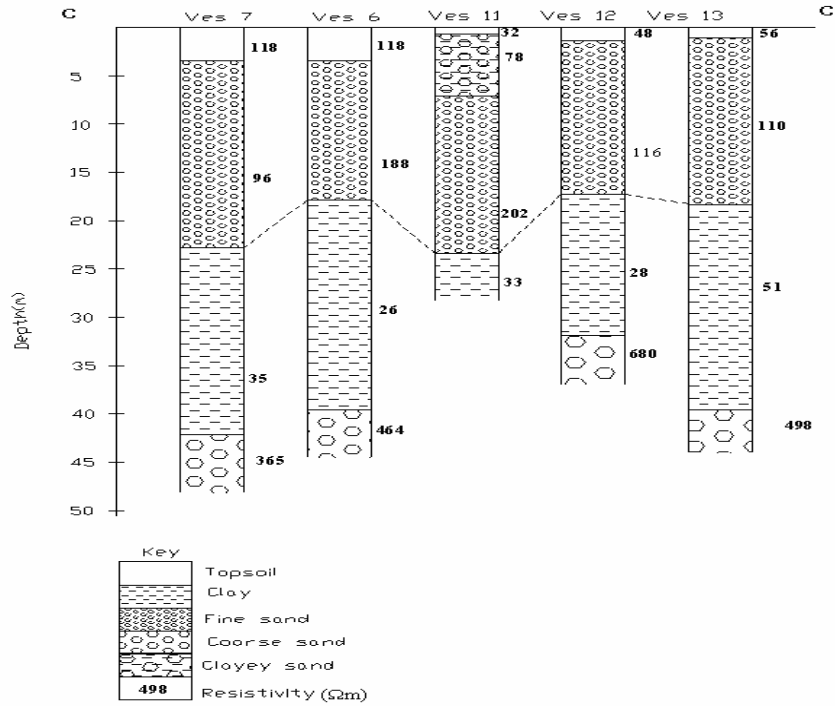


Fig 3c: Geoelectric section across C to C' beneath VES 7, 6, 11, 12 and 13

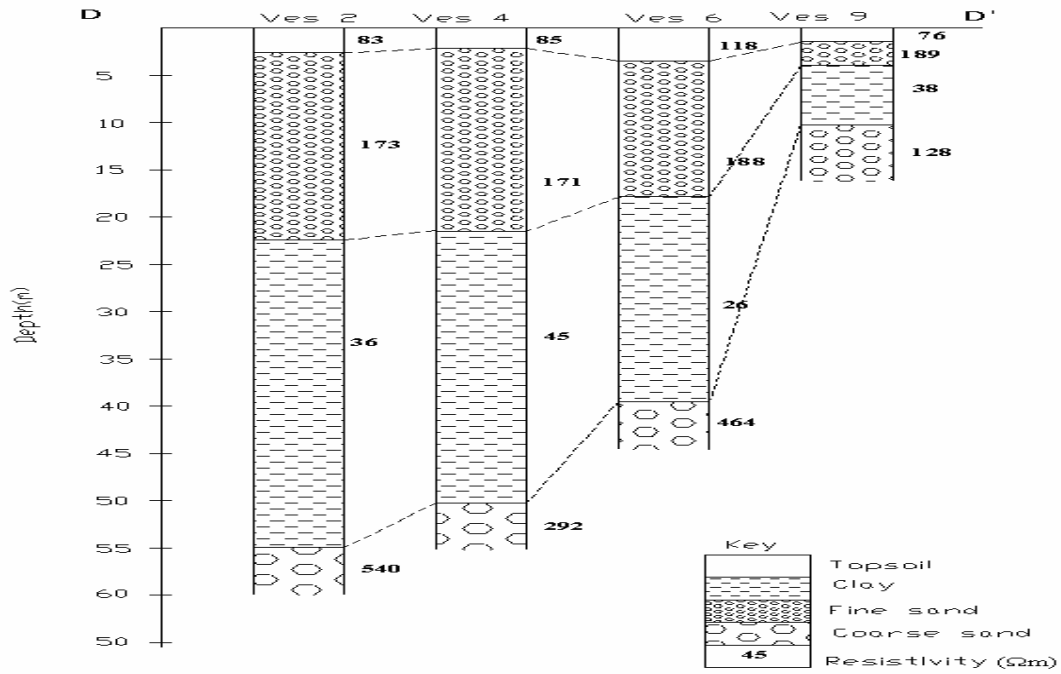


Fig 3d: Geoelectric section across D to D' beneath VES 2, 4, 6 and 9.

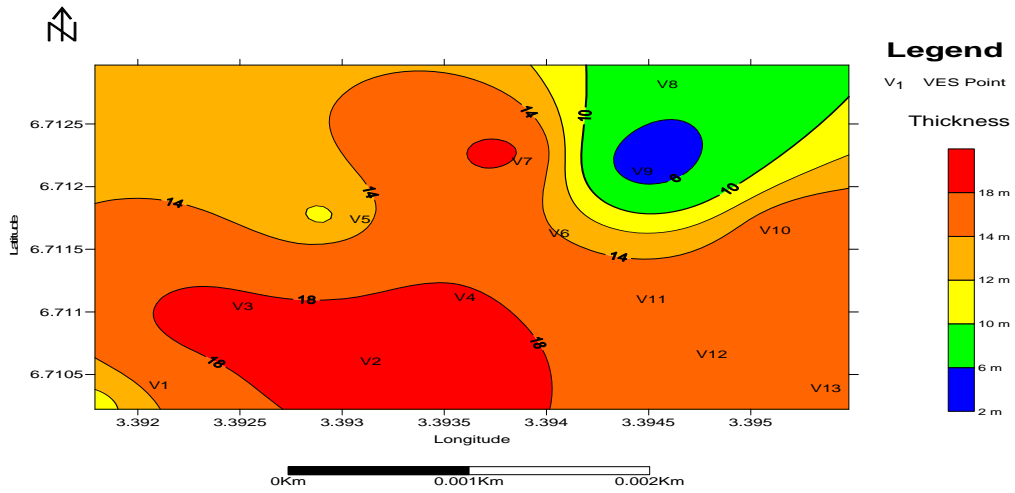


Fig 4: Isopach map of sand layers.

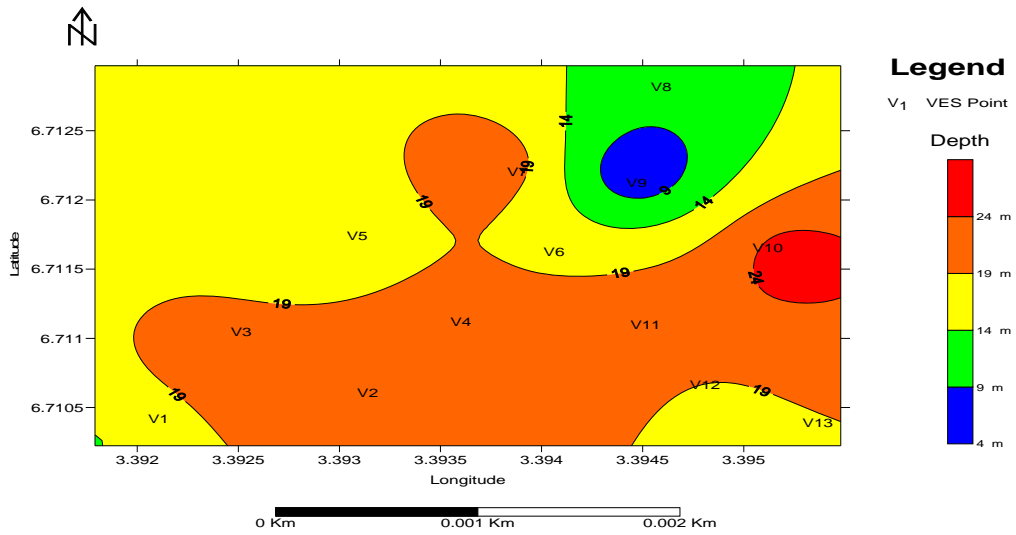


Fig 5: Isopach map of depth to clay layers.

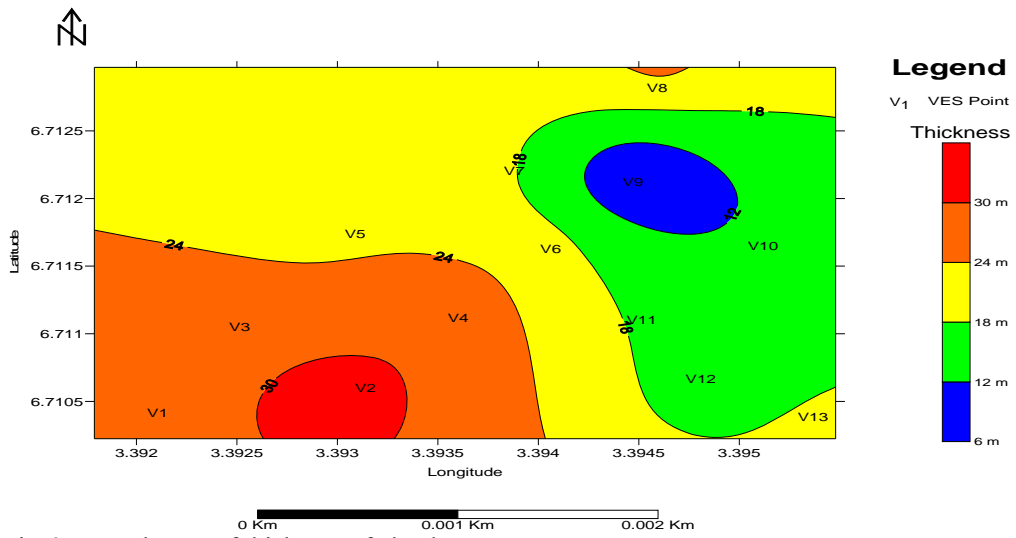


Fig 6: Isopach map of thickness of clay layers.

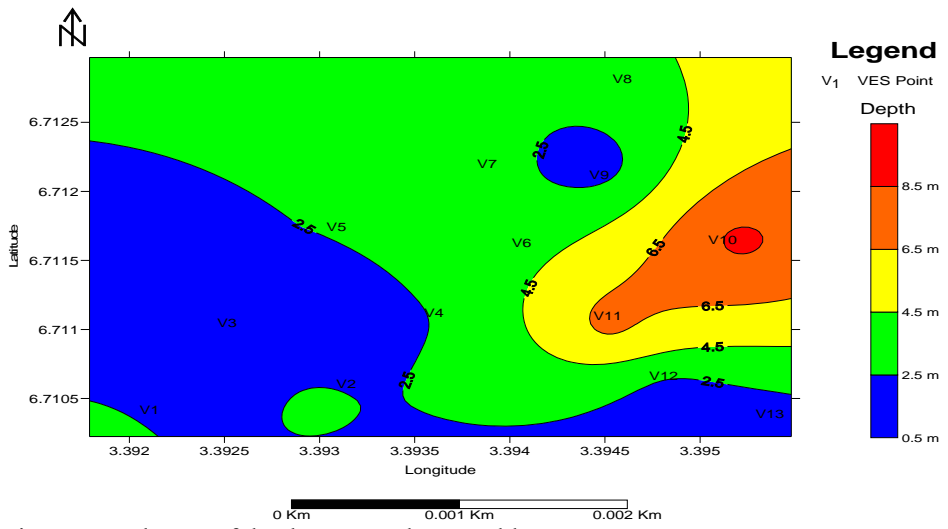


Fig 7: Isopach map of depth to groundwater table.

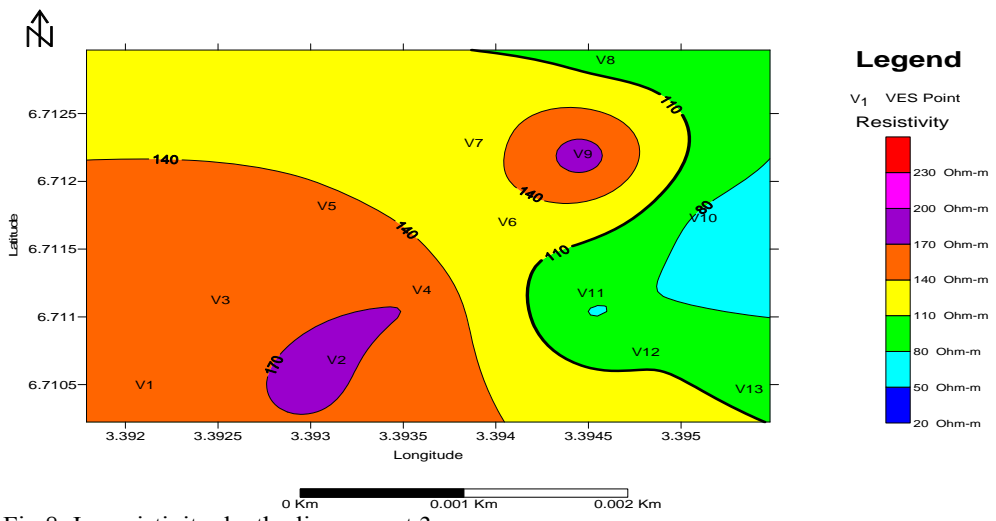


Fig 8: Isoresistivity depth-slice map at 3m.

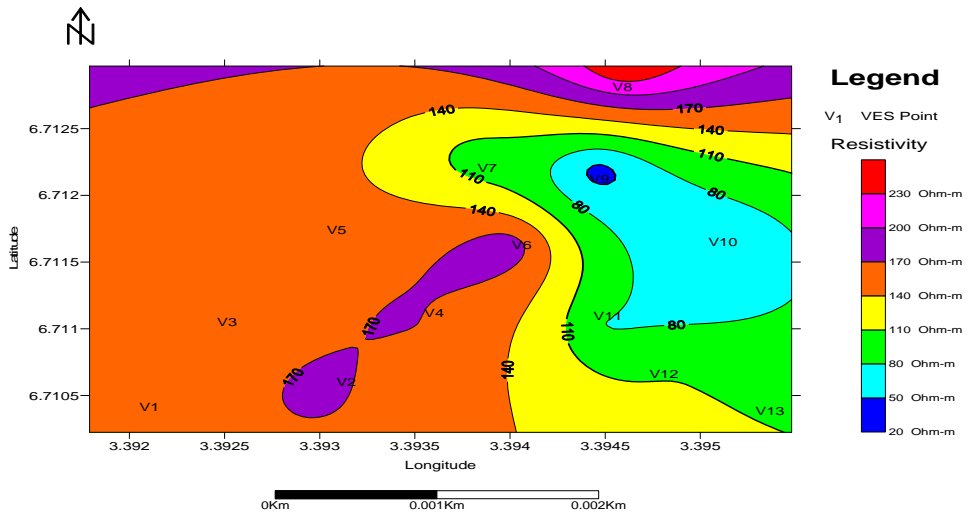


Fig 9: Isoresistivity depth-slice map at 7m.

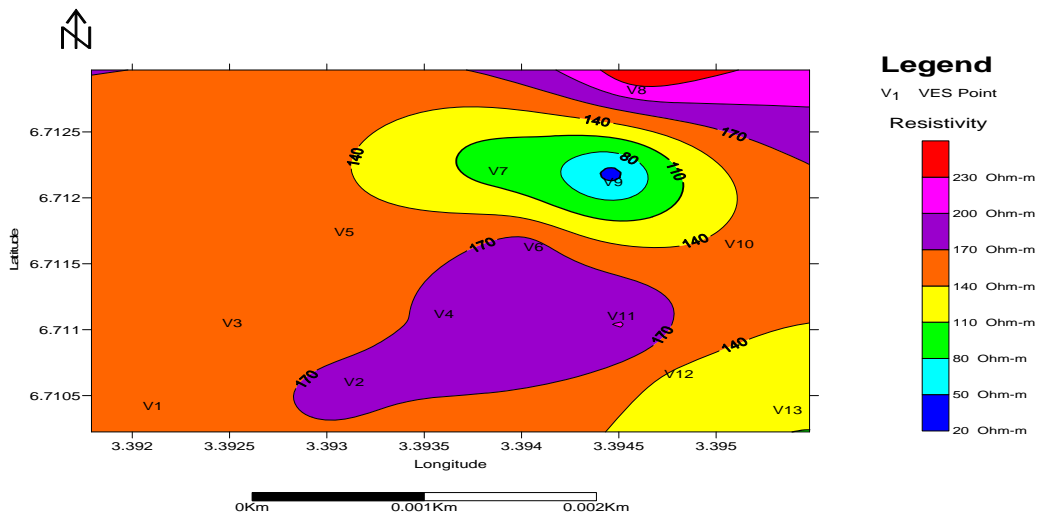


Fig 10: Isoresistivity depth-slice map at 10 m.

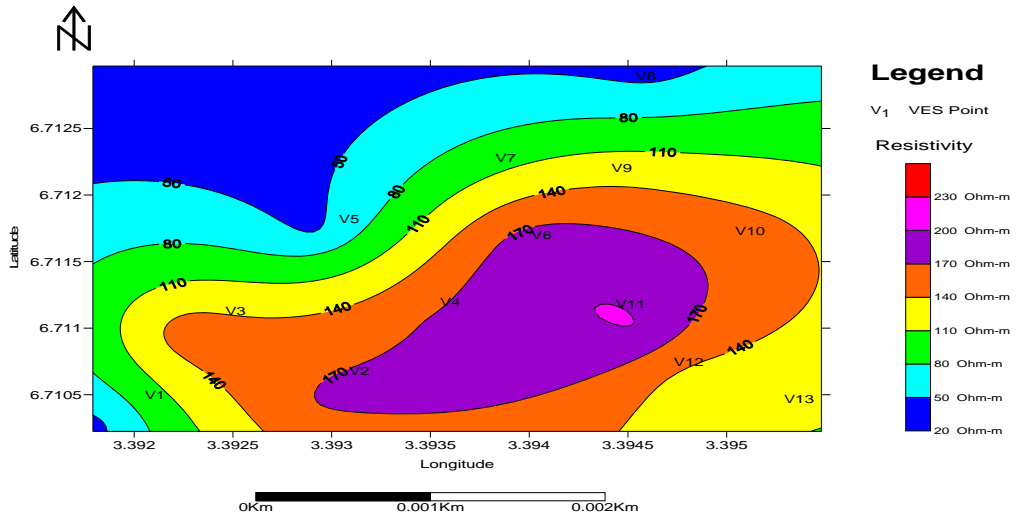


Fig 11: Isoresistivity depth-slice map at 15 m.

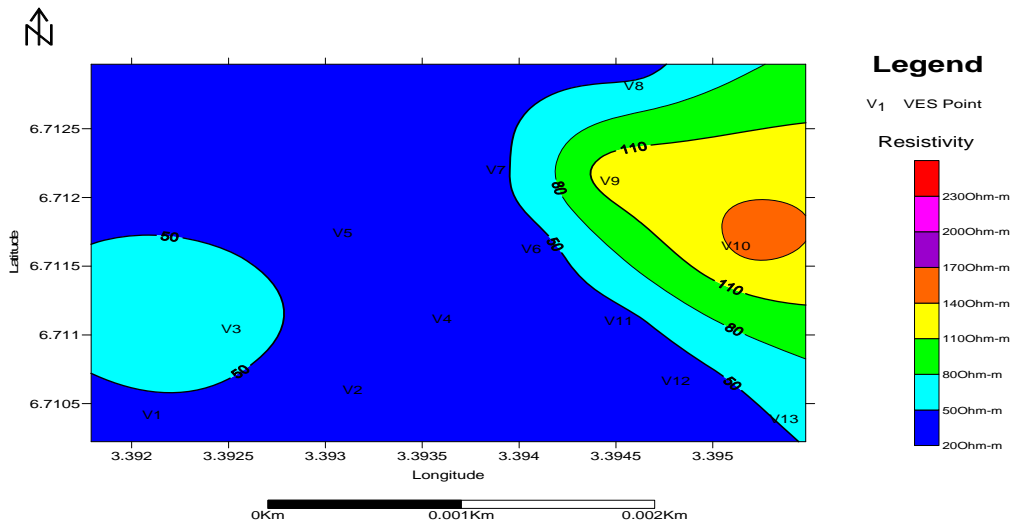


Fig 12: Isoresistivity depth-slice map at 25 m.

Table 1: Interpreted resistivity measurements.

| VES Station | Layer | Resistivity (Ωm) | Thickness (m) | Depth (m) | Lithology |
|-------------|-------|----------------------------------|---------------|-----------|-----------------------|
| 1 | 1 | 73.54 | 2.78 | 2.78 | Topsoil (clayey sand) |
| | 2 | 153.07 | 10.86 | 13.64 | Fine sand |
| | 3 | 39.68 | 25.06 | 38.7 | Clay |
| | 4 | 403.58 | - | | Coarse Sand |
| 2 | 1 | 83.17 | 2.63 | 2.63 | Topsoil (clayey sand) |
| | 2 | 173.29 | 19.83 | 22.46 | Fine sand |
| | 3 | 36.06 | 32.49 | 54.95 | Clay |
| | 4 | 539.92 | - | - | Coarse Sand |
| 3 | 1 | 85.13 | 1.56 | 1.56 | Topsoil (clayey sand) |
| | 2 | 155.95 | 19.87 | 21.43 | Fine sand |
| | 3 | 62.54 | - | - | Clay |
| 4 | 1 | 84.81 | 2.19 | 2.19 | Topsoil (clayey sand) |
| | 2 | 170.98 | 19.31 | 21.5 | Fine sand |
| | 3 | 44.6 | 28.73 | 50.23 | Clay |
| | 4 | 292.17 | - | - | Coarse Sand |
| 5 | 1 | 83.17 | 2.51 | 2.51 | Topsoil (clayey sand) |
| | 2 | 149.72 | 11.5 | 14.01 | Fine sand |
| | 3 | 43.82 | 21.79 | 35.8 | Clay |
| | 4 | 332.29 | - | - | Coarse Sand |
| 6 | 1 | 118.42 | 3.5 | 3.5 | Topsoil (clayey sand) |
| | 2 | 187.98 | 14.33 | 17.83 | Fine sand |
| | 3 | 26.34 | 21.71 | 39.54 | Clay |
| | 4 | 463.93 | - | - | Coarse Sand |
| 7 | 1 | 118.22 | 3.45 | 3.45 | Topsoil (clayey sand) |
| | 2 | 95.92 | 19.37 | 22.82 | Fine sand |
| | 3 | 34.73 | 19.29 | 42.11 | Clay |
| | 4 | 364.82 | - | - | Coarse Sand |
| 8 | 1 | 89 | 4.11 | 4.11 | Topsoil (clayey sand) |
| | 2 | 265.24 | 7.64 | 11.75 | Fine sand |
| | 3 | 35.9 | 25.59 | 37.34 | Clay |
| | 4 | 311.76 | - | - | Coarse Sand |

| | | | | | |
|----|---|--------|-------|-------|-----------------------|
| 9 | 1 | 76.42 | 1.45 | 1.45 | Topsoil (clayey sand) |
| | 2 | 188.58 | 2.53 | 3.98 | Fine sand |
| | 3 | 38.24 | 6.26 | 10.24 | Clay |
| | 4 | 127.53 | - | - | Medium Sand |
| 10 | 1 | 29.43 | 1.14 | 1.14 | Topsoil (clayey sand) |
| | 2 | 61.42 | 7.88 | 9.02 | clayey sand |
| | 3 | 152.25 | 17.27 | 26.29 | Medium sand |
| | 4 | 26.36 | - | - | Clay |
| 11 | 1 | 31.72 | 0.68 | 0.68 | Topsoil (clayey sand) |
| | 2 | 78.05 | 6.44 | 7.12 | Clayey sand |
| | 3 | 201.97 | 16.22 | 23.34 | Fine sand |
| | 4 | 32.87 | - | - | Clay |
| 12 | 1 | 48.29 | 1.4 | 1.4 | Topsoil (clayey sand) |
| | 2 | 115.97 | 15.86 | 17.26 | Fine sand |
| | 3 | 28.31 | 14.59 | 31.85 | Clay |
| | 4 | 679.81 | - | - | Coarse Sand |
| 13 | 1 | 55.98 | 1.09 | 1.09 | Topsoil (clayey sand) |
| | 2 | 109.57 | 17.3 | 18.39 | Fine sand |
| | 3 | 51.23 | 21.18 | 39.57 | Clay |
| | 4 | 497.55 | - | - | Coarse Sand |

Correspondence to:

Oyedele, K. F. and Bankole, O. O.

Department of Physics (Geophysics Programme)

University of Lagos, Nigeria

kayodeunilag@yahoo.com

References

- Gowd, S.S. (2004). Electrical resistivity surveys to delineate groundwater potential aquifers in Peddavanka watershed, Ananatapur District, Andhra Pradesh, India. *Jour. of Environmental Geology*. Vol. 46, 118 – 131pp.
- Kampsax, K. and Sshued, P.(1987).Hydrogeology of Lagos metropolis, A report submitted to the Ministry of works and Housing. Open File Records. 205pp.
- Jones, A.A. and Hockey, R.A. (1964).The geology of part of Southern Nigeria. *Geol.Survey, Nigeria. Bull.* **31**,101pp.
- Neil, A. and Ahmed,I. (2006).A generalized protocol for selecting appropriate geophysical techniques. *Dept.of Geol. and Geophys.University of Missouri-Rolla, Rolla, Missouri*, 19pp.

- Lambe, W. T. and Whitman, V. R. (1979). Soil Mechanics, S.I.Version. John Wiley and Sons. 530pp.
- Susan, E.P. (2004). The role of geophysics in 3-D mapping. Geol. Survey. Canada. ON, KIA 0E8, Canada 61-65pp.
- Oyedele, K. F.(2006). Geoelectric mapping of saline water intrusion into the coastal aquifers of Lagos, Nigeria (Ph.D Thesis), 102pp.
- Telford, W. M., Geldart, L. P. and Sheriff, R.E .(1990). Applied geophysics. Cambridge University Press.
- Ward, S. P. (1990). Resistivity and induced polarization method. In Ward, S. P. (edition). Geotechnical and Environmental Geophysics vol. 1. Investigation in Geophysics, No.5. SEG; Tulsa Oklahoma.

12/3/2008

论核场

陈果仁

湖南省邵阳市新产品开发研究所
中国湖南省邵阳市城北路 82 号
电话：0739—2393750
传真：0739—2339801
E-mail: renzichen@yahoo.cn

摘要：质子带正核场，中子带负核场，它们同性相斥、异性相吸。所有原子核都象晶体一样具确定的空间点阵。当核子在核子势阱中振动时，将产生 γ 射线。[New York Science Journal. 2009;2(2):46-50] (ISSN: 1554-0200).

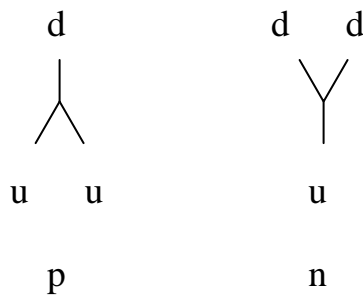
关键词：正负核场、夸克对接、核键、核子势阱、核能。

原子核由质子(p)和中子(n)构成，统称为核子，但是核子模型是什么？质子和中子为什么可以结合在一起？为什么中子数通常大于质子数，且比例不大于 2？放射性元素放射出来的为什么是氦核而不是质子或中子？所有这些问题至今没有一个具说服力的答案。现行教科书上不但说核子相对运动，还说质子和中子以核力或强作用力相互结合，而核力是通过所谓媒介子如 π 介子或胶子

之类来传递的，这些说法也太牵强了。

我们都知道，除了单个的质子或中子外，任何核子都只能由质子和中子共同构成而不能由单一的质子或单一的中子构成，这说明质子和质子或中子和中子相互排斥，即它们同性相斥，由此宇宙中既不可能有质子星，也不可能中子星。质子和中子能够相互结合又说明它们异性相吸。正如电场同性相斥、异性相吸，质子和中子也以同性场相互排斥，以异性场相互吸引，核子的这种场称为核场。如果设质子具正核场，那么中子就具有负核场。核场只在 10^{-15}m 范围内有效，以相同距离计，核场力是电场力 100 多倍。

质子和中子都是成 Y 形的三夸克粒子，质子有两个 u 夸克和一个 d 夸克，中子有一个 u 夸克和两个 d 夸克，如下图：



我们已经知道，u 夸克带 $2/3$ 单位正电场，d 夸克带 $1/3$ 单位负电场，正负电场中和后，质子带 1 单位正电场，中子则显电中性。与此相似，u 夸克带 1 单位正核场，d 夸克带 1 单位负核场，

正负核场中和后，质子带 1 单位正核场，中子带 1 单位负核场。u 夸克和 d 夸克可以结合，虽然一个质子有 2 个 u 夸克和一个 d 夸克，似乎一个质子可以和三个中子相结合，但同时中子同性相斥，故一个质子最多只能和两个中子相结合如 ${}^3\text{H}$ 核，同理一个中子最多只能和两个质子相结合如 ${}^3\text{He}$ 核，这就是为什么在多核子体中，质子数不能超过中子数的 2 倍，中子数不能超过质子数的 2 倍。由于质子带正电，而中子显电中性，质子之间的斥力大于中子之间的斥力，因此多数情况下，多核子体的中子数大于质子数。又由于核场力是电场力的 100 多倍，因此在没有外来压力作用的情况下，原子核中的质子数只能为 100 多个。

核子以 u 夸克和 d 夸克是以对接的方式相互结合的，而对接形成 u-d 键，又称核键，因此核子中的质子和中子是相对静止的，事实上质子和中子相互围绕旋转是不可想象的。正如每种晶体都有其固定的空间点阵，每种核子也都有其固定的空间点阵。和化学键相同，核键也具键长、键角、键强、键力、键势等各种参数。在多核子体中，通常存在着空位的 u 夸克和空位的 d 夸克，因此核子往往既可吸纳质子也可吸纳中子。 ${}^4\text{He}$ 核中的质子和中子都以它们的 u 夸克和对方的 d 夸克相互结合。 ${}^4\text{He}$ 核中没有空位夸克，它一旦在原子核中产生，就会被排出黑枣。 ${}^4\text{He}$ 核是最稳定的核子，

故我们世界中氦含量最大。 ${}^4\text{He}$ 核中的两个质子分别和两个中子相结合，构成一对称的四边形。在核场、电场、磁场等场的作用下，原子核的结构可自动调整，故核子结构有稳定和不稳定之分，放射性元素的放射过程就是多核体自动调整的过程，调整的结果是产生 α 射线即 ${}^4\text{He}$ 核。核子结构调整有快有慢，不同放射性元素有着不同半衰期。核子越大，其内在斥力越大，其结构也就越松散，故人类至今不能任意地制造出超大核子来。

在核键作用范围内，核键的长度是可变的。当 u 夸克和 d 夸克对接时，核键成为核子势阱。当核子发生核聚变、核裂变或核子结构调整时，核子将在核子势阱中产生振动。由于核场是强场，由核场形成的核键是强键，当核子在核子势阱振动时，将产生高频率的电磁波，这就是 γ 射线的产生。我们知道，正反电子湮灭产生 γ 射线， γ 射线可产生电子，当放射性元素产生 γ 射线时，部分 γ 射线产生电子，这就是 β 射线的形成。

质子、中子、电子是构成物质世界的基础，然而基本粒子从何而来？基本粒子及其夸克由什么构成？为什么夸克是禁闭的？为什么核子中的中子是稳定的，而单个中子寿命不到 10 分钟？为什么核子中的质子和中子会发生质量亏损？放射性元素为什么能高速发射 α 射线？何谓场？正负电场、正负核场、S 极和 N 极磁

场都是同性相斥、异性相吸的对称场，万有引力场有对称场吗？原子核中的质子和中子保持距离吗？核外电子绕核旋转吗？怎样解释质子和中子的三夸克形成的三喷注现象？物体表面暗线是什么？光线为什么会发生弯曲和折射？如此等等，请参考作者所著《以太旋子学》。

参考书：普通大学各学科相关教材。

陈果仁E-mail: renzichen@yahuu.cn

nucleus field

Chen Guoren

renzichen@yahoo.cn

Abstract: This article describes the nucleus field. [New York Science Journal. 2009;2(2):46-50] (ISSN: 1554-0200).

Keywords: nucleus; field; physics

An Incidence of Substratum Discolouration in a Tropical West African Lagoon.

Onyema, I.C. and Nwankwo, D.I.
Department of Marine Sciences, University of Lagos, Nigeria.

I.C. ONYEMA Ph.D.

Dept. of Marine Sciences

Faculty of Science

University of Lagos, Akoka.

Lagos, Nigeria.

iconyema@yahoo.com.au, iconyema@gmail.com

+2348023446934, +2348060442323

Abstract: A greenish discolouration of the lagoon floor at the Bayeku area of the Lagos lagoon was observed in January 2006. We report here an investigation of the area between December, 2005 and February, 2006 as part of a larger study. A total of 19 species from 13 genera were reported. *Oscillatoria tenuis* (95,800 trichomes per ml) was implicated as the causative organism for the substratum discolouration. Increased insolation, especially reaching the lagoon floor, low salinity, absence of flood conditions, suitable sediment type (fine – medium sand) and high nutrient ($\text{PO}_4 - \text{P} > 0.24 \text{ mg/L}$; $\text{NO}_3 - \text{N} > 4.40 \text{ mg/L}$) levels possibly encouraged the algal proliferation and subsequent substratum discoloration. It is suggested that improving water quality indices and salinity after January caused the disappearance of the discolouration on the substratum. [New York Science Journal. 2009;2(2):51-60]. (ISSN: 1554-0200).

Keywords: algae, water quality indices, substratum.

INTRODUCTION.

Coastal algal blooms respond to nutrient load from anthropogenic sources (Lee, 1999; Onyema, 2007). South-western Nigeria is endowed with an intricate network of rivers, creeks and lagoons, that serve as conduits transferring highly nutrified waters from hinterland to coastal areas. Bloom conditions have been reported in some of these waters (Nwankwo *et al.*, 2003a; Nwankwo *et al.*, 2008). Blooms of *Microcystis aureginosa*, *M. flos-aquae* and *M. wesenbergii* were reported in the Lagos lagoon (Nwankwo, 1993), Ogun river at Iju (Nwankwo, 1993) causing bluish colouration, anoxia, odour, impacting taste to the water (Nwankwo *et al.*, 2003a) and kuramo lagoon (Nwankwo *et al.*, 2008). Blooms of *Trichodesmium thiebautii* have also been reported off the

Lagos coast (Nwankwo, 1993) during thermocline conditions and more recently a bloom of *Bellerochea malleus* that caused brownish discolouration off the Light house beach, Lagos (Nwankwo *et al.*, 2004) was documented. Blooms of *Anabaena flos-aquae*, *A. spiroides* (cyanobacteria), *Cerataulina bergoni*, *Chaetoceros convolutus*, *Coscinodiscus centralis* (diatoms) and *Ceratium furca*, *C. fusus*, *C. tripos* and *Noctiluca scintillans* (dinoflagellates) are known to induce harmful effects in waters of south-western Nigeria (Nwankwo, 1993; Nwankwo *et al.*, 2003a, b, Onyema, 2008). There is at present a report of substratum discolouration in the Lagos lagoon system (Onyema and Nwankwo, 2006) implicating *Beggiatoa alba* and *Oscillatoria* spp as causative species.

Between December, 2005 and February, 2006, a greenish discolouration of the substratum at Bayeku was observed and thoroughly investigated. We report here the composition of the organisms before, during the bloom period and after the collapse. Water quality indices before, during and after the substratum discolouration were also estimated and investigated. This report is part of a larger study that was already ongoing at the time of the occurrence.

MATERIALS AND METHODS.

Description of study area.

The Lagos lagoon opens into the sea via the Lagos harbour all through the year. The tidal height is low (<1.5m) and the tidal exchange weak. It is shallow (<2m) and connected to the Epe lagoon to the east. The area investigated was (Fig 1) the Bayeku area of the Lagos lagoon (Latitudes 6° 32'N and 6° 31'N and Longitudes 3° 31'E and 3° 32'E). A greenish, slimy covering of suspected algae on the lagoon floor was observed for the very first time in this area. Nutrient rich water is known to flow from eutrophic creeks and creeklets systems in the area. Furthermore, poor sewerage systems are the common state of the rural dwellers of the immediate area. Hence direct dumping of domestic wastes is carried out in the closet water body.

Collection of samples

Water samples for determining water quality characteristics were collected at the site before substratum sample collection. The boat was anchored throughout sample collections. Water samples were collected in 1L plastic bottles with screw cap from 0.5m depth from the water surface. This was labeled and transported to the laboratory for chemical analysis.

Substratum samples (top 5cm) were collected within a 5cm² quadrat carefully placed on the greenish material / lagoon floor. A spatula was gently used underwater to scrape the topmost part. After carefully scooping up the greenish scum, it was gently spooned into a plastic bag while still underwater. Duplicate samples were collected on each occasion. Out of water and in the boat, samples were transferred to 75cl screw capped plastic containers. Samples were fixed with formalin (4% unbuffered) and labeled appropriately on the field before onward transportation to the laboratory. This process was carried out on each sampling occasion.

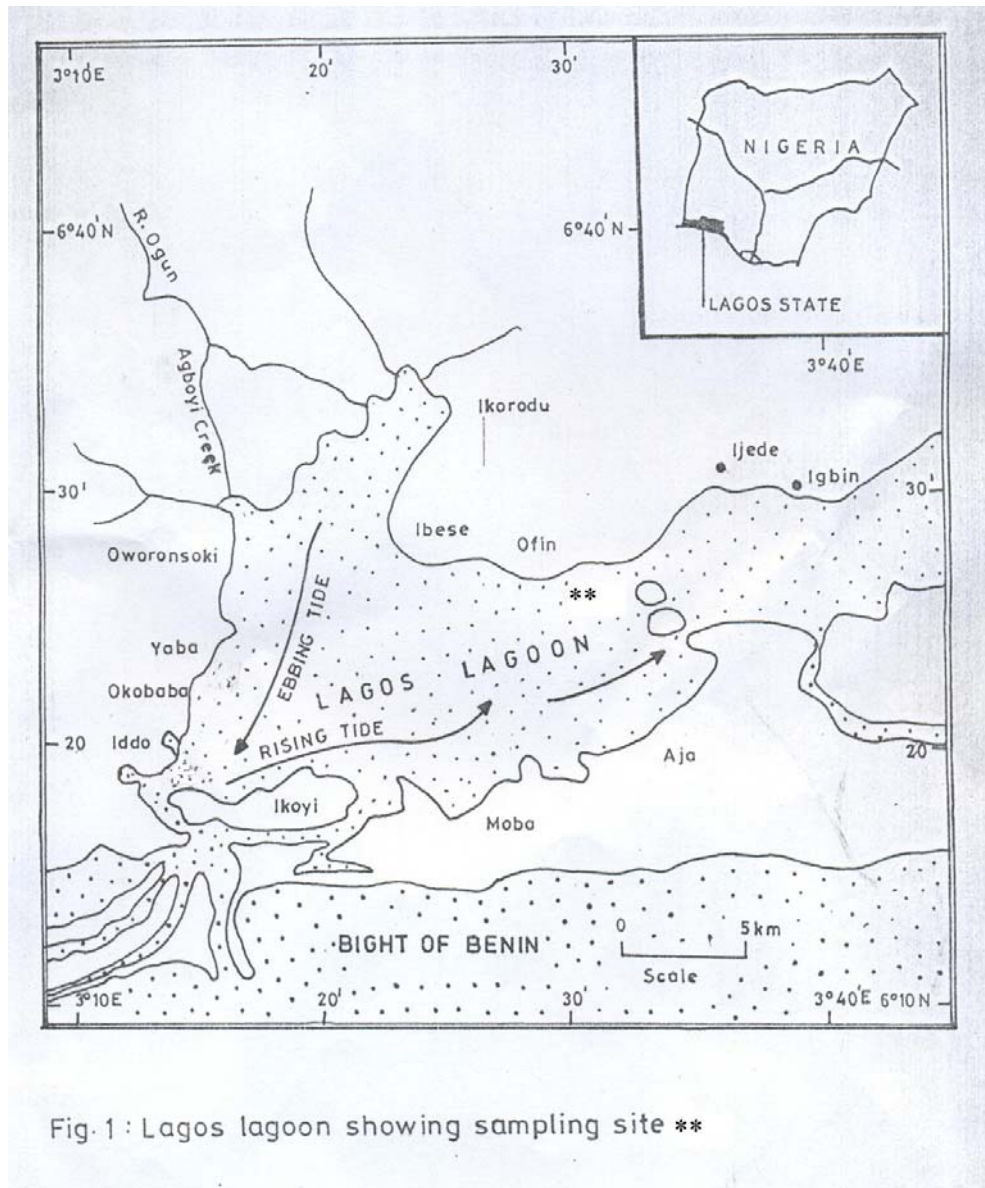


Fig. 1 : Lagos lagoon showing sampling site **

Physico-chemical analysis

Air and surface water temperatures were measured in-situ using a mercury thermometer while water depth was estimated with a calibrated pole. Total dissolved solids was determined by evaporating 100ml aliquot at 105°C and total suspended solids estimated by filtering 100ml of sample through a pre-weighed filter paper, dried to constant weight and reweigh. Conductivity was measured using the HANNA instrument while salinity was determined using the silver-nitrate chromate method. The surface water pH was determined with a Griffin pH meter (Model 80) while dissolved oxygen was measured using a Griffin oxygen meter (Model 40). Biological and chemical oxygen demands were measured using methods described in APHA (1998) for water analysis. Calorimetric methods using a Lovibond Nesslerier were adopted for the direct determination of phosphate-phosphorus and nitrate-nitrogen values while sulphate levels were measured using the gravimetric method. Calcium and magnesium ions were determined using a 400 single channel, low flame photometer. Concentrations of copper, iron and zinc were determined with an atomic absorption spectrophotometer (A.A.S.) Uni cam 99model.

Biological Analyses

In the laboratory, the drop count microscope analysis method described by Onyema (2007) was used to estimate the substratum algal flora. Microscope analysis was carried out on samples within 48hours of collection. Identification materials were used to assist and confirm identification of species (Smith 1950; Hendey, 1958, 1964; Desikachary, 1959; Wimpenny, 1966; Patrick and Reimer, 1966, 1975; Whitford and Schmacher, 1973; Vanlandingham, 1982; Nwankwo, 1990, 2004a; Bettrons and Castrejon, 1999; Siver, 2003; Rosowski, 2003).

RESULTS.

Physico-chemical.

Air (31 - 32 °C) and water (30 - 31 °C) temperatures were high through out the sampling period while the sampling depth was averagely 1.31m. The water remained slightly alkaline throughout the study (7.01 – 7.10). The total dissolved solids (20 - 33 mg/L), salinity (2.30 - 20.60 ‰), chloride content (770.0 – 6930 mg/L), conductivity (2335 – 12,500 µS/cm), acidity (3.0 - 8.8 mg/L), alkalinity (28.5 - 100.3 mg/L), total hardness (562.5 - 4687.0 mg/L), sulphate (6.1 – 60 mg/L) and cation content (Calcium 111- 500, Magnesium 35.6- 859 mg/L) increased as the dry season progressed, while there was a corresponding decrease in total suspended solids (1590 – 8260 mg/L), nitrate (2.5 - 4.8 mg/L), biological (5 - 11mg/L) and chemical oxygen demands (10 – 49 mg/L) and heavy metals levels (Iron 0.14 - 0.35, Zinc 0.003 - 0.006mg/L) (Table 1).

With regard to the algae, just one species each was recorded for December 2005 (*Microcystis aureginosa* Kutzing) and January 2006 (*Oscillatoria tenuis* Agardh), However, 17 species were recorded in February (Table 2). Although, total biomass in terms of cell numbers was high in January (95,800 trichomes per ml) it was for a sole species. This organism (*Oscillatoria tenuis* Agardh) is the implicated microalgae responsible for the greenish discolouration of the lagoon floor at Bayeku. Furthermore, February recorded 3 cyanobacteria, 8 centric diatoms and 6 pennate diatoms species. *Actinophycus splendens* Ralfs and *Biddulphia laevis* Ehrenberg were important diatoms and *Oscillatoria limnosa* Agardh for the cyanobacteria in terms of numbers in February.

Table 1: Monthly variation in water quality characteristics at Bayeku area of the Lagos lagoon (Dec., 2005 – Feb., 2006).

| Physico-chemical parameters | Dec., 2005 | Jan., 2006 | Feb., 2006 |
|---------------------------------|------------|------------|------------|
| Air temperature (°C) | 32 | 31 | 31 |
| Water temperature (°C) | 30 | 31 | 30 |
| Depth (m) | 1.42 | 1.24 | 1.41 |
| Total Suspended Solids (mg/L) | 33 | 27 | 20 |
| Total dissolved Solids (mg/L) | 1590 | 5120 | 8260 |
| Salinity (‰) | 2.30 | 9.20 | 20.60 |
| Chloride (mg/L) | 770.0 | 3086.0 | 6930 |
| Conductivity (µS/cm) | 2335 | 7877 | 12500 |
| pH | 7.05 | 7.01 | 7.10 |
| Acidity (mg/L) | 3.0 | 8.8 | 8.1 |
| Alkalinity (mg/L) | 28.5 | 30.4 | 100.3 |
| Total Hardness (mg/L) | 562.5 | 360.0 | 4687.0 |
| Nitrate- Nitrogen (mg/L) | 4.4 | 4.8 | 2.5 |
| Sulphate (mg/L) | 6.1 | 10.8 | 60 |
| Phosphate- Phosphorus (mg/L) | 0.24 | 0.26 | 0.04 |
| Silica (SiO ₂ mg/L) | 1.9 | 2.6 | 2.1 |
| Dissolved Oxygen (mg/L) | 5.5 | 4.2 | 4.3 |
| Biological Oxygen Demand (mg/L) | 11 | 9 | 5 |
| Chemical Oxygen Demand (mg/L) | 49 | 27 | 10 |
| Calcium (mg/L) | 165 | 111 | 500 |
| Magnesium (mg/L) | 35.6 | 50 | 859 |
| Copper (mg/L) | 0.002 | 0.002 | 0.002 |
| Iron (mg/L) | 0.35 | 0.22 | 0.14 |
| Zinc (mg/L) | 0.005 | 0.006 | 0.003 |

Table 2: Substratum algal composition (before, during and post bloom) at Bayeku (per ml).

| Algal Taxa | Dec., 2005 | (Bloom) Jan., 2006 | Feb., 2006 |
|---|------------|-----------------------|------------|
| Class – Cyanophyceae | | | |
| Order I – Chroococales | | | |
| <i>Microcystis aureginosa</i> Kutzing | 170 | - | - |
| | | | |
| Order II – Hormogonales | | | |
| <i>Lyngbya limnetica</i> Lemm | - | - | 5 |
| <i>Oscillatoria curviceps</i> C.A. Agardh | - | - | 10 |
| <i>Oscillatoria limnosa</i> Agardh | - | - | 60 |
| <i>Oscillatoria tenuis</i> Agardh | - | 95,800 | - |
| | | | |
| Class – Bacillariophyta | | | |
| Order I - Centrales | | | |
| <i>Actinophycus splendens</i> (Sch adbolt) Ralfs | - | - | 205 |
| <i>Biddulphia laevis</i> Ehrenberg | - | - | 125 |
| <i>Coscinodiscus centralis</i> Ehrenberg | - | - | 10 |
| <i>Coscinodiscus eccentricus</i> Ehrenberg | - | - | 10 |
| <i>Coscinodiscus radiatus</i> Ehrenberg | - | - | 5 |
| <i>Cyclotella meneghiniana</i> Kutzing | - | - | 15 |
| <i>Melosira moniliformis</i> (O.F. Muller) Agardh | - | - | 10 |
| <i>Melosira nummuloides</i> Agardh | - | - | 35 |
| | | | |
| Order II – Pennales | | | |
| <i>Cymbella affinis</i> Kutzing | - | - | 15 |
| <i>Navicula mutica</i> Kutzing | - | - | 5 |
| <i>Nitzschia palea</i> (Kutzing) Wm Smith | - | - | 5 |
| <i>Pleurosigma angulatum</i> (Quekett) Wm Smith | - | - | 55 |
| <i>Pleurosigma elongatum</i> Wm Smith | - | - | 15 |
| <i>Synedra crystallina</i> Kutzing | - | - | 20 |
| | | | |
| Number of species (S) | 1 | 1 | 17 |
| Species abundance (N) | 170 | 95,800 | 605 |
| | | | |

DISCUSSION.

The water quality status at the site ranged between low and high brackish water conditions. Low brackish condition (S=2.30‰) was experienced in December while high brackish condition (>9.20‰) reflected the dry months. As the rain ceased, turbidity reduced while transparency increased. Furthermore, insolation increased probably reaching the lagoon floor. This coupled with high nutrient levels ($\text{PO}_3^{2-} > 0.24\text{mg/L}$, $\text{NO}_3^- > 4.4\text{mg/L}$, $\text{SO}_4^{2-} > 6.1\text{mg/L}$), low brackish condition (<9.2‰) and low depth (<1.42m), favorable sediment type (fine – medium sand) and absence of

flood conditions probably encouraged the proliferation of the epipelagic algal population in January. According to Valangdiham (1982), *Oscillatoria tenuis*, the causative cyanobacterium, in the substratum discoloration, is a saprobiont which can exist either as plankton or as an attached form. Palmer (1969) reported that *Oscillatoria tenuis* is the second most tolerant *Oscillatoria* species to organically induced stress. It's important to note that both sole species in December and January are known pollution tolerant cyanobacteria forms for the region (Nwankwo, 2004b). Importantly, the highest level of nitrate (4.8 mg/L) recorded for this study was in January at the time of the greenish occurrence.

Oscillatoria spp are reported in literature to have wide tolerance limits to pH, salts and organically enriched environments (Valangdiham, 1982; Lee, 1999; Nwankwo, 2004b; Onyema, 2008). In Nigeria, Onyema *et al.*, (2003) has reported *Oscillatoria tenuis* in organically polluted parts of Lagos lagoon. Similarly, Chindah and Pudo (1991) have reported *Oscillatoria tenuis* from the Bonny river associated with oil related effluent. According to Valangdiham (1982) *Oscillatoria* species are heavily favoured in organically nutrified waters. The existence of high BOD levels in excess of 9mg/L at this site may be pointer to the probably stressed water quality status. According to Hynes (1960), BOD above 8.0mg/L may indicate severe organic pollution.

The disappearance of the bloom in February may be associated with increased salinity ($\geq 20.6^0/_{00}$) and reduced nutrient load ($PO_4 - P$ 0.04mg/L; NO_3-N = 2.05mg/L). Onyema and Nwankwo (2006) reported a high abundance of epipelagic algal forms in the dry months at some organically polluted sites of an estuarine creek in Lagos.

This investigation highlights the bane of increasing levels of pollutants from anthropogenic sources in the Lagos lagoon and the role of algal indicators in capturing changes in water quality.

Correspondence to:

I.C. ONYEMA Ph.D.

Dept. of Marine Sciences

Faculty of Science

University of Lagos, Akoka.

Lagos, Nigeria.

iconyema@yahoo.com.au, iconyema@gmail.com

+2348023446934, +2348060442323

REFERENCES.

- American Public Health Association. (1998). *Standard Methods for the Examination of Water and Waste Water*. 20th ed. APHA New York. 1270pp.
- Bettrons, D.A.S. and Castrejon, E.S. (1999). Structure of benthic diatom assemblages from a mangrove environment in a Mexican subtropical lagoon. *Biotropica*. **31**(1): 48 – 70.
- Chinda, A.C and Pudo, J. (1991). A preliminary checklist of algae found in plankton of Bonny River in Niger Delta, Nigeria. *Fragm flor. Geobot.***36** (1): 112-126.
- Desikachary, T.V. (1959). *Cyanophyta*. Indian Council of Agric. Research, New Delhi. 686pp.
- Hendey, N.I. (1958). Marine diatoms from West African Ports. *Journal of Royal Microscopic Society*. **77**: 28-88.
- Hendey, N.I. (1964). An introductory account of the smaller algae of British coastal waters. Part 5. Bacillariophyceae (diatoms) London. N.M.S.O. 317pp.
- Hynes, H.B. (1960). The biology of polluted waters. Liverpool University Press, Liverpool, 1-202 pp.
- Lee, R.E. (1999). *Phycology*. Cambridge University Press, New York. 614pp.
- Nwankwo, D.I. (1993). Cyanobacteria bloom species in coastal waters of South-Western Nigeria. *Archiv Hydrobiologie Supplement*. **90**: 553-542.
- Nwankwo, D.I. (1990). Contribution to the Diatom flora of Nigeria. Diatoms of Lagos lagoon and the adjacent sea. *Nigerian Journal of Botany*. **3**: 53-70.
- Nwankwo, D.I. (2004a). *A Practical Guide to the study of algae*. JAS Publishers, Lagos. Nigeria. 84pp.
- Nwankwo, D.I. (2004b). The Microalgae: Our indispensable allies in aquatic monitoring and biodiversity sustainability. University of Lagos Press. Inaugural lecture seris. 44pp.
- Nwankwo, D.I., Onyema, I.C. and Adesalu, T.A.(2003a). A survey of harmful algae in coastal waters of south-western Nigeria. *Journal of Nigerian Environmental Society*. **1**(2). 241 – 246.
- Nwankwo, D.I., Onyema, I.C., Adesalu, T.A., Olabode, R.J., Osiegbu, G.O. and Owoseni, T.I. (2003b). Additions to a Preliminary Checklist of Planktonic Algae in Lagos lagoon, Nigeria. *Journal of Science Technology and Environment*. **3**(1): 8 – 12.

- Nwankwo, D.I., Onyema, I.C., Labiran, C.O., Otuorumo, O.A.; Onadipe, E.I.; Ebulu, M.O. and Emubaiye, N. (2004). Notes on the observations of brown water discolouration off the light house beach, Lagos, Nigeria. *Discovery and Innovation*. **16** (3). 111 – 116.
- Nwankwo, D.I., Owoseni, T.I., Usilo, D.A., Obinyan I., Uche, A.C. and Onyema, I.C. (2008). Hydrochemistry and plankton dynamics of Kuramo lagoon. *Life Science Journal*. **5** (3): 50 – 55.
- Onyema, I.C. (2007). Mudflat microalgae of a tropical bay in Lagos, Nigeria. *Asian Journal of Microbiology, Biotechnology and Environmental Sciences*. **9** (4): 877 – 883.
- Onyema, I.C. (2008). Phytoplankton biomass and diversity at the Iyagbe lagoon Lagos, Nigeria. University of Lagos, Akoka. Department of Marine Sciences. 266pp
- Onyema, I.C. and Nwankwo, D.I. (2006). The epipellic assemblage of a polluted estuarine creek in Lagos, Nigeria. *Pollution Research*. **25**(3): 459 - 468.
- Onyema, I.C., Otudeko, O.G. and Nwankwo, D.I. (2003). The distribution and composition of plankton around a sewage disposal site at Iddo, Nigeria. *Journal of Scientific Research Development*. **7**: 11-24.
- Smith, G.M. (1950). *The fresh-water algae of the United States*. McGraw-Hill, London. 719pp
- Siver, P.A. (2003). Synurophyte algae. **In:** *Freshwater Algae of North America*. Ecology and Classification. Wehr, J.D. and Sheath, R.G. (Eds). Academic Press, New York. pp 523 - 558.
- Palmer, C.M. (1969). A composite rating of algae tolerating organic pollution. *Journal of Phycology*. **5**(1): 78 – 82.
- Patrick, R. and Reimer, C.W. (1966). The diatoms of the United States exclusive of Alaska and Hawaii (Vol. 1). *Monogr. Acad. Nat. Sci.* Philadelphia. 686pp.
- Patrick, R. and Reimer, C.W. (1975). The diatoms of the United States exclusive of Alaska and Hawaii (Vol. 2, part 1). *Monogr. Acad. Nat. Sci.* Philadelphia. 213pp.
- Rosowski, J.R. (2003). Photosynthetic Euglenoids. **In:** *Freshwater Algae of North America*. Ecology and Classification, Wehr, J.D. and Sheath, R.G. (Eds). Academic Press, New York. pp 383 – 422.
- Round, F.E. (1953). An investigation of two benthic algal communities in Malham Tarn, Yorkshire. *J. Ecol.* **41**: 174-187.
- Vanlandingham, S.L. (1982). Guide to the identification and environmental requirements and pollution tolerance of freshwater blue-green algae (cyanophyta). U.S. Environmental Protection Agency, EPA – 60.

Whitford, L.A. and Schmacher, G.H. (1973). *A manual of freshwater algae*. Sparks press Raeigh. 324pp.

Wimpenny, R.S. (1966). *The plankton of the sea*. Faber and Faber Limited, London. 426pp.

12/13/2008

Enhancement of Thermal Capabilities of A Solar Concentrator

I. O. Ohijeagbon¹, A. S. Adekunle², and O.D. Awolaran

^{1 & 2}Department of Mechanical Engineering, University of Ilorin, P. M B 1515, Ilorin, Nigeria
¹idehaiohi@yahoo.com

ABSTRACT: In order to continue to explore the enormous potential of solar energy as a veritable source of energy, physical constraints inherent in science and technological must steadily be converted to advantageous concepts and processes. This study investigates methods for enhancing thermal capabilities of a parabolic dish solar collector or concentrator. Optical lenses of different focal lengths and diameters were utilised to determine various output characteristics of thermal radiation. Convergent temperature (T_c), rate of energy emitted (\dot{q}), and intensity of radiation (i_n) were found to increase with steady increase in ambient temperature (T_a). Larger diameter lenses and shorter focal length lenses were more advantageous than smaller diameter lenses and longer focal length lenses in producing higher thermal outputs respectively. It was further observed that actual drop in thermal outputs are obtained with lenses of 15 and 30 cm focal lengths compared with no-lens condition at upward of 31 °C of ambient temperature. Also, the farther away the temperatures measured, the lower the thermal output temperature. This was as a result of radiation effects from the collector which influenced the output temperatures around the lenses. The study therefore concluded that enhanced thermal capabilities of solar energy devices operating on thermal radiations could be achieved by this method. [New York Science Journal. 2009;2(2):61-68]. (ISSN: 1554-0200).

Key words: *thermal capabilities, concentrator, optical lenses, converged temperature, rate of energy emitted, and intensity of radiation.*

1. INTRODUCTION

In view of increasing interest of finding enhanced and effective temperature output and thermal capabilities of solar energy radiations, which is described by Adegoke and Bolaji (2000) as the most attractive energy source for the future; this work is intended to further corroborate various existing methods and applications of solar energy devices operating on principles of thermal radiations. Many areas of applications of solar energy devices such as, solar cooker, solar furnaces, cooling of building, solar water and air heating, solar drying, among others, show that obviously, the availability of solar energy that have lend to very useful researches, which have continued to show that it is a safe and environmentally friendly source of energy in enhancing and transforming hitherto traditional techniques to modern scientific methods on energy utilisation and applications (Mc Veigh, 1977, Adegoke, 1998, Pelemo et al., 2002). Solar radiation does not contaminate environment or endanger ecological balance. It avoids major problems like exploration, extraction and transportation (Rajput, 2006). More so that mankind and especially engineering is today facing one of the most severe challenges ever. Present energy engineering leads to resource depletion and environmental destruction. Thus we need to develop energy engineering in harmony with nature (Wall, 2002).

Being a free gift of nature, solar energy is in most abundant supply compared with other naturally existing forms of energy such as fossil fuel, coal, oil and natural gas which are fast depleting due to increased global dependence on energy (Richard, 1984); hence more effective methods of exploring its use should be encouraged. Solar energy is not only inexhaustible, it is non-polluting and therefore can be utilised to provide all our energy needs (Richard, 1977). The finiteness of the fossil-fuel-based sources of energy has brought home to mankind the stark reality of the need to develop other sources of energy. Hence, an upsurge of small and large scale renewable energy programmes all over the world (Bamiro, 1983).

The enormous potential of solar energy as a veritable source of energy is in no doubt, however, its effective exploration and utilisation is determined by the extent and limitations that science and technological advances may allow. Although the total amount of energy is enormous, the collection and conversion of solar energy into useful forms must be carried out over a large area which entails a large capital investment (Rajput, 2006). In the past, the exploitation of solar energy reaching the earth's surface as a viable alternative energy source has been pursued vigorously through the development of different solar powered systems with varying degrees of efficiencies (Pelemo et al., 2002).

This study therefore is aimed at investigating methods of enhancement of thermal capabilities of a parabolic dish solar collector or concentrator. The process involves the use of optical lenses of different focal lengths and diameters to determine the output characteristics of temperature, rate of energy emitted, and intensity of radiation respectively. Improvements in thermal capabilities as a result of implementation of the optical lenses will lead to very useful information and optimised processes of solar energy devices operating on thermal radiations.

2. THEORETICAL FRAMEWORK

According to Rogers and Mayhew (1992), the framework for establishing the total energy emission per unit time by unit area of a surface and also for the intensity of radiation of a surface is hereby given.

The total energy emitted per unit time by unit area of a black surface is proportional to the 4th power of the absolute temperature T. This relation is expressed by the Stefan-Boltzmann law:

$$\dot{q}_b = \sigma T^4 \quad (1)$$

where, σ = Stefan-Boltzmann constant = 56.7×10^{-12} KW/m²K⁴

The spatial distribution of energy emission from an element can be represented as follows:

$$d\dot{Q}_{bn} = i_n dw_n dA \quad (2)$$

$$d\dot{Q}_{b\phi} = i_\phi dw_\phi dA \quad (3)$$

where, $d\dot{Q}_{bn}$ is the rate of flow of energy through dA_1 and $d\dot{Q}_{b\phi}$ is the rate of flow of energy through dA_2 .

i_n is the intensity of radiation in the normal direction and i_ϕ is the intensity of radiation in the ϕ direction.

The spatial distribution of i_ϕ is expressed by Lambert's cosine law:

$$i_\phi = i_n \cos \phi \quad (4)$$

Combination of equations (3) and (4) gives:

$$d\dot{Q}_{b\phi} = i_n \cos \phi dw_\phi dA \quad (5)$$

The solution of equation (5) gives:

$$\dot{Q}_b = i_n \pi dA \quad (6)$$

Equation (1) can be re-written as:

$$\dot{Q}_b = \sigma T^4 dA \quad (7)$$

Combination of equations (6) and (7) gives:

$$i_n = \frac{\sigma T^4}{\pi} \quad (8)$$

This equation, giving the intensity of normal black radiation, is a consequence of the Stefan-Boltzmann law and Lambert's law.

Therefore for a grey body the following laws are valid:

$$\dot{q} = \varepsilon \dot{q}_b = \varepsilon \sigma T^4 \quad (9)$$

$$i_n = \frac{\varepsilon \sigma T^4}{\pi} \quad (10)$$

where ε = total hemispherical emissivity or simply emissivity, and is defined as the ratio of the total energy \dot{q} emitted by a surface to the total energy \dot{q}_b emitted by a black surface at the same temperature.

Thus,
$$\varepsilon = \left(\frac{\dot{q}}{\dot{q}_b} \right)_T \quad (11)$$

The ratio of the total hemispherical emissivity to the normal emissivity $\frac{\varepsilon}{\varepsilon_n}$ is equal to unity for a grey body. Assuming a glass as a silver polished surface, its normal emissivity ε_n is given as 0.02 (Rogers and Mayhew, 1992). Hence, $\varepsilon = \varepsilon_n$ for a grey body. Equations (9) and (10) are respectively used to analyse the experimental data collected.

3. MATERIALS AND METHODS

3.1 Conditions and Materials

The major equipment used to carry out this research study is a focusing type solar collector or concentrator. This collector was previously constructed by Gbodiyan and modified for better performance by Abiola (Gbodiyan, 2003, Abiola, 2003), and then used by Awolaran for research studies (Awolaran, 2005). The surface area of the collector surface is 1.1314 m² with an estimated focal length of 69 cm, obtained as a cumulative value from the pieces of mirrors attached to the collector surface.

The geographical location of Ilorin, Nigeria where the study was conducted is estimated as Latitude: 8.43 °N, Longitude: 4.5 °E and Altitude: 366m, percentage annual average of actual to theoretical hours of sunshine in a day: $\frac{n}{N} = 53$, where, n = actual hours of sunshine in a day, N = theoretical maximum possible sunshine hours in a day, solar irradiance: 640 (Fagbenle, 1990, NMA, 2005).

Three thermometers were used (0-45)⁰C, (0-100)⁰C and (0-350)⁰C respectively. Four converging lenses with the following specifications were use; 10 cm focal length lens (5 cm in diameter), 15 cm focal length lens (5 cm in diameter), 30 cm focal length lens (5cm in diameter) and 15 cm focal length lens (10 cm in diameter) respectively. The lenses were used to investigate the effects of the lens' focal length and diameter respectively on the thermal output of the concentrator. A stop watch was used to time and monitor temperature changes within specific time-intervals during the experimental investigation.

3.2 Methods

The concentrator solar device without the use of lenses was positioned to ensure no shading effect and to guarantee a maximum radiation from the sun, between the hours of 12.00 noon and 2.00 pm when the experiment was conducted. During this period it was assumed that the sun radiation is at its peak. The concentrator laced was also placed so that the angle between the rays of the sun and the collector axis is minimised in order to obtain the maximum solar irradiance, that is, the total radiation incident on unit area of surface per unit time (Rogers and Mayhew, 1992). This was accomplished by making sure the shadow of the concentrator on the

ground forms approximately a perfect circle and radiation rays approximately at a normal angle to the concentrator surface.

The (0-350)⁰C thermometer was placed at the region of convergence of the concentrator to measure the air temperature (T_c) at converging point. The (0-45)⁰C thermometer was placed at a distance of about 3 meters away from the concentrator system in order to measure the ambient air temperature (T_a) without undue interference or influences. The setting up of the apparatus was done 30 minutes before the commencement of taking the readings, so that the apparatus will adapt to the ambient state. The readings of T_a and T_c were taken and recorded at 10 minutes interval between the hours of 12.00 noon and 2.00 pm for Day 1, without the use of any lens. The entire procedure was repeated for Days 2, 3 and 4 respectively, fixing the converging lenses of different focal lengths at the region of convergence of the solar concentrator in order to investigate the effects of focal lengths of lenses on convergent temperatures. Therefore the (0-350)⁰C thermometer was now placed at the new region of convergence of the lenses, to measure the temperature (T_c) at the new focal point.

All the above procedure was repeated for 3 more weeks to get a better view of the variations of the parameters over time. Lenses of different surface areas/diameters was then used on the fourth week respectively for another 3 days each to study the effects of lenses dimensions on convergent temperatures accordingly.

4. DISCUSSION OF RESULTS

4.1 Effects of Lenses Focal Length on Radiation Output Characteristics

Table 1: average ambient and convergent temperatures of concentrator-using lenses with different focal lengths below shows the data collected for the ambient and convergent temperatures of the concentrator (Awolaran, 2005). These being the average values over a 3 weeks period, that is 29th August 2005 to 1st September 2005, 5th September 2005 to 8th September 2005, and 12th September 2005 to 15th September 2005 respectively. The data is for no lens condition and with lenses of 10 cm, 15cm and 30 cm focal lengths respectively with each of the lens been 5 cm in diameter.

The output characteristics of solar radiation indicates a consistent increasing temperature (T_c) of converged radiations with time with respect to increasing ambient temperatures (T_a) as shown in table 1, and figure 1: variation of energy emitted with time for different focal lengths of lenses respectively. Consequently, the rate of energy emitted (\dot{q}), and intensity of radiation (i_n) given by equations (9) and (10) would also increase correspondingly with the exception of the ambient values which appears constant.

Figure 1 further reveals that higher thermal output characteristics are achievable with lens of shorter focal length of 10 cm compared with 15 and 30 cm lenses. It should however be noted that actual drop in thermal outputs are obtained with lenses of 15 and 30 cm focal lengths compared with no-lens condition at upward of 31 ⁰C of ambient temperature; this situation further reveals that the farther away the temperatures observed and measured from the primary solar collector at some significant point in the ambient temperature, the lower would be the thermal outputs with further increasing ambient temperatures. Hence, it can be deduced that thermal and radiation measurements through the lenses is also partly influenced by radiation effects from the collector.

4.2 Effects of Lenses Diameter on Radiation Output Characteristics

Table 2: average ambient and convergent temperatures of concentrator-using lenses with different diameters and Focal Lengths = 15 cm as shown below, the data collected is for the ambient and convergent temperatures of the concentrator for lenses of 5 and 10 cm diameter respectively (Awolaran, 2005); with each of the lens been 15 cm focal length. These being the average value of 3 days readings each for each lens. That is 31st August 2005, 7th September 2005 and 14th September 2005 for the 5 cm diameter lens, and 30th September 2005, 1st October 2005 and 3rd October 2005 for the 10 cm diameter lens respectively.

In addition to increasing convergent temperatures with respect time and increasing ambient temperatures as shown in table 2, figure 2: variation of energy emitted with time for different lenses diameters also reveals that appreciable gain can be achieved in the rate of energy emitted (\dot{q}), and intensity of radiation (i_n) if an increased diameter lens is utilised in solar collector devices. Figure 2 also indicates equivalent values of the rate of energy emitted (\dot{q}) for ambient measurement of both lenses, as their curves overlap one another.

5. CONCLUSION

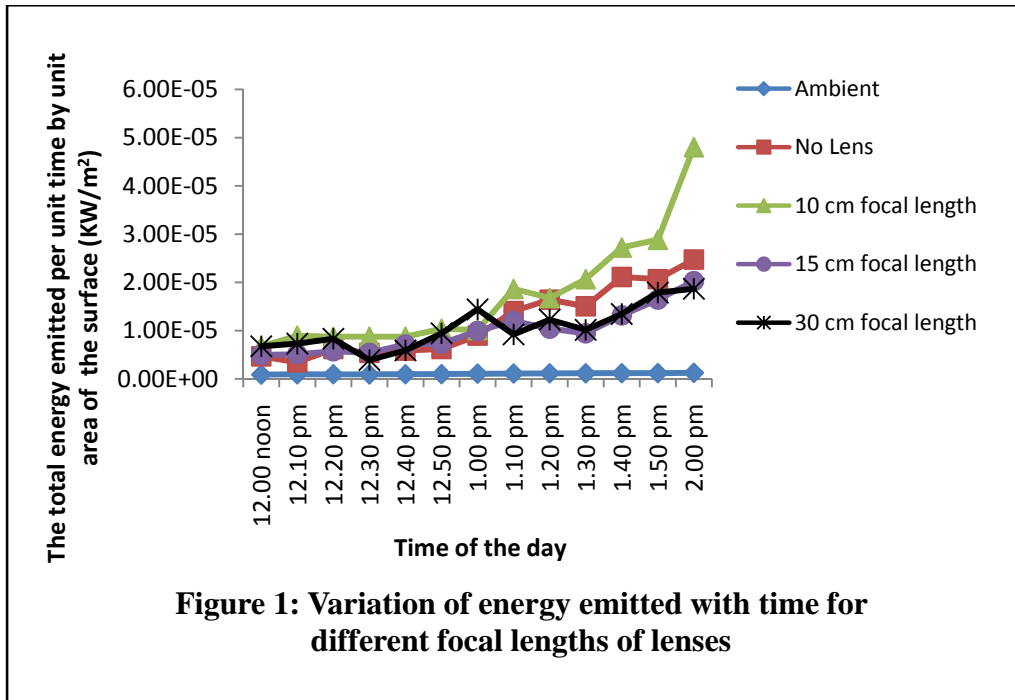
From the results, the study shows that enhancement of thermal capabilities of a solar concentrator is achievable through the use of converging lenses. Larger diameter lenses should be preferred over smaller diameter ones as this will permit more radiation to be captured. And shorter focal lengths are more advantageous than longer focal lengths, as a result, allowing the converged radiation closer to the collector surface which is also influenced by thermal radiations from the solar collector itself. Hence, improved and optimised output characteristics of temperature, rate of energy emitted, and intensity of radiation respectively could be achieved and employed for better performances of solar energy devices operating on thermal radiations.

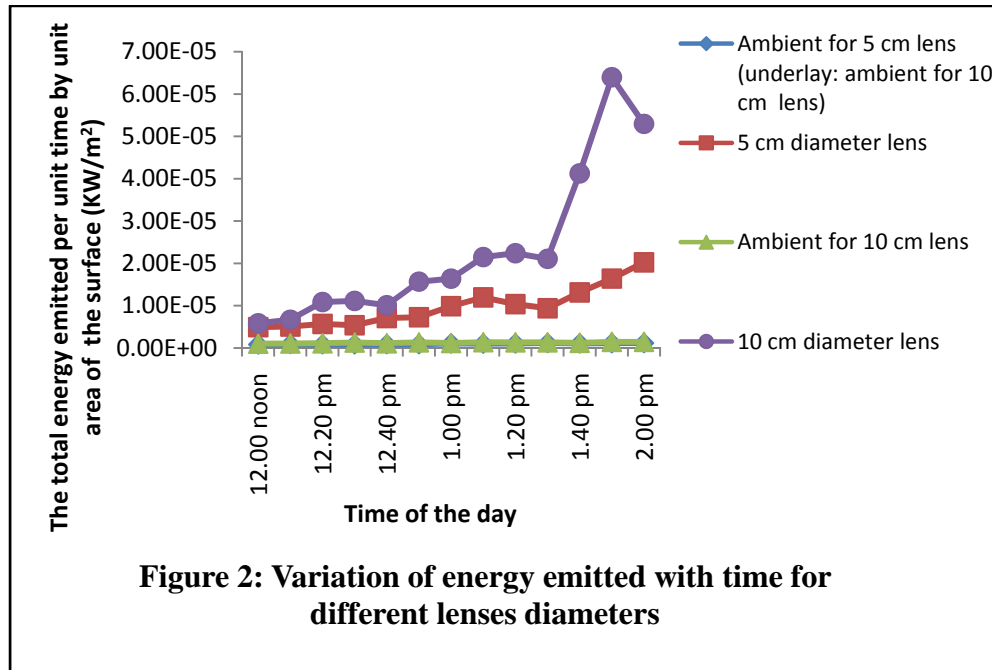
Table 1: Average Ambient and Convergent Temperatures of Concentrator-Using Lenses with Different Focal Lengths

| Time | Average Ambient Temperature, T_a ($^{\circ}\text{C}$) | Average Convergent Temperature, T_c ($^{\circ}\text{C}$) | | | |
|------------|---|--|------------------------------|--------------------|--------------------|
| | | With No Lens | With Lenses Diameters = 5 cm | | |
| | | | 10 cm Focal Length | 15 cm Focal Length | 30 cm Focal Length |
| 12.00 noon | 29.50 | 45.00 | 49.33 | 45.67 | 49.33 |
| 12.10 pm | 30.00 | 41.67 | 53.00 | 46.00 | 50.33 |
| 12.20 pm | 30.17 | 48.33 | 52.67 | 47.33 | 52.00 |
| 12.30 pm | 29.92 | 46.67 | 52.67 | 46.67 | 43.00 |
| 12.40 pm | 30.17 | 47.67 | 52.67 | 50.00 | 47.67 |
| 12.50 pm | 30.25 | 48.33 | 55.00 | 50.33 | 53.67 |
| 1.00 pm | 31.17 | 53.00 | 54.67 | 54.33 | 59.67 |
| 1.10 pm | 31.33 | 59.33 | 63.67 | 57.00 | 53.33 |
| 1.20 pm | 31.67 | 61.67 | 62.00 | 55.00 | 57.33 |
| 1.30 pm | 31.67 | 60.33 | 65.33 | 53.67 | 54.67 |
| 1.40 pm | 31.75 | 65.67 | 70.00 | 58.33 | 58.67 |
| 1.50 pm | 31.83 | 65.33 | 71.00 | 61.67 | 63.00 |
| 2.00 pm | 32.33 | 68.33 | 80.67 | 65.00 | 63.67 |

Table 2: Average Ambient and Convergent Temperatures of Concentrator-Using Lenses with Different Diameters and Focal Lengths = 15 cm

| Time | Average Values of Temperature | | | |
|------------|---|--|---|--|
| | 5 cm Diameter Lens | | 10 cm Diameter Lens | |
| | Ambient Temperature, T_a ($^{\circ}\text{C}$) | Convergent Temperature, T_c ($^{\circ}\text{C}$) | Ambient Temperature, T_a ($^{\circ}\text{C}$) | Convergent Temperature, T_c ($^{\circ}\text{C}$) |
| 12.00 noon | 29.33 | 45.67 | 31.00 | 47.67 |
| 12.10 pm | 30.33 | 46.00 | 31.33 | 49.33 |
| 12.20 pm | 29.67 | 47.33 | 31.67 | 55.67 |
| 12.30 pm | 29.67 | 46.67 | 32.67 | 56.00 |
| 12.40 pm | 30.00 | 50.00 | 31.67 | 54.67 |
| 12.50 pm | 30.00 | 50.33 | 33.00 | 61.00 |
| 1.00 pm | 31.33 | 54.33 | 32.00 | 61.67 |
| 1.10 pm | 31.00 | 57.00 | 33.33 | 66.00 |
| 1.20 pm | 31.33 | 55.00 | 33.00 | 66.67 |
| 1.30 pm | 32.00 | 53.67 | 33.00 | 65.67 |
| 1.40 pm | 31.33 | 58.33 | 32.33 | 77.67 |
| 1.50 pm | 31.67 | 61.67 | 33.67 | 86.67 |
| 2.00 pm | 32.00 | 65.00 | 33.67 | 82.67 |





6. REFERENCES

- Abiola, A. O. (2003)**, Temperature Magnification and Applications of a Parabolic Solar Energy Collector, B. Eng. Thesis, Department of Mechanical Engineering, University of Ilorin, Ilorin, Nigeria.
- Adegoke, C. O. (1998)**, Alternative Energy Option for Nigeria as a Reaction to Impending Global Climate Change, *Journal of Science, Engineering and Technology*, Vol. 5(3), pp1341-1348.
- Adegoke, C. O. and Bolaji, B. O. (2000)**, Performance Evaluation of Solar-Operated Thermosyphon Hot Water System in Akure, *International Journal of Engineering and Engineering Technology*, School of Engineering and Engineering Technology, Akure, Nigeria, Vol. 5(1), pp35-40.
- Awolaran, O. D. (2005)**, Investigation of Methods of Increasing Temperature of a Parabolic Solar Energy Collector, B. Eng. Thesis, Department of Mechanical Engineering, University of Ilorin, Ilorin, Nigeria.
- Bamiro, O. A. (1983)**, Empirical Relations for the Determination of Solar Radiation in Ibadan, Nigeria, *Solar Energy*, Pergamon Press Ltd., UK., Vol. 31(1), pp85-94.
- Fagbenle, R. L. (1990)**, Estimation of Total Solar Radiation in Nigeria Using Meteorological Data, *Nigerian Journal of Renewable Energy*, Vol. 1, pp1-10.
- Gbodiyan, M. F. (2003)**, Design and Construction of a Solar Steam Producer, B. Eng. Thesis, Department of Mechanical Engineering, University of Ilorin, Ilorin, Nigeria.
- Mc Veigh, J. C. (1977)**, Sun Power, An Introduction to Application of Solar Energy, Pergamon Press, London.
- Nigerian Meteorological Agency (NMA, @ 2005)**, Record of Climatic Conditions in Ilorin (September 2002-August 2005), Federal Airport Authority, Ilorin, Nigeria.
- Pelemo, D. A., Fasasi, M. K., Owolabi, S. A., and Shaniyi, J. A. (2002)**, Effective Utilisation of Solar Energy for Cooking, *NJEM*, Vol. 3(1), pp13-18.

- Rajput, R. K. (2006)**, Thermal Engineering, Laxmi Publications (P) Ltd., New Delhi.
- Richard, C. D. (1984)**, Energy Resources and policies, Academic Press, New York.
- Richard, J. W. (1977)**, Solar Energy Technology and Application, Ann Arbor Science, New York.
- Rogers, G. F. C. and Mayhew, Y. R. (1992)**, Engineering Thermodynamics-Work and Heat Transfer, Longman Group, UK. Ltd.
- Wall Goran (2002)**, Conditions and Tools In the Design of Energy Conversion and Management Systems of a Sustainable Society, Energy Conversion and Management Vol. 43, pp1235–1248, www.elsevier.com/locate/enconman

1/6/2009

对黑洞的新观念和新的完整论证：黑洞内部根本没有奇点（上篇）***

====所有黑洞之最后命运就是由于发射霍金辐射而收缩成为宇宙中的最小引力黑洞

($M_{bm} \approx 10^{-5}g$) 在爆炸中消亡于普朗克领域 Planck Era, 而不是塌缩成为奇点====

张 洞 生

Dongsheng Zhang

1/10/2009

1957年毕业于北京航空学院,即现在的北京航空航天大学

永久住址: 17 Pontiac Road, West Hartford, CT 06117-2129, U.S.A.

E-mail: ZhangDS12@hotmail.com

The New Concepts and The Complete Demonstrations to Black Holes: Any Black Holes Had No Singularity At All (Part I)

==== The final destiny of all black holes would contract to the minimum Schwarzschild black hole of

$M_{bm} \approx 10^{-5}g$ (MSBH), and to explode in Planck Era, but not to contract to Singularity====

Abstract: In this article, the conclusion of “No Singularity in any black hole at all” is derived out from 4 reliably classical formulas and demonstrated by author’s unique and simple way. Formula (4e) $m_{ss}M = hC/8\pi G = 1.187 \times 10^{-10}g^2$ in this article is the most important conservation formula on the Event Horizon of any black hole(BH). It is got from the special solution of formula(1a) $dP/dR = -GM\rho/R^2$ with other 3 classical formulas as the complementary conditions, which are (1b) $P = n\kappa T = \rho\kappa T/m_s$, (1c) $R_b = 2GM_b/C^2$, $C^2/2 = GM_b/R_b$ ^[6] and (1d) $T_b = (C^3/4GM_b) \times (h/2\pi\kappa) \approx 10^{27}/M_b$ ^[2]. In formula (4e), M is the mass of a whole BH, m_{ss} is a particle balanced by thermodynamics and a quantum of Hawking radiation on Event Horizon (EH). Due to the maximum m_{ss} is only equal to the minimum M_{bm} under the extreme condition, so, $m_{ss}^2 = M_{bm}^2 = hC/8\pi G$, i.e. $m_{ss} = M_{bm} = (hC/8\pi G)^{1/2} = 1.058 \times 10^{-5}g$ (6a). However, (6a) is completely and exactly equal to Planck particle m_p , i.e., $m_{ss} = M_{bm} = m_p = (hC/8\pi G)^{1/2} = 1.058 \times 10^{-5}g$. It is completely and exactly proved that, once a BH could contract its volume to the limit because of emitting Hawking radiations, its final destiny would be to become a basic particle of $M_{bm} = m_p$, and finally explode, disintegrate and vanish in Planck Era, but have no way to contract continuously its volume to Singularity. It clearly shows that no Singularity would appear in any BHs and that the General Theory of Relativity(GTR) is sure to become invalid in Planck Era. (The whole article will be translated in English later.) [New York Science Journal. 2009;2(2):69-93] (ISSN: 1554-0200).

笛卡儿：“在怀疑中寻找真理。”

内容提要：在本篇中，作者在没有提出任何附加的假设条件和数据的情况下，尝试用一种独特而简易的新方式方法直接论证推导出“黑洞内部没有奇点”，取得了令人比较满意的结果。这种新方式方法就是综合运用相对论的基本原理，结合其它的经典理论(霍金的黑洞理论，经典力学和热力学等)的4个基本公式，以黑洞视界上的一般热动力平衡公式(1a)为基础， $dP/dR = -GM\rho/R^2$ ，用另外3个基本公式作为补充条件，简单地解出了黑洞在其视界半径上的物理状态参数之间的1组守恒公式，这几个守恒公式只与4个基本物理常数(h, C, G, κ)发生关系，并且得出其中之一的重要公式如下，

$$m_{ss} M = hC/8\pi G = 1.187 \times 10^{-10}g^2 \quad (4e)$$

上式中M是任何一个黑洞的质量， m_{ss} 是该黑洞在其视界半径R上霍金辐射粒子的质量， m_{ss} 也在R上达到了引力和热动力的平衡。由此得出 $m_{ss}M$ 的乘积是一个常数。(4e)式直接简单地告诉我们，在物理世界和真实宇宙中， m_{ss} 不可能 = 0，所以任何黑洞质量M不可能为无限大， m_{ss} 更不可能为无限大，使黑洞质量M不可能集中在一点而成为“奇点”。运用部分不能大于全体的公理，黑洞M所能发射出的粒子 m_{ss} 的最大质量不可能大于M，其极限只能是 $m_{ss} = M$ 。因而得出一个宇宙中最小黑洞质量(6a)式， $M_{bm} = (hC/8\pi G)^{1/2} = m_{ss} \approx 10^{-5}g$ 。而 M_{bm} 又完完全全等于普郎克质量 m_p ，即 $M_{bm} = m_p = (hC/8\pi G)^{1/2}$ 。这就充分证明当任何一个黑洞发射霍金辐射收缩到最后，其命运是同时分裂成为两个宇宙的最小黑洞 $M_{bm} \approx 10^{-5}g$ ，即达到普郎克量子领域，它们唯一的可能是在宇宙最高温度下爆炸解体消亡，“其质量转变成能量，这种能量以一种高强度的伽玛射线爆发的形式消散。以最后一刻的爆炸而告终”^[1]（霍金）。因此， M_{bm} 根本不可能再继续收缩成为“奇点”。由于(4e)式对任何大小的黑洞都普遍有效，从而也证明了“奇点”不可能存在于恒星所塌缩成的黑洞和所有黑洞的中心。恒星在塌缩过程中，最终形成稳定的黑洞后，黑洞既然连光都不能逃出去，它近似于一个绝对黑体，仅能发出微量的量子辐射（霍金辐射）。恒星塌缩成的黑洞所产生的高温度和高密度以及粒子之间的泡利不相容原理就能够对抗与平衡其内部引力塌缩，使黑洞内部达到了极其平衡和稳定，而成为一个极长寿命的实体。因此，“奇点”也根本不可能出现在恒星塌缩成的黑洞内部。这清楚地表明广义相对论在普郎克领域是失效的，不适用的。[New York Science Journal. 2009;2(2):69-93] (ISSN: 1554-0200).

关键词：黑洞内没有奇点，黑洞的本质属性，黑洞的霍金辐射，宇宙中的最小引力黑洞 $M_{bm} \approx 10^{-5}g$ ，所有黑洞的最终命运是塌缩为最小黑洞 $M_{bm} \approx 10^{-5}g$ 而爆炸消失，最小黑洞 $M_{bm} = 10^{-5}g = m_p$ 普郎克粒子(Planck particle)，普郎克尺寸，

*** 本文全部共分上下两篇，这两篇是相互连接而不可分割的姊妹篇。下篇为“对宇宙起源的新观念和新的完整论证：宇宙不可能诞生于奇点。”（下篇）<18>，请同时参看本文的下篇。

本文只讨论史瓦西 Schwarzschild 引力黑洞 (即无电荷,无旋转的球对称黑洞)。

I, 黑洞状态和运动的 4 个基本公式: 粒子 m_s 在史瓦西黑洞视界半径 R 上的平衡

为了研究恒星级黑洞的发生，应首先参考宇宙中原始星际星云的塌缩过程，如果原始星云处于热动力平衡状态，(1a)式正确地规范了气体粒子的压强 P 与其在同一处的引力 F 相平衡。如将(1a)用于规范粒子在史瓦西黑洞视界半径 R 上的平衡也应该是适合的，根据牛顿方程和热力学；

$$dP/dR = -GM\rho/R^2 \quad (1a)$$

$$P = n\kappa T = \rho\kappa T/m_s \quad (1b)$$

M - 为黑洞在视界半径 R 内的总质量；R 为视界半径， ρ 为 M 在 R 上的密度； m_s 为粒子在 R 上的质量，T 为对应于 R 处的温度；

波尔兹曼常数 $\kappa = 1.38 \times 10^{-16} g \cdot cm^2/s^2 \cdot k$ ，引力常数 $G = 6.67 \times 10^{-8} cm^3/s^2 \cdot g$ ，光速 $C = 3 \times 10^{10} cm/s$ ，普郎克常数 $h = 6.63 \times 10^{-27} g \cdot cm^2/s$ ， n = 单位体积内的粒子数，

按照史瓦西对广义相对论的特解，以此作为黑洞存在的必要条件。得出黑洞视界半径 R_b 与黑洞质量 M_b 的关系如下：

$$R_b = 2GM_b/C^2, \quad C^2 = 2GM_b/R_b \quad (1c)$$

由霍金黑洞理论得出在视界半径 R_b 上的霍金辐射量子的阈值温度公式如下:

$$T_b = (C^3/4GM_b) \times (h/2\pi\kappa) \approx 0.4 \times 10^{-6} M_\theta / M_b \approx 10^{27} / M_b \quad (1d)$$

M_θ - 太阳质量 $\approx 2 \times 10^{33}$ g, t_b - 为黑洞内光从中心到视界的时间. 在此定义下, 任何物质与光都不能逃出黑洞.

$$C \times t_b = R_b, \quad t_b = 2GM_b/C^3, \quad (1e)$$

$$\text{球体公式 } M_b = 4\pi\rho R_b^3/3 \quad (1f)$$

上面 4 个公式 (1a), (1b), (1c) 和 (1d) 都是理想化的, (1a), (1b), 应能有效地应用到黑洞的视界和内部各处. (1c) 和 (1d) 只能应用于黑洞视界半径 R 上. 它们 4 个公式一起构成了任何瞬时粒子 m_s 在黑洞视界上的引力与热压力的平衡与稳定. 其实这种平衡与稳定的关系正如罗伊·克尔 (Roy Kerr) 黑洞是一样的, 在该黑洞视界上的任何瞬时以光速转动的粒子 m_s 的离心排斥力与引力达到了平衡. 按照广义相对论, 公式 (1c) 是构成一个黑洞的必要条件. 公式 (1d) 来源于霍金的黑洞理论, 它规定了黑洞视界面上量子辐射的阈值温度. (1b) 是气体的理想状态方程. 公式 (1a) 用于规定黑洞视界半径上的粒子 m_s 的引力和热压力的平衡. 因有公式 (1c) 和 (1d) 作为边界条件, (1a) 就比 Tolman-Oppenheimer-Volkoff [7] 方程能更加简化地解出来. 原来的 TOV 方程对 (1a) 的修正包括 3 项, 内部的热压力, 每个核子平均的熵和内部的化学成分结构. [7] 由于这 3 项修正需要许多的假设和数据, 所以 TOV 方程很难准确的解出来. 用公式 (1a), (1b) 描述黑洞内部的状态应当是合适的. 因为本文在讨论黑洞内部的“奇点”问题时并不需要知道黑洞内部各点的状态参数的数值和微观结构. 本文的目的就是要找出公式 (1a) 的可用于球对称的史瓦西黑洞在其视界半径 R 上的特殊解—各个参数在 R 上的守恒公式, 并将这些公式推广应用到所有黑洞. 即从粒子 m_s 在 R 收缩时从其平衡状态去分析了解黑洞内部不可能像广义相对论所论断的那样: 中心出现和存在“奇点”.

结论: 上述 4 个公式 (1a), (1b), (1c) 和 (1d) 来源于不同的经典理论的基本公式. 因而本文以后对黑洞的概念和结论是与单独的广义相对论的结论截然不同的.

II, 从黑洞的 4 个基本公式求出黑洞在其视界半径 R 上的 4 个重要的守恒公式— (1c), (1d), (4d) 和 (4e) 式: 将上面的牛顿力学, 热力学, 状态方程和霍金温度公式等 4 个公式用于求解黑洞在其视界半径上的引力与压强的平衡和特解, 即如 TOV 方程的简化解: 即得到式 (2c), 有了这一组共 6 个守恒公式, 就可以从黑洞的收缩中研究黑洞是否最后收缩成为“奇点”: 在此, R —黑洞的视界半径. M 为 R 内的黑洞质量, m_s —视界半径 R 上粒子的能量-质量, P — R 上的热压力, T —粒子 m_s 在视界半径 R 上的阈温值,

$$dP/dR = -GM_p/R \quad (1a)$$

$$P = n\kappa T = \rho\kappa T/m_s \quad (1b)$$

对于任何一个史瓦西黑洞, $M = 4\pi\rho R^3/3$, 以及从 (1d), $T = (C^3/4GM) \times (h/2\pi\kappa)$,

$$P = \rho\kappa T/m_s = \kappa/m_s \times (3M/4\pi R^3) \times (C^3/4GM) \times (h/2\pi\kappa) = 3hC^3/(32\pi^2 GR^3 m_s),$$

$$dP/dR = d[3hC^3/(32\pi^2 GR^3 m_s)]/dR = -(9hC^3)/(32\pi^2 Gm_s R^4), (\therefore dP/dR \text{ 正比例于 } R^{-4}), \quad (2a)$$

$$-GM_p/R^2 = -(GM/R^2) \times (3M/4\pi R^3) = -(3G/4\pi R^3) \times (M^2/R^2),$$

由 (1c), $M_b/R_b = C^2/2G = M/R$. 故
 $-GM \rho/R^2 = -3C^4/(16\pi GR^3)$, (正比例于 R^{-3}) (2b)

将 (2a), (12b) 代入 (1a),

$$-(9hC^3)/(32\pi^2 Gm_s R^4) = -3C^4/(16\pi GR^3),$$

$$\text{或 } 3h/(2\pi m_s R^4) = C/R^3$$

$$\mathbf{R = 3h/(2\pi C m_s), \text{ 或者 } R m_s = 3h/(2\pi C) = 1.0557 \times 10^{-37} \text{ cmg}} \quad (2c)$$

相应得出的黑洞的其它几个在其视界半径上的重要的守恒公式如下:

$$\mathbf{T \times R = (C^3/4GM) \times (h/2\pi\kappa) \times (2GM/C^2) = Ch/4\pi\kappa = 0.1154 \text{ cmk}} \quad (2ca)$$

$$\mathbf{M/R = C^2/2G \approx 0.675 \times 10^{28} \text{ g/cm,}} \quad (1c)$$

$$\mathbf{m_s M = 3hC/4\pi G = 7.123 \times 10^{-10} \text{ g}^2} \quad (2cb)$$

$$\mathbf{T \times M = (C^3/4G) \times (h/2\pi\kappa) \approx 0.4 \times 10^{-6} M_\theta \approx 0.779 \times 10^{27} \text{ gk}} \quad (1d)$$

$$\rho R^2 = 3C^2/\pi G. \quad \rho M^2 = 3C^6/32\pi G^3 \quad (2cc)$$

以下将利用上面所得出的守恒公式探讨分析各种大小不同的黑洞及其属性。

III, 黑洞的本质属性之一: 一旦一个黑洞形成之后, 无论它是因辐射能量-物质而缩小还是因吞噬外界能量-物质而膨胀, 它会永远是一个黑洞。

根据史瓦西黑洞公式 (1c), $R_b = 2GM_b/C^2$,

$$\text{可得, } C^2 dR_b = 2G dM_b \quad (3a)$$

$$\text{于是, } C^2 (dR_b + R_b) = 2G(dM_b + M_b) \quad (3b)$$

(3b) 式表明, 一旦一个黑洞形成之后, 无论它是因辐射能量-物质而缩小还是因吞噬外界能量-物质而膨胀, 它会永远是一个黑洞。

设有另外一个黑洞, $C^2 R_{ba} = 2GM_{ba}$ (3c)

$$\text{由(3c) + (1c), } C^2 (R_{ba} + R_b) = 2G (M_{ba} + M_b) \quad (3d)$$

(3d)式表明, 两个黑洞相碰撞或者合并也仍然是一个黑洞。

结论: 黑洞的膨胀只是因为吞噬进来外界的能量-物质, 黑洞的收缩只是因为向外界发射能量-物质, 即霍金辐射。但黑洞无论是膨胀到多么大还是收缩到多么小, 在其最后收缩到宇宙最小引力黑洞 $M_{bm} \approx 10^{-5} \text{ g}$ 以前, 却始终是一个黑洞。

作者根据此原理前不久论证了 1998 年所发现的我们宇宙的加速膨胀是由于在宇宙早期我们宇宙大黑洞与另外一个宇宙大黑洞碰撞和合并的结果。^[4]

IV. 黑洞的本质属性之二: 发射霍金量子辐射是黑洞的本性。黑洞的视界半径 R_b 上的温度 T_b 就是霍金辐射量子 m_{ss} 的阈温, 即 $m_{ss} = \kappa T_b/C^2$ 。因为黑洞总是不停地在从外部吞噬能量-物质的同时, 不停地向外发射霍金量子辐射 (能量-物质)。所以每个黑洞在最后收缩成为最小引力黑洞 $M_{bm} \approx 10^{-5} \text{ g}$ 而消失之前, 黑洞的视界半径 R_b 永无休止地振动 (扩大或缩小) 是黑洞的本性。

从第 2 节的黑洞守恒公式(2ca), (2cb) (1c)和(1d)可知, 当黑洞发射霍金辐射时, 它同时缩小视界半径提高温度和增加密度。当黑洞吞噬进来外界的能量-物质时, 它同时增大视界半径降低温度和减小密度。黑洞在有外界能量-物质可吞噬的情况下, 都是同时吞噬外界能量-物质和发射霍金辐射。不过一般黑洞除了特别小的黑洞和孤立于接近宇宙真空中的黑洞之外, 其所吞噬的粒子的质量绝大多数大于霍金

辐射的质量，所以实际能观测到的黑洞都是膨胀的黑洞。下面来探讨黑洞发射霍金辐射的状况，

设 m_s 是黑洞质量 M_b 的视界半径 R_b 上的粒子的质量，由公式(2a)，(2b)可知，当 m_s 在 R_b 上处于黑洞的引力与热压力的平衡状态时， m_s 还必须符合黑洞守恒公式(2cb)和(1d)而成为：

$$m_s = 3hC / (4\pi GM_b) = (3hC / 4\pi G) \times (4GT_b / C^3) \times (2\pi\kappa / h) = 6\kappa T_b / C^2 \quad (4a)$$

在(4a)式中，由于 m_s 并不能绝对地保持其恒定的温度和动能，因此， m_s 的温度和动能的少许涨落就会离开 R_b 而进入黑洞附近内部或者跑出黑洞。由于在 R_b 的霍金辐射是量子辐射，因此在 R_b 上发射的每一个 m_s 的阈值温度还必须符合 R_b 上的阈值温度，那么，为什么(4a)中即 $m_s \neq \kappa T_b / C^2$ ，而是 $m_s / 6 = \kappa T_b / C^2$ ？

$$\text{设有 } m_{ss} = m_s / 6, \quad \text{则 } m_{ss} = m_s / 6 = \kappa T_b / C^2 \quad (4b)$$

这就是说，只有(4b)式才是正确的，符合黑洞视界半径上的真实情况的。所以在黑洞视界半径 R_b 上所真正发射的霍金辐射量子应该是 m_{ss} 而不是 m_s ，为什么呢？因为在第 II 节中求解(1a)式时无法知道黑洞的内部结构和密度分布，只能是用整个黑洞的平均密度 ρ_{ba} 作为视界上的实际密度 ρ_{be} 从而得出了(2c)式。因而使视界上用于(1a)的密度成为 ρ_{ba} ，它是黑洞视界上的实际密度 ρ_{be} 的 6 倍，这就造成在(1a)中的 m_s 等于实际 m_{ss} 的 6 倍，因而得出(4b)式，即 $m_s = 6m_{ss}$ ，从而相应地得出，

$$\rho_{ba} = 6\rho_{be} \quad (4c)$$

因此，(2c) 式和(2cc)式就应当作出相应地修正如下的(4d)和 (4e)式：

$$Rm_{ss} = h / (4\pi C) = 0.176 \times 10^{-37} \text{ cmg} \quad (4d)$$

$$m_{ss} M = hC / 8\pi G = 1.187 \times 10^{-10} \text{ g}^2 \quad (4e)$$

虽然从(4c)中知道整个黑洞的平均密度 ρ_{ba} 等于黑洞视界上的实际密度 ρ_{be} 的 6 倍，但是整个黑洞内部的密度分布仍然无法知道。然而，这却是黑洞内部没有无穷大密度的奇点的另一个有力的佐证。

现在来看这 m_{ss} 是如何发射出去的。

A. 当黑洞外附近的温度 T_w 低于视界半径 R_b 上的温度值 T_b (等于 m_{ss} 的阈值温度 T_b) 时，如果外界粒子的质量 m_{ssw} 均小于 m_{ss} 时(此时外界没有能量-物质可以被吞噬进入黑洞内部)，则在 R_b 上面和附近内部的 $\leq T_b$ 辐射能量和 $\leq m_{ss}$ 的粒子会很自然地由高温逃向低温，由高能奔向低能，而以霍金辐射的形式逃出黑洞的 R_b 进入外界。而后，黑洞由于失去 m_{ss} 而相应地缩小 R_b 和提高 R_b 上阈值温度 T_b ，而这提高后的 T_b 就成为比原来 m_{ss} 更大的粒子 m_{sb} 的阈值温度，这样，具有较高阈温的 m_{sb} 的辐射和粒子就更易于以霍金辐射的形式射入外界。如此这般，黑洞就一直不停地向外界发射霍金辐射，收缩体积和提高温度和密度，直到最后收缩成为质量 $M_{bm} \approx 10^{-5} \text{ g}$ 的最小引力黑洞后在强烈的爆炸中消亡于普朗克领域。

B. 当外界 R_b 附近的温度 T_w 高于 R_b 上的阈温度，即高于 m_{ss} 的阈值温度 T_b 时，或者外界粒子的质量 m_{ssw} 大于 m_{ss} 时， m_{ss} 会很自然地吸收外界的高温能量以提高自己能级而被吸入黑洞内或者随着外界的高温高能量辐射一起流向低温的黑洞体内。当然 m_{ssw} 也会被吞噬进黑洞。黑洞于是扩大体积并降低温度和密度，这样一来，黑洞 R_b 与外界的温差就更加大，外界的高温高能量辐射和粒子就更容易被黑洞吞噬。黑洞一边吞噬外界能量-物质，一边膨胀体积和降低温度。直到吞噬完外界所有能量-物质为止，此后，黑洞即不再膨胀，转而向空空的外界发射霍金辐

射，并同时收缩体积和提高温度和密度，这个过程会不停地继续下去，直到最后收缩成为质量 $M_{bm} \approx 10^{-5}g$ 的最小引力黑洞在强烈的爆炸中消亡。

C. 由于黑洞内部的强大引力场，黑洞好像绝对黑体。因此，当黑洞视界半径 R_b 内的粒子的质量大于阈温的 m_{ss} 的粒子时，这些粒子是不可能成为霍金辐射而逃出黑洞的。换句话说，黑洞的霍金辐射只会发射等于和小于 m_{ss} 而在 R_b 内附近的能量和粒子。同理，黑洞只会吞噬外界高于阈温和质量大于 m_{ss} 并在 R_b 外附近的能量和粒子。至于向黑洞飞奔过来的粒子，不管其质量大于或者小于 m_{ss} ，黑洞会完全吞噬。一个太阳质量的黑洞 $M_{0b} = 2 \times 10^{33}g$ ，其视界半径 $R_{0b} = 2.96 \times 10^5 cm$ ，而 R_{0b} 上的阈温温度 $T_{0b} = 0.4 \times 10^{-6}k$ ，与其阈温相对应的粒子质量仅仅是， $m_0 = 0.6 \times 10^{-43}g$ 。

可见， m_0 是非常小的能量粒子，因此，这个不大的太阳质量的黑洞 M_{0b} 几乎可以吞噬其邻近的任何能量-物质。这就是黑洞可以几乎吞噬任何能量-物质的原因。

D. 再来分析当外界温度 T_w 等于黑洞 M_b 的 R_b 上的温度 T_b 时，黑洞是向外界发射霍金辐射而收缩呢？还是吞噬外界能量-物质而膨胀呢？这种 $T_w = T_b$ 看似稳定的动平衡情况其实是极不稳定的。首先，假设 m_{ss} 是对应于 T_b 阈温的粒子质量，那么，在黑洞内，大于 m_{ss} 的能量和粒子是不会逃出黑洞而奔向外界的，但在 R_b 附近而等于和大于 m_{ss} 的许多外界能量粒子却会被吸入黑洞。这样黑洞就会在吞噬外界能量-物质后而降低温度和膨胀体积，使黑洞与外界的温度差距加大，并使黑洞更易于吞噬外界能量-物质，而直到吞噬完外界能量-物质为止。此后，黑洞即不再膨胀，转而向空空的外界发射霍金辐射，收缩体积，这个过程会不停地继续下去，直到收缩成为质量 $M_{bm} \approx 10^{-5}g$ 的最小引力黑洞在强烈的爆炸中消亡。

E. 对黑洞视界半径 R_b 上霍金量子辐射 $m_{ss} = \kappa T_b / C^2$ 的物理意义的推测和探讨：此式表明，在阈温 T_b 下从 R_b 上辐射出去霍金量子 m_{ss} 是将其所有惯性质量完全转变成为了辐射能量 κT_b 而发射出去的，所以 R_b 的作用就像是一个能量过滤器，它限制大于 m_{ss} 的能量-粒子流出黑洞，也它限制外界小于 m_{ss} 的能量-粒子流入黑洞。在辐射和粒子能转换的条件下，这种能量的转变形式如下，设 ν —辐射的频率，

$$m_{ss}C^2 = \kappa T_b = h\nu/2\pi \quad (4f)$$

现在来看 m_{ss} 的位能 $Gm_{ss}M_b/R_b$ 能为辐射出去的霍金量子 m_{ss} 提供出多少能量，

$$\text{令 } Gm_{ss}M_b/R_b = \kappa T_{b1} \quad (4g)$$

但是对于黑洞来说， $GM_b/R_b = C^2/2$ ，所以， $m_{ss}C^2/2 = \kappa T_{b1}$ ，或者，

$$m_{ss}C^2 = 2\kappa T_{b1} \quad (4h)$$

$$\text{所以， } T_b = 2T_{b1} \quad (4i)$$

(4i)式表明， m_{ss} 的位能只为辐射出去的霍金量子提供了 1/2 的能量。因为所谓 m_{ss} 的全部惯性质量是由所有不同的能量提供的，除了其中的 1/2 的位能以外，还有那些能量贡献到 m_{ss} 的另外 1/2 的惯性质量中去以填补其空缺呢？

F. 黑洞与黑洞的碰撞和合并—小黑洞吞噬大黑洞：当两个黑洞 M_{b1} 和 M_{b2} 发生碰撞和合并时，虽然较小的黑洞 M_{b1} 由于其 T_{b1} 温度较高而向大黑洞发射少量的霍金辐射，但由于 m_{ss1} 很小，而大黑洞 M_{b2} 内有大量大于 m_{ss1} 的能量-物质粒子会被黑洞 M_{b1} 吞噬而膨胀。大黑洞 M_{b2} 也会因内部有小黑洞 M_{b1} 而扩张。最后当小黑洞 M_{b1} 吞噬完大黑洞 M_{b2} 所有能量-物质后。二者完全合并成一个更大的黑洞，这个新黑洞的质量 = $M_{b1} + M_{b2}$ ，而其视界半径 = $R_{b1} + R_{b2}$ 。新黑洞的归属如上面的 A 或 B。

G. 由上面的分析可见, 任何一个 M_b 的 R_b 上的温度 T_b 只是 R_b 的阈温值, 即该黑洞在 R_b 上与外界可交换量子 m_{ss} 的阈温值。因此, T_b 并不代表黑洞内部的温度。因为对于大黑洞来说, 其内部辐射能量与粒子的能量差别太大, 不能相互转换, 因而这种黑洞的内部处于热不平衡状态, 各处的温度是不一致的。即使当黑洞内部的辐射能量与物质粒子能量相当而能在各处互相转换达到热平衡时, 黑洞 R_b 上的辐射 m_{ss} 的阈温 T_b 也不可能与黑洞内部的温度达成一致。只有当整个黑洞收缩成为两个单个粒子 $M_{bm} \approx 10^{-5}g$ 时, 温度才会相同。

V. 黑洞的本质属性之三: 任何一个黑洞从它生成的一刻起直到它收缩成为两个质量 $M_{bm} \approx 10^{-5}g$ 的最小引力黑洞在强烈的爆炸中消亡时为止, 无论它如何变化, 收缩还是膨胀, 它始终遵循和服从(4d), (2ca), (2cb)和 (4e)等守恒公式, 而且永远是一个黑洞, 所有视界半径 R 相同的黑洞都具有相同的其它的各种参数值, 并有完全相同的黑洞属性。在这些公式中, 黑洞各个参数之间的关系都是单值的。当黑洞的一个参数确定之后, 其他的参数也就相应的唯一的被跟着确定了。而在视界半径 R 上具有相同参数的黑洞有完全相同的黑洞属性。因此, 比如说, 一个黑洞的质量 M_b 被确定之后, 其它的任何在视界半径 R 上的参数如 R_b , T_b 都不可能有两个不同的数值。因此, 黑洞的演变规律是完全一致的和唯一的, 而唯一的区别是由于黑洞吞噬外界能量-物质时, 不同质量的黑洞内部可有不同的膨胀速率, 即有不同的哈勃常数 H 。从这个意义上说, 黑洞的属性是宇宙所有物体中属性最简单的实体, 这就是本文能够用几个简单可靠的基本公式而能精确地计算出黑洞各个参数数值变化的根本原因。至于黑洞内部的状况—物体的种类和结构, 各物质物体之间的相互作用和运动状况, 愈大的黑洞, 内部的状况愈复杂, 但这些并不影响其作为黑洞而存在和变化, 不影响其服从黑洞在其视界半径 R_b 上的各个守恒公式, 如 $m_{ss}M = hC/8\pi G = 1.187 \times 10^{-10}g^2$ 。

VI. 黑洞的本质属性之四: 所有黑洞的最后归属不是“奇点”, 而是收缩成为两个质量相等的 $M_{bm} \approx 10^{-5}g$ 的最小引力黑洞在强烈的爆炸中消亡在普朗克领域。

A. 从第 4 节中可知, 无论是正在收缩的黑洞或者正在膨胀的黑洞, 其最后的命运就是收缩分裂成为两个相等的最小引力黑洞, 而在强烈的爆炸中消亡在普朗克领域。该黑洞质量 $M_{bm} \approx 10^{-5}g$, 因为任何一个黑洞, 无论它在死亡之前如何变化, 它必须服从黑洞的守恒公式(1c), (1d)和(4d) (4e)。从公式(4e), $m_{ss}M_{bm} = hC/8\pi G = 1.187 \times 10^{-10}g^2$, 可以得出黑洞质量 M_{bm} 与在其视界半径 R_b 上与 m_{ss} 的乘积等于常数。 m_{ss} 也是黑洞在 R_b 所能发射出的霍金辐射。因此, 当一个黑洞因发射出霍金辐射而不停地收缩时, 其收缩的最后极限只能是达到 $m_{ss} = M_{bm}$ 的极限时为止, 不可能发生 $m_{ss} > M_{bm}$ 的情况, 即部分不能大于整体, 正如一个人的腿的重量不可能重于整个人体的重量一样。在 $m_{ss} = M_{bm}$ 时, 从公式(4e)得出,

$$m_{ss} = M_{bm} = (hC/8\pi G)^{1/2} = (1.187 \times 10^{-10}g^2)^{1/2} = 1.058 \times 10^{-5}g \quad (6a)$$

从(6a)可见, 当黑洞收缩到 $m_{ss}M_{bm} = 1.187 \times 10^{-10}g^2$ 时, 黑洞还可以作最后一次的分裂而发射最后一次霍金辐射, 这是完全地一分为二, 分为两个完全相等的粒子而同时在宇宙最高的温度下爆炸解体湮灭。当黑洞 M_{bm} 最后发射出一个 $m_{ss} =$

$M_{bm}=1.058 \times 10^{-5}$ g 后。就再也不能发射霍金辐射粒子了，再发射就只能将本身 $M_{bm}=1.058 \times 10^{-5}$ g 整个质量当作霍金辐射粒子暴发出去。也不能再收缩了。因为如果再发射霍金辐射粒子而收缩必然造成 $m_{ss} > M_{bm}$ ，而这是不可能发生的，也违反黑洞的守恒公式的。所以一个不能再收缩的最小黑洞 $M_{bm} = 1.058 \times 10^{-5}$ g 就只能在其高温下爆炸解体和消亡。设最后分裂之前的黑洞质量为 M_{bm1} ，则

$$M_{bm1} = m_{ss} + M_{bm} = 2.116 \times 10^{-5} \text{g} \quad (6a1)$$

现在来看看黑洞在发射最后分裂之前的一次霍金辐射发射状况，假设那次所发射的霍金辐射粒子为 m_{ss2} 。

$$\text{则 } m_{ss2} = 1.187 \times 10^{-10} / 2M_{bm} = 1.187 \times 10^{-10} / 2 \times 1.058 \times 10^{-5} = 0.561 \times 10^{-5} \text{g}, \quad (6a2)$$

$$\text{而当时整个黑洞的质量就是 } M_{bm2} = 2M_{bm} + m_{ss2} = 2.677 \times 10^{-5} \text{g} \quad (6a3)$$

B. 任何黑洞收缩的极限是收缩到最小引力黑洞 $M_{bm} = 1.058 \times 10^{-5}$ g 为止，而后在高温下爆炸解体和消亡在普朗克领域，不会收缩到 R_b 趋于 0 的状况。而且，黑洞的收缩因为要遵循其黑洞的守恒公式，这几个守恒公式中没有有一个参数可以趋于 0 而导致另外一个参数发散成为无限大，所以不可能收缩成为“奇点”。再比如(4d)式中， $Rm_{ss} = h/(4\pi C) = 0.176 \times 10^{-37} \text{cmg}$ 。 m_{ss} 不可能为 0，因为 $m_{ss} = \kappa T_b / C^2$ ，根据热力学定律， T_b 不可能为 0，所以 R 就不可能成为无限大，而在最大的 $m_{ss} = M_{bm} = 1.058 \times 10^{-5}$ g 时，其最小的 $R_{bm} = 10^{-33} \text{cm}$ 。

C. 当大黑洞内部有小黑洞时，小黑洞必定吸收大黑洞内部空间内的能量物质而膨胀扩张其视界半径直到与大黑洞合而为一。而不是大黑洞继续收缩成为小黑洞，然后继续收缩下去成为“奇点”。

从守恒公式可见，如果大黑洞内部有小黑洞，该小黑洞也必定遵守其视界半径上的守恒公式。

设大黑洞的参数为 $M_b = R_b C^2 / 2G$ ，小黑洞的参数为 $M_s = R_s C^2 / 2G$ ，因为 $M_b > M_s$ ， $R_b > R_s$ ，所以在大黑洞 $R_b - R_s$ 的空间内，必定存在有 $M_b - M_s$ 的能量-物质。小黑洞 M_s 只发射极少量的霍金量子辐射，而在其外面大量的 $M_b - M_s$ 的能量-物质就会为具有强大引力的小黑洞 M_s 所吞噬，但大黑洞 M_b 发射霍金量子辐射比 M_s 更少更慢，所以 M_s 视界半径 R_s 就会不断地快速扩大直到 $R_s = R_b$ 为止。同样，如果大黑洞 M_b 内有許多小黑洞 M_s ，那么，在 M_b 与许多 M_s 外的空间内仍然存在有能量-物质，这许多小黑洞 M_s 就会一面相互碰撞合并，一面吞噬其外界的剩余的能量-物质，最后达到内部的许多小黑洞 M_s 合并成为一个整体而与 M_b 合而为一。因此，从现实的情况看，我们这个宇宙大黑洞内部只可能出现恒星级小黑洞，它们是由宇宙中最剧烈的超新星爆炸所产生的，但不可能在其内部出现“奇点”。

D. 宇宙中最小引力黑洞 $M_{bm} = 1.058 \times 10^{-5}$ g 的其它参数如下，可根据黑洞的守恒公式计算出来， τ_b —寿命， t_b —光通过黑洞半径的时间，黑洞比质子重的倍数 n_{bm} ，

$$M_{bm} = (hC/8\pi G)^{1/2} = 1.058 \times 10^{-5} \text{g}, \quad (6a)$$

$$R_{bm} = 2GM_{bm}/C^2 = (hG/2\pi C^3)^{1/2} \approx 1.61 \times 10^{-33} \text{cm}, \quad (6aa)$$

$$T_{bm} = M_{bm} C^2 / \kappa \approx 0.72 \times 10^{32} \text{k}, \quad (6ab)$$

$$M_{bm} C^2 \approx 10^{19} \text{GeV}, \quad (6ac)$$

$$\rho_{bm} \approx 6.4 \times 10^{92} \text{g/cm}^3, \quad (6ad)$$

$$t_b = 2GM_{bm}/C^3 = 5 \times 10^{-44} \text{s}, \quad (6ae)$$

$$\tau_b \approx 10^{-27} M_b^3 (s)^{1/2} \approx 10^{-42} \text{s} \quad (6af)$$

$$n_{bm} = M_{bm}/m_p = 10^{-5}/1.67 \times 10^{-24} \approx 10^{20}, \quad (6ag)$$

E. 现将上述 $M_{bm} = (hC/8\pi G)^{1/2} \approx 10^{-5} \text{ g}$ 最小引力黑洞的各种数值与引力量子论中的普朗克 Planck 数值比较如下。

引力量子论是将量子力学中的侧不准原理引入到引力理论中.由侧不准原理给出,^[3]

$$\Delta E \times \Delta t \approx h/2\pi \quad [3] \quad (6b)$$

将上式用于两个基本粒子的反应过程,

$$\Delta E = 2mC^2 \quad [3] \quad (6ba)$$

则产生或湮灭两个基本粒子的时间量级为,

$$\Delta t = t_c = h/4\pi mC^2 \quad [3] \quad (6bb)$$

t_c 称为康普顿时间 (Compton time),光穿过质量为 m 的基本粒子的史瓦西半径的时间为,

$$t_s = 2Gm/C^3 \quad [3] \quad (6bc)$$

t_s 称为史瓦西时间,一般来说, $t_c < t_s$,当 $t_c = t_s$ 时, 对应的质量为,

$$\text{普朗克质量 } m_p = (hC/8\pi G)^{1/2} = 1.058 \times 10^{-5} \text{ g} \quad [3] \quad (6c)$$

$$\text{普朗克长度 } L_p = (Gh/2\pi C^3)^{1/2} = 1.61 \times 10^{-33} \text{ cm} \quad [3] \quad (6d)$$

于是 $m_p/L_p = C^2/2G$, $T_p = 10^{32} \text{ k} \quad [3]$,

光通过质量为 m 的基本粒子的史瓦西半径的时间 t_s ,

$$t_s = 2Gm/C^3 \quad [3] = 5 \times 10^{-44} \text{ s} \quad (6e)$$

将此段内的各个公式及其所得的数值与上面 C 段中相对应的各个公式及其所得的数值相比较, 可以得出结论, 各相对应的公式和数值完全相等,

$$M_{bm} = m_p = (hC/8\pi G)^{1/2} = 1.058 \times 10^{-5} \text{ g}, \quad R_{bm} = L_p = (Gh/2\pi C^3)^{1/2} = 1.61 \times 10^{-33} \text{ cm},$$

$$t_b = t_s = t_c = 2GM_{bm}/C^3 = 5 \times 10^{-44} \text{ s}, \quad M_{bm}/R_{bm} = m_p/L_p = C^2/2G,$$

$$T_{bm} = T_p = M_{bm}C^2/\kappa \approx 0.72 \times 10^{32} \text{ k}, \quad (6f)$$

(6f)式完全证明当所有的黑洞最后收缩而分裂至两个 $M_{bm} \approx 10^{-5} \text{ g}$ 时, 各自都到达了 Planck Era 而量子化, 其湮灭的时间应符合康普顿时间 $t_c \leq t_s$, 在此领域,

“量子效应将起作用, 时间将不可能准确地测量出来, 经典的引力和时空概念失效。”^{[3] [5]}, 也就是说, 广义相对论到此就已失效。更不可能收缩到广义相对论中称之为现有物理定律所无法了解的“奇点”。^[5]同时, 因为 $M_{bm} \approx 10^{-5} \text{ g}$ 整体是一个 10^{32} k 的宇宙中最高温的能量粒子, 它内部的引力因发不出小于本身质量的 m_{ss} 而无法再收缩, 从而只能在最高温的辐射压力下爆炸粉碎消亡。

由(6b)式看,为什么刚刚由 $M_{bml} = 2.116 \times 10^{-5} \text{ g}$ 分裂出来的两个 $m_{ss} = M_{bm} = 1.058 \times 10^{-5} \text{ g}$ 最小粒子黑洞必定各个爆炸解体消失而不会重新聚合并在一起而合而为一呢? 首先, 两个粒子黑洞合并需要大于 2 倍 $t_s = t_c$ 的时间才能传递其引力, 而其湮灭解体的时间 t_c 只有 $t_c \leq t_s$ 。其次, 因分解后的 m_{ss} 和 M_{bm} 的温度已经高于 M_{bml} 在分解前的温度的 1 倍, 二者的热排斥力使其无法再接近。第三, m_{ss} 和 M_{bm} 二者内部都已成为一个不可能再收缩的整体, 即宇宙最高温的整体能量粒子, 又处在自由空间, 如果外部没有如此巨大的力量迫使二者接近, 那么, 内部能量量子之间的热排斥力和不相容必然使其爆炸粉碎消亡。

F. 最小黑洞 $M_{bm} \approx 10^{-5} \text{ g}$ 的整体惯性能量 E_b ,

$$E_b = M_{bm}C^2 = 10^{-5} \times 9 \times 10^{20} = 10^{16} \text{ g} \cdot \text{cm}^2/\text{s}^2 = 10^{19} \text{ GeV} \quad (6g)$$

而黑洞内部一个粒子的热能或者发出一个霍金辐射粒子所需的能量 E_{b1} ,

$$E_{b1} = \kappa T_{mb} = 1.38 \times 10^{-16} \times 0.72 \times 10^{32} = 10^{16} \text{ g} \cdot \text{cm}^2 / \text{s}^2 = 10^{19} \text{ GeV}$$

$$= hC / 4\pi\lambda = 6.63 \times 10^{-27} \times 3 \times 10^{10} / (4\pi \times 1.61 \times 10^{-33}) = 10^{16} \text{ g} \cdot \text{cm}^2 / \text{s}^2 = 10^{19} \text{ GeV} \quad (6h)$$

可见, 黑洞 M_{bm} 的粒子数 $n_b = E_b / E_{b1} = M_{bm} C^2 / \kappa T_{mb} = 1$ (6i)

既然最小黑洞 $M_{bm} \approx 10^{-5} \text{ g}$ 的整体已是一个基本粒子, 那么, 它的整体温度就是 T_{bm} . $T_{bm} = 0.72 \times 10^{32} \text{ k}$, 因此, 可以估算出它的热压力 P_{mb} 已达到,

$$P_{bm} = \rho_{bm} \kappa T_{bm} / M_{bm} = 6.4 \times 10^{92} \times 1.38 \times 10^{-16} \times 0.72 \times 10^{32} / 10^{-5} = 6.36 \times 10^{113} = 10^{107} \text{ atm} \quad (6j)$$

G. **结论:**所有的黑洞最后都会发射霍金辐射 $m_{ss} = \kappa T_b / C^2$ 而收缩蒸发下去, 只不过大的黑洞由于 T_b 很低, 所以沸腾得较慢, 它们的辐射非常微弱, 因此令人难以觉察。但是随着黑洞逐渐变小, 这个过程会加速, 以至最终失控。黑洞收缩时, 在其视界半径上引力虽然会变大, 但热压力增加的更大。因此会产生和排斥出更多更重的逃逸粒子, 从黑洞中带出去的能量和质量也就越多。黑洞反而收缩的越来越快, 促使蒸发的速度变得越来越快, 当黑洞质量减少达到 $M_{bm} \approx 10^{-5} \text{ g}$ 时, 因 M_{bm} 等于普朗克粒子 m_p 而达到普朗克量子领域, 温度达到 $T_{bm} \approx 0.72 \times 10^{32} \text{ k}$, 黑洞就会在普朗克量子领域中爆炸毁灭, 由辐射自己的质量而完全蒸发掉。因为 M_{bm} 已经成为一个完整基本粒子 m_p , 其湮灭的时间应为康普顿时间 $t_c \leq t_s$ 。

第一. 比较 (6f) 式与 (1e) 式, 可见二者是完全等同的。这完全证明当黑洞收缩到 $M_{bm} \approx 10^{-5} \text{ g}$ 的最小引力黑洞而最后爆炸消亡时, 它就踏进量子引力时代— Planck Era, 而且 T_{bm} , R_{bm} 也完全与普朗克时代的 T_p , L_p 的数值相符合。反过来说, **Planck Era (普朗克时代) 的物质结构状态就是最小引力黑洞爆炸消亡时的量子状态。**这再次证明黑洞塌缩的最终归属不是广义相对论的结论: “奇点”, 而是 Planck Era。“奇点”是一个无法量度的物理量和一个非理性的概念, 它的产生和转换与真实的物理世界无法发生可观测量的因果联系。“奇点”只能由上帝创造。

第二. 从 (6i) 式 $M_{bm} C^2 = \kappa T_{bm}$ 和 (6a), (6a1) 来看, 当黑洞收缩到普朗克领域, 而分裂成为两个 $M_{bm} \approx 10^{-5} \text{ g}$ 的最小黑洞时, 每个黑洞 M_{bm} 整体就是一个高温高能量粒子, 黑洞不可以将其内部的惯性能分裂出一部份转变为霍金辐射-高温量子, 更无法再收缩而发射出等于或大于本身质量的霍金辐射。再从 (6a), (4e) 来看, 比 M_{bm} 本身小的霍金辐射又根本发射不出来。从 (1d) 式 $T_{bm} \approx 10^{27} / M_{bm}$ 来分析, 就是说, 当 $M_{bm} \approx 10^{-5} \text{ g}$ 时, M_{bm} 的引力收缩将剧烈地增高霍金辐射的温度和热斥力。由此可见, $M_{bm} \approx 10^{-5} \text{ g}$ 的最小黑洞内部所能产生的引力收缩力必然剧烈地增高内部的热斥力。因此, M_{bm} 唯一的出路是将整个黑洞爆炸解体, 使其全部的惯性能分散转变为宇宙最高温的许多高能量量子。宇宙中所有物体的爆炸解体都是其内部热压力(热能)突然急剧增高而突破其引力约束和其结构间结合力的结果。

从公式 (2ca) 可知,

$$T \times R = (C^3 / 4GM) \times (h / 2\pi\kappa) \times (2GM / C^2) = Ch / 4\pi\kappa = 0.1154 \text{ cmk} \quad (2ca)$$

于是, $\Delta T_b = -0.1154 \Delta R_b / R_b^2$ (6k)

从上面可知, 当黑洞收缩到 $M_{bm} = 10^{-5} \text{ g}$ 时, $T_{bm} \approx 0.72 \times 10^{32} \text{ k}$, $R_{bm} = L_p = 10^{-33} \text{ cm}$, 因为 M_{bm} 不能再发出霍金辐射, 如果 ΔR_b 收缩一个极小量 ε , 即 $\Delta R_b = R_b - \varepsilon \approx R_b$, 从 (6k) 可见, 温度的增加量 $\Delta T_b \approx 0.1154 / R_b \approx 10^{32} \text{ k}$. 可见 M_{bm} 只能爆炸消亡。所以霍金说, M_{bm} 只能爆炸成为极高能量的 γ 射线。

第三. 广义相对论在普朗克领域失效的根本原因: 按照广义相对论, 物质粒子之间的引力是绝对存在的, 可以收缩小到任何尺寸, 甚至到无穷小的尺寸, 如果真实世界的物质粒子间的距离可以无限小地收缩下去, 当然会达到“奇点”。但是(6i)式表明, 当黑洞收缩到 $M_{\text{bm}} \approx 10^{-5} \text{ g}$ 最小黑洞的普朗克尺寸时, 其所有物质的引力能都会因爆炸解体而变成许多的高温热能的量子分散在普朗克自由空间, 它们之间的引力或许变成不连续和不确定了, 或许因引力微弱而不能对抗其热排斥力而无法重新聚集在一起再继续塌缩下去了。所以普朗克尺寸就是广义相对论所能达到的最小极限尺寸。在小于等于此尺寸的领域, 广义相对论无效。广义相对论可以宣告牛顿力学在接近光速运动时失效。同样, 黑洞量子理论也可以宣告广义相对论在普朗克领域内失效。现在尚只从理论的推论知道黑洞收缩到最后能进入普朗克领域, 除此之外, 现代科学对普朗克领域还知之甚少。未来人类也未必能观测到普朗克领域的物质结构及其运动状态。人类对宇宙和物质的认知有无极限?

第四. 既然所有黑洞的最后命运是塌缩成为 $M_{\text{bm}} \approx 10^{-5} \text{ g}$ 的最小黑洞而爆炸消亡, 而不是塌缩为“奇点”, 那么, 坚持根据广义相对论的数学公式推演到极端而存在“奇点”的结论的学者们就是非理性的, 他们只不过是维护自己对广义相对论的信仰而已, 很明显, 广义相对论在微观的普朗克量子领域是失效的。在真实物理世界中, 物质的引力塌缩会在其内部出现结构和运动状态的改变, 这就是相变(临界点), 而没有“奇点”。物体进入普朗克领域就是发生“相变”。现有的数学尚无法将物质结构转变的临界点和其一般的运动状态结合在一个统一的方程内加以描述和解决。统一微观世界与宏观世界的终极理论和数学方程也许超越人类的认识能力的范围。

VII, 恒星级黑洞 $M_{\text{bh}} \approx (1.9 \sim 15 \sim 50) M_{\odot}$: 所有宇宙中独立存在的实体, 特别是能够较长期存在的个体, 其内部结构都存在对抗自己引力塌缩的机制, 即其内部的引力与斥力, 塌缩力与其对抗力能够达到较长期的平衡和稳定的结果, 各种星体和黑洞也不例外。物体和各种能量粒子团的本性表明: 在其体积收缩时所增强的热压力是引力如影随形的对抗力量, 因此, 只要能够保持其热量不流失和温度不降低, 它就不会收缩。其次, 物质的结构之间的结合力和其组成的粒子之间的不相容也对抗着引力的收缩, 即以结构的内能对抗其收缩的引力能。黑洞在宇宙中长期存在的事实就表明其内部斥力与引力达到了极好的平衡, 所以能保持长期的稳定存在, 这就否定了黑洞内部具有无法平衡的无穷大密度的物理量的“奇点”存在的可能。

质量小于 10^{15} g 的物体中, 其氢原子的数目 $n_{\text{p}} < 10^{15} / 1.67 \times 10^{-24} = 10^{39}$. 由于物质质量小, 所产生的引力往往能为该物体的外层电子结构所承受, 而形成不改变结构的热胀冷缩, 因而可以没有一个较坚实的核心。

A. 在宇宙中独立存在和运行的物体都有较大的质量。一个典型的彗星质量也有大约 10^{15} g . 太阳的质量 $M_{\odot} = 2 \times 10^{33} \text{ g}$, 这些大质量的星体为了阻止外层物质向中心的引力塌缩, 用三种方式共同对抗外层物质向中心的引力塌缩。

第一: 小于 $0.08 M_{\odot}$ 质量的行星: 其中心都有密度较大温度较高的较坚实的核心。它一方面承受外围物质压力以对抗引力的塌缩, 一方面又维持对外围物质的足够引力使其不会逃离出去, 以保持该物体的整体的稳定性。这种气体或者固态行星的中心多为固态或液体的铁所形成较坚实核心以平衡和对抗外围物质的引力塌缩。

第二：质量大于 $0.08 M_0$ 天体会成为恒星：这类恒星能够点燃其中心的核聚变，只要核聚变所提供的热能能够保持住高温高压不下降，就能长期地对抗物质向其中心的引力塌缩，

太阳和正在其中心进行核聚变的所有恒星，都是用其中心核聚变所提供的高能量以维持其内部的高温高压，能量向外辐射的流失与核聚变供给的能量的平衡能长期地对抗其引力塌缩达到数亿年至百亿年之久。最后，只有当氢被耗尽时，内核收缩，包层膨胀形成巨大红色星球--红巨星，再过几千年后，太阳将坍缩成一个逐渐冷却的白矮星。

太阳内部稳定的状态使得我们能够估算出太阳中心的压力 P_s ：由(1b)式. 太阳中心密度 $\rho_s \approx 10^2 \text{g/cm}^3$ ，太阳中心温度 $T_s \approx 1.5 \times 10^7 \text{k}$ ，

$$P_s = \rho_s \kappa T_s / m_p = 10^2 \times 1.38 \times 10^{-16} \times 1.5 \times 10^7 / 1.67 \times 10^{-24} \approx 1.5 \times 10^{11} \text{ atm.} \quad (7a)$$

这就是说，太阳中心的压力 P_s 是地球表面压力的 1.5×10^{11} 倍。

第三：不同质量的致密天体结构内粒子之间的泡利不相容原理能够对抗其内部物质塌缩成为“奇点”：宇宙原始星云含有 3/4 氢，只要其质量 $M > 0.08 M_0$ ，它们就能靠自己引力的收缩达到大约高于 10^7k 的高温以点燃其中心核聚变，从而长期对抗其引力收缩. 等到所有氢燃烧完毕时，在通过红巨星或者新星超新星爆发之后，它的余烬（星核） M_r 的塌缩根据其质量的大小会形成不同的结果：白矮星，中子星，黑洞或成为一团尘埃. 大致上来说原始质量小于 $3.5 M_0$ 的恒星，可能变成白矮星^[9]. 质量在 $(3.5 \sim 8) M_0$ 之间的，可能成为“中子星”^[9] 质量大于 $8 M_0$ 倍或更大的恒星，可能最终将塌缩成为“黑洞”。^[9] 但还有多种不同的说法，尚无共识。

B. 白矮星：白矮星的质量 M_w ，当老年原始恒星演变到最后阶段，它的余烬（星核） $M_r < 1.44 M_0$ ，会成为白矮星. 这就是钱德拉塞卡极限. 白矮星的密度 ρ_w ，原子之间的距离 d_w ，单位体积内的质子数 n_w ，白矮星的表面温度 $T_w \approx 10000 \text{k}$ 。

$$\rho_w \approx 10^6 \text{g/cm}^3, \quad d_w \approx 1.2 \times 10^{-10} \text{ cm}, \quad n_w = 10^{30} \text{ 个/cm}^3. \quad M_w < 1.44 M_0 \quad (7b)$$

原子核的直径 d_a 尺寸大约是 10^{-13} cm ，所以在白矮星内部，原子与原子之间尚有不小的空隙与距离，使电子脱离了原子轨道变为自由电子，这些空隙间成为充满电子的海洋。由于电子间泡利不相容原理而产生的“斥力”能抗衡住万有引力的塌缩，形成密度为 10^6g/cm^3 左右的白矮星。但是白矮星是非常稳定的，释放能量以降低温度和冷却极其缓慢，经过数千亿年之后，白矮星才会冷却到无法发光，成为黑矮星。但是目前普遍认为宇宙的年龄（150亿年）不足以使任何白矮星演化到这一阶段。如白矮星有伴星而形成密近双星时，白矮星会从其伴星中吸取物质，当白矮星的质量增大到 $1.44 M_0$ 接近钱德拉塞卡质量极限时，会成为碳-氧白矮星通过聚变中心的碳和氧所引发的热核爆炸能产生 Ia 型超新星大爆炸，而可能将整个白矮星炸得粉碎而抛掷空中。

C. 中子星：中子星质量 M_n 的下限 $M_n > 0.1 M_0$ ， M_n 的上限 $M_n = (1.5 \sim 2) M_0$ ，当超新星爆发之后，它的余烬（星核） $M_r > 1.44 M_0$ 而超过钱德拉塞卡极限，即 $M_r = (1.5 \sim 2) M_0$ 时，会成为中子星。由于中子星表面是固体，很有可能是固态铁。中子星的构造分为 4 层，其密度由外层到中心核的密度大致是 $\rho_n \approx 5 \times 10^{11} \sim 5 \times 10^{15} \text{ g/cm}^3$ ，相应地原子之间的距离 $d_n \approx 1.2 \times 10^{-13} \text{ cm}$ = 原子核的直径，所以在中子星内，原子核是紧紧地挤在一起没有任何“真空”留下了。电子不再可以在原子核外活动，

而是被挤进核内使质子变成为中子。特别是其核心的核子因能量的增高已成为超子的海洋，能够承受外层物质的引力塌缩。最大中子星的直径大约为33公里。

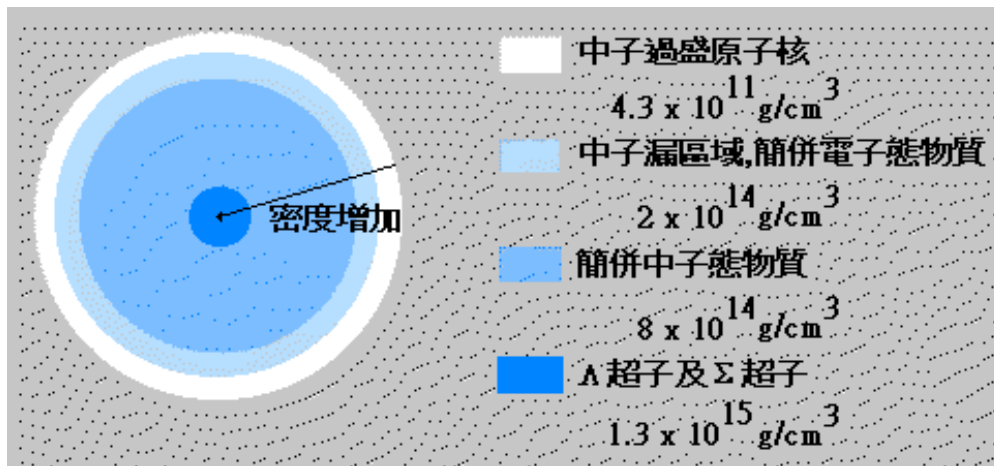
中子星 M_n 的一些状态参数如下：

$$M_n = (1.5 \sim 2)M_0, \rho_n \approx 10^{14} \sim 10^{15} \text{ g/cm}^3, d_n \approx 1.2 \times 10^{-13} \text{ cm}, n_n = 10^{39} \text{ 个/cm}^3. \quad (7c)$$

中子星的表面温度 $T_n \approx 10^7 \text{ K}$ ，因此，其表面的热压力 P_n 估计大到：

$$P_n = \rho_n T_n k / m_p = 10^{15} \times 10^7 \times 1.38 \times 10^{-16} / 1.67 \times 10^{-24} \approx 10^{24} \text{ atm}. \quad (7d)$$

这就是说，超新星的爆炸力 $P_n \approx 10^{24} \text{ atm}$ 一方面会压缩恒星的星核成为中子星，另一方面将其外壳以极高的速度炸飞而抛向外空。由于 P_n 过高造成的不稳定，使其高速旋转而快速释放能量-物质，快速降温变为冷星。 $10^{15} \times 10^7 \times 1.38 \times 10^{-16} / 1.67 \times 10^{-24}$



中子星的结构图(圖: LKL Astro-Group)^[13]

² 而 $1.3 M_0 \sim 2M_0$ 中子星不太可能自己塌缩成为黑洞，因为其外层温度非常高，旋转非常快，无法向内塌缩，而核心虽然密度高，但质量小，不可能在核心形成黑洞。中子星只有在吸收其大质量伴星的物质后，如果质量超过奥本海默-沃尔科夫极限，即 $M_n \geq 3M_0$ 时，中子间的“泡利斥力”顶不住万有引力的作用，将继续坍塌而成为夸克星，或者成为黑洞。如果中子星外部没有伴星的物质可供吸收，就不会增大，而在快速降低温度后而成为一个黑星。

D. $M_b \approx (1.9 \sim 15 \sim 50) M_0$ 的恒星级黑洞的形成：

第一. 原始质量 $> 8 M_0$ 倍的恒星在超新星爆发之后，只有当它的余烬（星核） $M_r \geq 3M_0$ (奥本海默-沃尔科夫极限) 时， M_r 才有可能塌缩成为一个 $> 3M_0$ 的恒星级黑洞。也有可能是在 M_r （星核）的核心先塌缩成为 $1.9 M_0$ 小黑洞，它在形成之后，就会很快地吞噬其外围的高密度能量-物质或者其伴星的物质而变成 $M_b > 3 M_0$ 的恒星级更大黑洞。“伍德介绍，形成黑洞有两种方式，一是质量非常大的恒星爆炸后产生黑洞，二是两个中子星合并后形成黑洞。基本上可以认为有两种不同类型的黑洞，一类是质量相当于太阳质量3~50倍的小黑洞，另一类是质量相当于太阳质量100万~10万亿倍的大黑洞。”^[11] “质量介于两者之间的黑洞是否存在，科学家们一直有争议。但近来美国密歇根大学的研究人员在《天体物理杂志通信》上发表论文说，位于双鱼座“梅西尔74”(M74)星系的一个黑洞，其质量可能相当于1万个

太阳，远远大于恒星级黑洞，但比“超级黑洞”小得多，符合中等质量黑洞的标准。

第二. 从理论的计算来看，黑洞 $M_{bh} \approx 1.9 M_0$ 是可能达到的恒星级最小黑洞，但它是极难出现和存在的：从上面中子星的结构图可见，其核心已被压缩成为超子（另一种说法是固态中子）。只是由于这个核心的质量较小，而不能形成黑洞。取中子星核心的密度 $\rho_n \approx 5 \times 10^{15} \text{g/cm}^3$ 。现求具有如此密度 $\rho_b > \rho_n \approx 5 \times 10^{15} \text{g/cm}^3$ 的黑洞应当具有的质量 M_{bh} 。按公式(1e)和(1f)，

$$R_b = C[3/(8\pi G\rho_n)]^{1/2} = 0.189 \times 10^{-4} C, \quad \therefore M_{bh} \geq R_b C^2 / 2G \approx 3.8 \times 10^{33} \approx 1.9 M_0, \quad (7h)$$

“美宇航局戈达德太空飞行中心天文学家尼古拉·沙波什尼科夫及同事在加州洛杉矶举行的美国天文学会高能天体物理分会的会议上公布了这一发现。这个“小”黑洞的代号为 **XTE J1650-500**，现这个黑洞的质量仅仅是太阳质量的 **3.8 倍**，比之前保持着最小质量记录的黑洞小了不少，它是太阳质量的 6.3 倍。那么最小黑洞的质量究竟有多少？按照天文学家估计，应是太阳质量的 1.7 倍至 2.7 倍。比这还小的天体只能是中子星了。找到迫近这一下限的黑洞，有助于物理学家更好地理解物质在这种极端环境下被碾碎时的表现。”^[8]

第三. 恒星级黑洞 $M_b \approx (2 \sim 3) M_0$ 的形成：由于现在在宇宙中尚未观测到这种级别的恒星级黑洞，很难以判断其形成的机制。很有可能是大质量恒星在超新星爆炸后，形成双中子星或其它密近双星系统而后碰撞塌缩变成 $M_b \approx (2 \sim 3) M_0$ 的恒星级黑洞。

第四. 夸克星：也许中子星在冷却后能逐渐吸收外界物质或与其伴星碰撞和降低温度后，可能先成为夸克星而后有可能再塌缩成为黑洞，现在已观测到在宇宙中存在着几个夸克星，如超高密度星 RX J1858-3754，但其寿命不会很长，这也许是在宇宙空间很难找到夸克星的原因。它一方面会吞噬外界能量-物质，另一方面，它也无足够大的引力禁锢其外层能量使其不致流失而保持温度。因此夸克星有可能会吞噬其伴星与外界能量-物质和降低温度而塌缩成为黑洞，当然也有可能在外界能量-物质可被吞噬的情况下向外抛射能量-物质而最后消亡。

E. 中子星与恒星级黑洞的比较：(a)。中子星和黑洞的重要不同之处，是中子星有一个固体表面，核心是超子。而黑洞则没有固体表面。(b)。中子星的逃逸速度约为光速 0.8C。而黑洞的逃逸速度为光速 C。(c)。中子星的表面温度非常高，热压力非常大，旋转非常快，辐射 χ 射线、 γ 射线和可见光，黑洞的表面温度低，旋转慢。(d)。中子星的典型质量为 $(1.5 \sim 2) M_0$ ，恒星级黑洞的质量按照现有的观测从 $3.8 M_0 \sim 15 M_0$ ，有可能达到 $50 M_0$ ，因为最近发现了质量 $\approx 150 M_0$ 的巨型恒星。

1.75 M_0 的中子星与黑洞的比较：“Strohmayer 所发现的中子星属于恒星系 EXO 0748-676 的一部分，坐落在南半球天空的飞鱼星座，离地球有 30000 光年的距离。这颗中子星的半径约为 7 英里（11.5 公里），质量约为太阳的 1.75 倍。”^[12]，该中子星的质量 $M_{n1.75} = 1.75 M_0 = 3.5 \times 10^{33} \text{g}$ ，则其它的参数值计算是，

$$M_{n1.75} = 1.75 M_0 = 3.5 \times 10^{33} \text{g}, R_{n1.75} = 11.5 \times 10^5 \text{cm}, \rho_{n1.75} = 5.5 \times 10^{14} \text{g/cm}^3, \\ T_{n1.75} \approx 10^7 \text{k}, \quad (7e)$$

设一个黑洞的质量 $M_{b1.75} = 1.75 M_0 = 3.5 \times 10^{33} \text{g}$ ，相应地各参数值计算是，

$$M_{b1.75} = 1.75 M_0 = 3.5 \times 10^{33} \text{g}, R_{b1.75} = 5.16 \times 10^5 \text{cm}, \rho_{b1.75} = 5.75 \times 10^{15} \text{g/cm}^3, \\ T_{b1.75} = 0.23 \times 10^{-6} \text{k}, \quad (7f)$$

由此可见, $R_{b1.75} = 1/2 R_{n1.75}$, $\rho_{b1.75} = 10 \rho_{n1.75}$, $T_{n1.75} \approx 10^{12} T_{b1.75}$ (7g)

由(7g)可见, 二者的巨大差别在于温度, 这表明中子星抛射出去的粒子的能量 $\approx 10^{12}$ 倍黑洞的霍金辐射粒子的能量。

F. 进一步的分析和结论, 恒星级黑洞内部不可能出现“奇点”: 第一. 在真实的宇宙物理界, 宇宙本身就是一个宇宙黑洞。^[18]无论是白矮星中子星和恒星级黑洞的形成都是由于恒星内部核聚变到最后, 当氢燃烧耗尽时, 所产生的爆炸或新星或超新星爆炸对其核心(余烬)产生巨大的内压力使其塌缩而成。这些致密星体形成和能长期稳定地存在本身就表明靠巨大星云物质自然的引力塌缩和新星或超新星爆炸只可能塌缩出宇宙中密度最大的(3.8~50) M_{\odot} 的小恒星级黑洞。在这些恒星级黑洞内部, 已经没有再产生核聚变的条件, 不可能出现密度更高的更小的黑洞, 怎么可能再出现奇点呢? 万一有我们尚不知道原因在其内部塌缩出小黑洞, 因为它们有极长的寿命。所以只能吞噬其外界周围的能量-物质而膨胀和降低密度, 最后与原黑洞合而为一。第二. 目前在宇宙中所观测到的恒星级黑洞的质量从(3.8~15) M_{\odot} , 其相对应的密度为从 $10^{15} \text{g/cm}^3 \sim 8 \times 10^{13} \text{g/cm}^3$ 。这就是说, 恒星级黑洞的密度与中子星的密度几乎是相同的, 即内部都有超子。只不过比中子星稍大的黑洞内部的超子比中子星内多许多而已。因此, 黑洞内部一定不会按照广义相对论的极端要求而产生“奇点”。中子星的核心密度高到使核子已变成超子而无法塌缩成为黑洞, 这证明超子之间的泡利不相容原理具有极其强大的对抗引力塌缩的能力, 因为两个超子之间的距离小于 $0.8 \times 10^{-13} \text{cm}$ 时核力表现为斥力。^[17]加上黑洞内在几乎不向外泄露辐射热能的条件下应比中子星能更有力地对抗其内部引力塌缩, 没有什么力量使其塌缩成为奇点。由(7b)式可知, 如果有 $1.9 M_{\odot}$ 的黑洞存在, 其密度也不过是等于中子星核心的密度 $\rho_n \approx 5 \times 10^{15} \text{g/cm}^3$, 而 $1.9 M_{\odot}$ 的黑洞的寿命约为 10^{66} 亿年, 比中子星的寿命更长得多, 这表明黑洞比中子星更加稳定。中子星的核心是超子, 而没有出现“奇点”, 同样是更多有超子而更稳定更长寿命的黑洞内更不可能反而出现“奇点”。更何况现在在宇宙中找到的最小黑洞只是 $3.8 M_{\odot}$, 其平均密度比 $1.9 M_{\odot}$ 的黑洞已经降低 4 倍而约为 10^{15}g/cm^3 , 就是说, 其核心可能已不是超子而是中子和质子了, 其内部更不可能出现奇点, 而比 $3.8 M_{\odot}$ 更大的恒星级黑洞因为其密度更低, 就更无可能在其内部塌缩出来奇点。第三. 既然黑洞时刻都在因发射霍金辐射而收缩其视界半径, 这说明黑洞内部空间不是如广义相对论所说的真空, 不是内部空间的所有能量-物质都集中到其中心的“奇点”, 而是充满能量-物质。只有这样, 黑洞的视界半径收缩到任何尺寸时, 才都会有霍金辐射发出。第四. 由(4c)式可见, 既然任何一个黑洞的平均密度 ρ_{ba} 只等于 6 倍的视界半径上的密度 ρ_{be} , 即 $\rho_{ba} = 6 \rho_{be}$, 那么, 恒星级黑洞中心就不可能出现和存在密度为无限大的“奇点”。这同时也意味着恒星级黑洞内不可能出现比超新星爆炸还强烈的爆炸, 所以既不可能在其中心塌缩出 $\rho \approx 10^{54} \text{g/cm}^3$ 的微型黑洞 $m_{bm} \approx 10^{15} \text{g}$, 更加不可能塌缩出密度高达 $\rho \approx 10^{94} \text{g/cm}^3$ 的 $M_{bm} \approx 10^{-5} \text{g}$ 宇宙最小黑洞, 再从(6j)式可知, $M_{bm} \approx 10^{-5} \text{g}$ 最小黑洞的热压力高达 10^{107}atm 。就是说, 恒星级黑洞内部根本不可能塌缩出 $M_{bm} \approx 10^{-5} \text{g}$ 最小黑洞, 那就绝无可能塌缩出“奇点”了。第五. 只要能够保持住物质物体的热能不损失, 温度不下降, 它就不会收缩。恒星级黑洞内部不可能出现“奇点”, 是因为一个太阳级质量的黑洞, 其寿命竟长达 10^{65} 年。具有如此长寿命的黑洞的内部是极其稳定的, 不可能

出现有无穷大密度的“奇点”存在，因为黑洞有极强大的引力，而近似绝对黑体，连光都逃不出黑洞，所以有温度的粒子也逃不出黑洞，这样，黑洞内部就能保持其温度成为对抗引力的塌缩的主要力量，从而能够保持极长的寿命。但它还是会因霍金量子辐射而极其少量和缓慢地失去能量而收缩。大黑洞由于密度的大幅降低内部更加稳定而更难塌缩，其寿命能维持非常的长久，如一个太阳级质量的黑洞， $M_0 = 2 \times 10^{33} \text{g}$ ，按照(6b)式，其寿命竟长达 10^{65} 年，而小黑洞由于辐射出高能量的霍金量子辐射，所以寿命变得很短。假如有一个小黑洞的质量 $M_b = 1000 \text{ton}$ ，其寿命就只有 1 秒。宇宙中一半以上的恒星都有伴星，成为双星系统，因此，各种恒星级黑洞在塌缩形成之后，就会马上吞噬其外界的能量-物质而膨胀以降低其密度，长成更大的黑洞。宇宙中也发现有几乎吞噬完其周围能量-物质后而孤独地在宇宙空间漂浮的黑洞(其外界并非绝对真空，只是能量-物质极其稀少而已)。第六. 参见第 VI 节的 C 段。

总之，在恒星所塌缩成的恒星级黑洞内，其中心所能达到的最高密度 $\approx 5 \times 10^{15} \text{g/cm}^3$ ，即 $1.9M_0$ 黑洞由均匀的超子构成的中心的密度。比 $1.9M_0$ 黑洞更大黑洞，其中心的密度就更低。这表明宇宙中超新星爆炸时的极限压力对其余烬 M_r 的中心所能形成的最高密度不会高于 $5 \times 10^{15} \text{g/cm}^3$ 。所以，在恒星级黑洞内部根本不可能塌缩出更小的黑洞，因为在其内部根本不可能再发生超新星爆炸和其它更剧烈的爆炸，更绝无可能塌缩出奇点。但是，各种大小不同黑洞形成的机制和过程现在还不清楚。普遍认为的是并非所有超新星爆炸都会形成中子星。而且当前的超新星爆发理论尚未完善，不能说明是否恒星的余烬(星核) M_r 可能被直接压缩成为黑洞而不经超新星爆发，是否有超新星形成的黑洞，以及恒星的初始质量和演化终点的准确关系。

1974 年乔治 (Georgi) 和格拉肖 (Glashow) 提出了把强、弱、电三种相互作用统一在一起的 SU(5) 大统一理论, 按照该理论, 质子是不稳定的, 它的寿命约为 $10^{28} \sim 2.5 \times 10^{31}$ 年, 但实际上美国, 印度和日本等国的实验尚未有确切的公认的证据证实质子有衰变的迹象。因此在现实宇宙中, 我们可以大致地认为恒星所塌缩成的史瓦西恒星最小黑洞 $M_{bh} \approx 1.9 M_0$ (参见 VII 节) 应该是中子(质子)被挤压到近乎极限而增高了能量变成为超子, 而仍然是“核粒子”, 但可能没有达到破坏其内部的夸克链成为自由夸克, 只可能是将夸克之间的距离压缩短了而已,

VIII. 微型黑洞 $m_{bm} \approx 10^{15} \text{g}$: 早在 1971 年, 霍金首先提出了“微型黑洞”的概念, 认为宇宙形成初期, 一些小团块物质在“宇宙浴缸”的巨大压力下, 会收缩成为不同尺度的黑洞, 有的是由一座山收缩而成的, 其体积仅相当现在的一颗基本粒子, 在宇宙大爆炸发生之际, 各种质量的黑洞都是有可能生成的; 因此, 宇宙空间里目前仍可能存在着“微型黑洞”这也就是“原初宇宙小黑洞 m_{bo} ”。

这样, 如果取(2c)式中黑洞辐射霍金粒子的质量 $m_s =$ 质子的质量 $m_p = 1.67 \times 10^{-24} \text{g}$, 则可得出一个史瓦西微型黑洞 m_{bm} , 其各种参数值如下:

该黑洞视界半径 $r_{bm} = 1.0557 \times 10^{-37} / 1.67 \times 10^{-24} \text{g} = 0.632 \times 10^{-13} \text{cm} =$ 原子核的半径,

该黑洞质量 $m_{bm} = r_m C^2 / 2G = 0.632 \times 10^{-13} \times 9 \times 10^{20} / 2 \times 6.67 \times 10^{-8} = 0.426 \times 10^{15} \text{g}$,

该黑洞在 r_{bm} 上的霍金辐射量子的阈温度值温度 $T_{bm} = 9.62 \times 10^{12} \text{K}$,

该黑洞内相当的质子数 $n_{bm} = m_{bm} / m_p = 0.426 \times 10^{15} / 1.67 \times 10^{-24} = 0.255 \times 10^{39}$

该黑洞之霍金辐射粒子的质量 $m_s =$ 质子的质量 $m_p = 1.67 \times 10^{-24} \text{g}$,
 该黑洞密度 $\rho_{\text{bm}} = 3m_{\text{bm}}/4\pi r_{\text{bm}}^3 = 3 \times 0.426 \times 10^{15} / (4\pi \times 0.632^3 \times 10^{-39}) = 0.4 \times 10^{54} \text{g/cm}^3$
 霍金的任何一个黑洞的寿命 τ 的公式如下:

$$\tau \approx 10^{-27} M_{\text{b}}^3 \text{ (s)}^{[2]} \quad (8a)$$

该黑洞寿命 $\tau_{\text{bm}} \approx 10^{-27} m_{\text{bm}}^3 \approx 10^{-27} \times (0.426 \times 10^{15})^3 \approx 0.0773 \times 10^{18} \text{s} \approx 24.5$ 亿年.

史瓦西微型黑洞 m_{bm} 与霍金在 1971 年所提出的原初宇宙小黑洞 m_{bo} 在同一个数量级。我们宇宙现今的年龄 $\tau_{\text{b0}} = 137$ 亿年, 如果 m_{bo} 现今尚能存在于宇宙中, 其质量应该是:

$$m_{\text{bo}} \geq (10^{27} \times 137 \times 10^8 \times 3.156 \times 10^7)^{1/3} = 0.756 \times 10^{15} \text{g} \quad (8b)$$

在 70 年代, 科学家们曾费力地力求在宇宙空间找到 m_{bo} 这种原初宇宙小黑洞, 但一无所获。因为它们不可能存在于现今宇宙中。(以下再详细论证)

从以上所计算的史瓦西微型黑洞 m_{bo} 的各种参数值与所有其它学者用其它公式所计算的结果是完全一致的。这证明本文中所采用的公式是没有错误的。

按照霍金的黑洞理论, 黑洞向外辐射能量的速率为:

$$dE/dt = 10^{46} M^{-2} \text{erg/s}^{[2]} \quad (8c)$$

假设 $M = M_{\theta} = 2 \times 10^{33} \text{g}$, 而 $T_{\text{b}} \approx 10^{-6} \text{k}$, 按照 $dE./dt \approx 10^{-20} \text{erg/s}$ 这个极其微小的霍金辐射速度, 一个太阳质量的黑洞约需 10^{65} 年才辐射完其所有能量-物质, 其寿命 τ_{θ} ;

$$\tau_{\theta} \approx 10^{-27} M_{\theta}^3 \text{ (s)}^{[2]} = 10^{-27} \times (2 \times 10^{33})^3 \approx 8 \times 10^{72} \text{s} \approx 10^{65} \text{年} \quad (8d)$$

按照霍金的黑洞理论, 任何恒星在塌缩过程中, 熵总是增加而信息量总是减少的。设 S_{m} —恒星塌缩前的原有的熵, S_{b} —恒星塌缩后的熵。霍金公式:

$$S_{\text{b}}/S_{\text{m}} = 10^{18} M_{\text{b}}/M_{\theta}^{[2]} \quad (8e)$$

Jacob Bekinstein 指出, 在理想的条件下, 即恒星塌缩前后熵不变的条件即得到一个恒星级黑洞的最小(下限)质量(m_{om})^[2].

$$\text{从 (8e), } m_{\text{om}} = M_{\theta}/10^{18} = 2 \times 10^{33}/10^{18} = 2 \times 10^{15} \text{g}, \quad (8f)$$

可见, m_{om} 与 m_{bm} 又是同一级别黑洞。这足以证明本文所用的公式和推导与 Jacob Bekinstein 是殊途同归。于是,

$$m_{\text{bm}} (0.426 \times 10^{15} \text{g}) \approx m_{\text{bo}} (0.756 \times 10^{15} \text{g}) \approx m_{\text{om}} (2 \times 10^{15} \text{g}) \quad (8g)$$

以下将讨论 m_{bo} 和 m_{om} 能否存在于现今宇宙中。

当 $m_{\text{bo}} \geq 0.756 \times 10^{15} \text{g}$ 时, 相应地, m_{bo} 的

$$R_{\text{bo}} \geq 1.12 \times 10^{-13} \text{cm}, \rho_{\text{bo}} \leq 0.1285 \times 10^{54} \text{g/cm}^3, T_{\text{bo}} \leq 10^{12} \text{k}. \quad (8h)$$

从本文的下篇^[18]可以查出或计算出, 当宇宙的密度 $= \rho_{\text{bo}} \leq 0.1285 \times 10^{54} \text{g/cm}^3$ 时, 宇宙的特征时间 t_{up} 是,

$$t_{\text{up}} = (3/8\pi \rho_{\text{bo}} G)^{1/2} = 0.37 \times 10^{-23} \text{s} \quad (8i)$$

从宇宙大爆炸后的宇宙演变膨胀图可知^[18], $t_{\text{up}} = 0.37 \times 10^{-23} \text{s}$ 是处于宇宙的重子时代, 即 Hadron Era, 此时单个的强子不能存在, 宇宙中大部分的物质形态是浓密的夸克和胶子的混合物, 又称为夸克时代。^{[2] [18]}这就是说, 此时的无数的质量为 m_{bo} 的原初宇宙小黑洞是紧密地均匀地在当时宇宙内挤在一起的, 随着时间的增加, 许多小黑洞 m_{bo} 就会碰撞和合并而变成更大的黑洞, 因此, 在宇宙密度当时高达 10^{54}g/cm^3 的状态下, 是不可能原初宇宙小黑洞 m_{bo} 既不吞噬其外围的能量-物质又不与其邻近的小黑洞合并而孤立的残存到现今的宇宙空间的。推而广之, 宇宙

膨胀到辐射时代 (Radiation Era) 结束之前^[18], 此时宇宙的密度虽然已降低到 $\approx 10^{-20} \text{g/cm}^3$, 即在大爆炸后的 30~40 万年之前, 但那时宇宙并不透明, 仍然处在辐射为主要的时代。宇宙由于原生的最小黑洞 $M_{\text{bm}} \approx 10^{-5} \text{g}$ 的合并仍然在不断地膨胀着, 但在每一时刻, 微波背景辐射的观测证实那时温度的差异仍然很小, 也就是说, 宇宙还是几乎近于热平衡状态。因此, 其内部密度在每一时刻都是相当均匀的, 不可能在以后密度降到远低于 10^{54}g/cm^3 的密度状态下又塌缩出 m_{bo} 如此小的质量和如此高密度的原初宇宙小黑洞。

在宇宙膨胀到物质占统治地位的时代, 即 Matter-dominated Era, 即在大爆炸 30~40 万年之后直到现在^[18], 宇宙的能量-物质密度从 $\approx 10^{-20} \text{g/cm}^3$ 已经降低到现在的 10^{-30}g/cm^3 。只有在物质形成后, 由于辐射能量与物质粒子能量之间的巨大差异而不能互换, 才在宇宙的小范围内(1~3 亿光年内)造成物质密度的极大不均匀。因而才出现星云星系和恒星, 恒星只能在死亡后通过新星或者超新星的爆炸, 其残骸才能塌缩成为如前所述的质量大约为 10^{33}g 的恒星级黑洞, 而不可能爆炸和塌缩出来质量 $\approx 10^{15} \text{g}$ 的原初宇宙小黑洞 m_{bo} , 因为其爆炸压力和温度都达不到 m_{bo} 所需要的条件。 m_{bo} 的热压力 P_{bo} 可估算如下:

$$P_{\text{bo}} = \rho_{\text{bo}} k T_{\text{bo}} / m_p = 0.1285 \times 10^{54} \times 1.38 \times 10^{-16} \times 10^{12} / 1.67 \times 10^{-24} \approx 10^{67} \text{atm} \quad (8j)$$

上面提到, Bekenstein 曾指出, 如令恒星塌缩前后的熵不变, 即令 $S_b/S_m = 1$, 则得到一个最小的恒星级黑洞最小(下限)质量(m_{om})^[21]。但是, 由 (8e) 式可知, 恒星没有可能在塌缩为黑洞前后保持熵不变。只有整个塌缩过程是极其缓慢的理想绝热过程才能保持熵不变。恒星的塌缩过程可以分为两步: 1. 从恒星的死亡爆炸到塌缩成为恒星级黑洞 $\approx 3M_{\odot}$, 这个过程是一个恒星死亡后的激烈和迅速的爆炸和塌缩的过程, 总的来说, 完全是一个从有序到无序的熵大大的增加的过程。也许变成恒星级黑洞的余烬 M_r 的有序性有所增加, 即熵有所减少, 但是 M_r 只占总体的一小部分, 所以 $S_b/S_m \neq 1 \gg 1$ 。 2. 从恒星级黑洞的质量大约为 $6 \times 10^{33} \text{g}$ ($3M_{\odot}$) 塌缩到 $\approx 2 \times 10^{15} \text{g}$ 的微小黑洞。假设这个过程能够出现的话, 它就是一个从低温低密度向高温高密度收缩转变的过程, 如果没有外部能量的供给和极高的压力, 这个转变不可能完成, 但是, 如前所述, 黑洞在吞噬外界能量-物质时不是收缩反而是膨胀。因此, 黑洞的收缩只能是如前所述的完全靠自己向外发射霍金量子辐射, 因此, 从大质量恒星级黑洞收缩到微型黑洞(m_{om})所需的时间是 = 恒星级黑洞的寿命-微型黑洞的寿命 $\approx (10^{66} \text{年} - 10^{11} \text{年})$ 。而这个过程也完全不是理想的等熵过程, 因为收缩的结果是向外发射了大量的无序的霍金量子辐射, 黑洞只是由一个质量 $6 \times 10^{33} \text{g}$ 恒星级黑洞缩小成 $2 \times 10^{15} \text{g}$ 的唯一一个微型黑洞, 而不是收缩成为与原来黑洞等量又等熵的 N_{min} ($N_{\text{min}} = 6 \times 10^{33} / 2 \times 10^{15} = 3 \times 10^{18}$) 个 m_{bo} 微型黑洞。虽然最后一个仅存的 $2 \times 10^{15} \text{g}$ 的微型黑洞的熵有所增加, 但它只是原先总体质量的 $1/N_{\text{min}}$, 因此, 其塌缩前后的熵比 $S_b/S_m \neq 1 \gg 1$ 。

结论: 根据 1989 年发射的 COBE 卫星测量结果进行分析计算后发现, 宇宙微波背景辐射与绝对温度 2.7 度黑体辐射非常吻合, 另外微波背景辐射在不同方向上温度有着极其微小的差异, 也就是说存在的各向异性非常小, 因而在宇宙的辐射时代结束之前不可能使在宇宙早期所产生原初宇宙小黑洞 m_{bo} 孤独地保持到现在。而在宇宙的辐射时代之后一直到现在, 即是物质占统治地位的时代, 在此期

间，只能产生恒星级黑洞，如果由恒星级黑洞以霍金辐射收缩成为原初宇宙小黑洞 m_{b0} ，需要再经过大约 10^{65} 年之后才会出现。

IX. ($10^7 \sim 10^{12}$) M_0 超级大黑洞与类星体 (Quasar)

在每个星系的中心都有一个超级大黑洞，其质量约为 ($10^7 \sim 10^{12}$) M_0 不等。最近“美国斯坦福大学的天文学研究小组在遥远的宇宙中发现了被称为 Q0906+6930 的黑洞。到目前为止堪称最庞大最古老的黑洞。其质量是太阳质量的 100 多亿倍，形成时间在 127 亿年前，即在宇宙的大爆炸之后大约 10 亿年”^[14]。

设上述黑洞质量 $M_q = 10^{10} M_0 = 2 \times 10^{43} \text{g}$ ，则其 $R_q = 2.96 \times 10^{15} \text{cm}$ ， $\rho_q = 1.74 \times 10^{-4} \text{g/cm}^3$ 。

而宇宙 10 亿年时的平均密度 $\rho_{10} = 3/(8\pi G t^2) = 1.8 \times 10^{-24} \text{g/cm}^3$ 。

再看中子星和恒星级黑洞的平均密度 $\approx (10^{14} \sim 10^{16}) \text{g/cm}^3$ ，

“2008-09-05 报道，天文学家首次清晰观测到银河系中心黑洞”，该黑洞的史瓦西半径 $R_y = 1609$ 万公里，即 $R_y = 1.6 \times 10^{12} \text{cm}$ ，其质量 $M_y \approx 10^{6.5} M_0$ ，平均密度 $\rho_y = 3 \times 10^2 \text{g/cm}^3$ 。

分析与推论：1. 从上面的密度比较和分析后可见，质量愈大的超级黑洞，其密度愈小，可能愈易于从该超巨大星系的原始星云中直接收缩而成。所以在宇宙物质占统治时代的早期，在密度较大的状态下，较易形成超级大黑洞，即类星体。**2.** 超级黑洞外的剩余能量-物质愈多，则黑洞因吞噬能量-物质而向宇宙空间发射的辐射能量也愈多。在宇宙空间也就愈亮。银河系中心的超级黑洞外围的能量-物质较少，所以也较暗。**3.** 这些超级黑洞是否由其原始大星云在中心先塌缩成许多恒星级黑洞和致密天体，然后由他们碰撞合并而成呢？这种可能性不大。因大量致密天体被黑洞所吞噬而形成上述如此大的超级黑洞需要很长的时间，特别是恒星级黑洞是需要花费数亿到百亿年的时间完成核聚变之后才能形成的。因此，超级黑洞的这种形成方式的可能性很小。也许小星系中心或者大星系中心外形成的 $10^5 M_0$ 的中型大黑洞可能由这种方式形成。**4.** 由此可见，应该是先有行星状星云的星系，然后收缩成为各种星体各种黑洞和超级黑洞，而不可能先有黑洞再吸引宇宙空间的能量-物质形成行星状星系。

什么是类星体？类星体其实就是遥远的超级黑洞，也是上述超级黑洞的婴儿和青少年时期。现简单介绍何香涛教授在其“观测宇宙学”^[3]中第 8 章的证明如下：

类星体的质量 M_Q 应该满足，

$$M_Q > L_Q M_0 / 1.5 \times 10^{38} = 3.3 \times 10^8 M_0 \quad (9a)$$

对于光变周期为 1 小时的类星体，其尺度 D 应该满足

$$D \leq C \Delta t = 1.1 \times 10^{14} \text{cm}, \quad (9B)$$

对于如此大小的一个史瓦西黑洞，其质量 M_S 应该是，

$$M_S = RC^2 / 2G = 1.9 \times 10^8 M_0 \quad (9C)$$

可见， $M_Q \approx M_S$ ，二者是极其接近的。(9a)式中之 $L_Q = 5 \times 10^{46} \text{erg/s}$ 。

X. 对上述史瓦西黑洞的论证再作进一步的分析和结论如下：

A. “两位英国学者，剑桥大学的史蒂芬·霍金和发明保角图的罗杰·彭罗斯在 60 年代证明，“奇点”是广义相对论的一个必不可少的组成部分。一个真实恒星的引力坍缩是否一定导致视界和黑洞的形成对此尚不明确，但是坍缩的结局是不可避免

地成为奇点，这是确定无疑”。这是“黑洞”一书作者约翰-皮尔·卢米涅在1995年写的。^[1]按照广义相对论，任何一个黑洞将由三部分组成。第一，视界为其边界。第二，奇点在 $R=0$ 的几何中心，在那里集中有无穷大的能量密度，时空弯曲成无穷大。第三，在视界与“奇点”之间的空间为真空。这表示奇点成为黑洞存在的前提，广义相对论还指出，由于空间与时间在黑洞内互换，其中心 $R=0$ 的点成为时间的终结，以后就成为“时间之外”。^{[1][6]}

广义相对论对“时间之外”无法解释。仅仅按照单独的广义相对论的数学方程的极端状态得出的上述解释是不适宜于研究黑洞内部状况的。我们所熟知的物理定律失效的奇点^[5]只是广义相对论的数学推导的极端结果，而不是真实的物理世界的图像。何况，广义相对论没有考虑温度和热压力如影随形地对引力的抗拒作用，没有考虑量子理论，它不能应用于普朗克量子领域。而“奇点”作为能量与密度为无限大的点，它不可能在真实的物理世界出现和存在。任何理论的数学方程都有其应用的极限，广义相对论也不例外。因为数学方程的连续性通常不大可能统一地描述物态之间的极端（极限）--相变及相变处的临界点。正如气体状态方程不能用于水的沸点一样，在自然界既能找到长期存在的黑洞实体，就应当应用其它的观点或机理以代替用单独的广义相对论对黑洞内部无能为力解释的“奇点”。既然黑洞以被观测和证实为宇宙中长期存在的物质实体，那么，其内部必然存在着对抗引力塌缩的机制以维持其平衡和稳定。

B. 本文前面是用4种不同经典理论的基本公式来解决黑洞内部没有奇点的问题，即用经典的热力学公式(1a) $dP/dR = -GM\rho/R^2$ 为基本，以史瓦西对广义相对论的特解公式(1c) $R_b = 2GM_b/C^2$ 作为黑洞存在的必要条件，以热状态方程(1b) $P = nkT = \rho\kappa T/m_s$ 和以霍金的黑洞量子辐射公式(1d) $T_b = (C^3/4GM_b) \times (h/2\pi\kappa)$ 作为边界的补充条件，求出了黑洞视界半径 R_b 上一组能普遍应用于所有黑洞守恒公式(2ca), (2cb) 等，和修正后的重要公式如(4d), $R_{m_{ss}} = h/(4\pi C) = 0.176 \times 10^{-37} \text{cm}$, 和(4e), $m_{ss}M = hC/8\pi G = 1.187 \times 10^{-10} \text{g}^2$ 。必须特别着重指出，所有这些守恒公式仅仅实用于黑洞视界半径 R_b 上。至于黑洞内部各点的状态特别是各点的温度 T 的状态与上述守恒公式无关，也不影响上述守恒公式。而 T_b 仅仅表示黑洞视界半径 R_b 上的霍金辐射量子的阈温。如果大黑洞内部有黑洞，则该小黑洞视界半径 R_b 上也适用这组守恒公式，而在黑洞内部的非黑洞区域的状态，只有公式(1a) 和 (1b) 可以使用，而必须再补充其它的边界的补充条件才能解出公式(1a)。

C. 由前面的论证可见，黑洞视界半径 R_b 的界面上实际上是黑洞能量位阶的最低界面。黑洞界面内外的能量-物质粒子只有通过界面才能交换和进出。界面内附近的粒子能量只有达 R_b 的位阶，即其小于或等于阈值 $m_{ss} \leq \kappa T_{om}/C^2$ 时才可能逃出黑洞。同样，界面外附近的粒子能量只有达 R_b 的位阶，即其大于或等于阈值 $m_{ss} \geq \kappa T_b/C^2$ 时才可能被吸入黑洞。黑洞界面 R_b 上不停地能量-物质交换使得 R_b 上不停地震荡—扩大或者缩小。当黑洞因不断地发射霍金量子辐射而内部空间一直缩小下去时，内部的能量物质也就一直不停地通过 R_b 向外辐射而后使 R_b 逐渐缩小，这就完全证明黑洞内部空间充满能量-物质，而在 R_b 逐渐缩小时能随时供给能量-物质，从而证实其内部空间绝对不是真空。因此，广义相对论所得出“黑洞内部除了奇点之外，所有空间都是真空”的结论是不符合黑洞的真实状况的。广义相对

论数学方程的极端处是不能用于真实的物理世界的，正如牛顿力学不能用于接近光速运动的物体一样。

D. 恒星在死亡时的塌缩大爆炸中，恒星将抛射掉自己大部分的质量，同时释放出巨大的能量。这样，在短短几天内，它的光度有可能将增加几十万倍，这样的星叫“新星”。如果恒星的爆发再猛烈些，它的光度增加甚至能超过 1000 万倍，这样的恒星叫做“超新星”。这些剧烈的爆炸现在已能真实的被观测到。设想如果所有的黑洞内均出现过“奇点”，那么每个奇点爆炸的剧烈程度将会比超新星的爆炸不知要大多少倍，似乎都会像广义相对论所设想的宇宙诞生的“大爆炸”一样地剧烈。从广义相对论的理论上讲，也许黑洞外面的人不能观察到黑洞内奇点大爆炸的图景。但是“奇点”的爆炸必定会爆出来无法估量的能量-物质迫使其视界半径以光速不断地向外扩张。在我们银河系的中心区域有许多小黑洞和一个超级大黑洞，如果所有这些黑洞内都有“奇点”而爆炸的话，那么，距离银河系中心仅仅 2.6 万光年的太阳系早就被这些扩张的黑洞所吞噬了。因此，我们银河系内及外围空间许多被观测到的黑洞的长期真实地存在就证明所有黑洞内没有出现和存在过“奇点”和“奇点的爆炸”。也证明了我们的太阳系不在银河系的某个黑洞之内。可见，用广义相对论数学方程的极端处存在“奇点”以证明真实的黑洞内存在“奇点”是一种错误的推论和结论，正如用经典力学证明电子会失去能量而坠落到原子核中的错误是一样的。

E. 在前面第 VI 节中已经证明所有黑洞的最后命运不是收缩成为奇点，而是收缩成为质量 $M_{bm} \approx 10^{-5}g$ 的最小引力黑洞在普朗克领域中强烈的爆炸消亡。既然所有黑洞的最后命运是如此，假设黑洞内部有可能发生这种极其强烈的引力收缩时，也必然而且只能是最后收缩成为质量 $M_{bm} \approx 10^{-5}g$ 的最小引力黑洞而在黑洞内部强烈的爆炸中消失后，其残渣就混入黑洞内的空间与能量-物质中。而实际上恒星级黑洞或者有中子星所塌缩成的恒星级黑洞是不可能发生这种情况的。前面已经说过，现在宇宙中由新星和超新星爆炸所形成的恒星级黑洞或者有中子星所塌缩成的恒星级黑洞的质量大约是 $3.8 \sim 15 M_{\odot}$ 。这种黑洞形成后，由于其霍金辐射的能量极其微小，其寿命按照公式 (6b) 将达到大约 $10^{65} \sim 10^{70}$ 年，这就是说，在视界半径 R_b 的界面上，黑洞内部的热压力几乎完全能够对抗和平衡其引力的塌缩，内部核心超子（所谓超子其实就是具有高能量和高温度的中子和质子）之间的斥力（泡利不相容原理的作用）能更强力地对抗外层物质的引力塌缩成为小黑洞，因而只可能在其中心存在一个较密实的超子核心，而内部空间则充满密实的能量-物质，其中密度由中心向外是连续降低的。这也就是说，恒星级黑洞一旦形成之后，其内部不可能再继续塌缩出更小的黑洞，因为塌缩出更小的黑洞需要更高得多的压力，而恒星级黑洞内已无再产生核聚变的可能。假如万一有更小的黑洞出现，它也只能会吞噬其外围的能量-物质而扩大其视界半径直到与原黑洞的半径合而为一。

F. 再从另一个角度来看，“所有黑洞的最后命运不是收缩成为奇点，而是收缩成为质量 $M_{bm} \approx 10^{-5}g$ 的最小引力黑洞在强烈的爆炸中消亡”。从公式(1d)看，黑洞 M_b 在其视界半径 R_b 上的阀温 T_b 的黑洞守恒公式如下：

$$T_b = (C^3/4GM_b) \times (h/2\pi\kappa) \approx 0.4 \times 10^{-6} M_{\odot} / M_b \approx 10^{27} / M_b \quad (1d)$$

从公式(1d)看，当 M_b 质量在 $10^{-x}g$ 以下收缩（缩小）时， T_b 的绝对值增加的很大，很显然，在自然界，阀温 T_b 不可能增加到无限大，而使 $m_{ss} (= \kappa T_b / C^2)$ 也增加到

无限大。同时，黑洞也必须遵循热力学第三定律，此定律可表述为：在通常的热力学系统中，不能通过有限次操作，把系统的温度降低到绝对零度或升高到无穷大。因此，黑洞质量 M_b 就不可能收缩到无穷小的奇点。这样，当黑洞收缩时， T_b 就存在一个最大值， M_b 就相对地存在一个最小值，从而只能收缩到 $M_b = M_{bm} \approx 10^{-5}g$ 为止。因此，相对应地粒子的尺度 R_b 也不可能收缩成无限小，而只能到 $R_b \approx 10^{33}cm$ 为止。密度也只能增加 $\rho_{bm} \approx 6.4 \times 10^{92}g/cm^3$ 为止，而不是无限大。再从(6f)式可知。每个黑洞收缩到 $M_{bm} \approx 10^{-5}g$ 时，就达到了Planck Era,因而只有在 $10^{32}k$ 的宇宙最高温度下爆炸解体消亡。

$$m_{ss}M = hC/8\pi G = 1.187 \times 10^{-10}g^2. \quad (4e)$$

再看(4e)式，对于任何一个黑洞而言， $m_{ss} \leq \kappa T_b / C^2$ 。而 $M \geq \kappa T_b / C^2$ ，只有当黑洞收缩到成为最后两个粒子时，就达到一个极限，即(6a)式，

$$M = m_{ss} = 1.058 \times 10^{-5}g, \quad (6a)$$

这是黑洞的最后一次发射霍金辐射粒子 $m_{ss} = M$ 。这也是真正地一分为二，一个最后的黑洞粒子分裂成为 2 个相等的辐射能量子，而后在相同的最高温度下爆炸消亡。所以最后的一次发射霍金辐射粒子 m_{ss} 的能量成为：

$$M C^2 = m_{ss} C^2 = \kappa T_b = 10^{16} g \cdot cm^2/s^2 = 10^{19} GeV \quad (10a)$$

其实，如果令 T_b 为黑洞 M_b 在其视界半径 R_b 上的阀温，即 $T_b = m_{ss}C^2/\kappa$ ，(1d) 式可直接变为(4e)式，即， $m_{ss}M = hC/8\pi G$ 。这再一次证明了本文前面对黑洞守恒公式的推演和结论都完全是正确的，符合量子力学和霍金黑洞理论等各种经典理论而圆满自洽的。所以，宇宙中事物之间的道理是一通百通的。但是，如果直接如上所述由 (1d) 式得出(4e)式，我们就不知道 m_{ss} 在黑洞 M_b 的视界半径 R_b 上处于热动力的平衡状态，这样就难以理解 m_{ss} 如何作为黑洞的霍金辐射在起作用，也难以从黑洞守恒公式收缩演变的观点分析黑洞的内部状况和收缩到最后成为 $M = m_{ss} = 1.058 \times 10^{-5}g$ 而消失。

G. 前面的分析和论证表明，用单独的广义相对论无法解决黑洞内部的奇点问题。直到现在,尚未有一个单独的理论能描述黑洞内部。在本质上，广义相对论是一个无热力学效应而以四维时空代替引力作用的时空几何学。因而，在用单一的广义相对论方程式描述黑洞内部时，没有热力作为对抗力，均匀的能量-物质空间的引力的塌缩(即时空收缩)也就必然会产生“奇点”。Tolman-Oppenheimer-Volkoff [7]方程已将热力学效应，粒子的熵和物质的结构效应作为修正项用以解决公式 (1a) [7]，但因 TOV 方程太复杂而又无某种确定的规范作为边界条件用于黑洞内部。更主要的是，在 40 年代，霍金的黑洞辐射理论尚未出现，所以，至今无人将 TOV 方程用于黑洞内部而又解决问题。本文用简化的公式(1a) $[dP/dR = -GM\rho/R^2]$ 以代替复杂的 TOV 方程。而用霍金黑洞理论中的温度公式于黑洞作为边界条件。因此，找出了一个简化的特殊解，即黑洞视界半径 R_b 上的几个守恒公式，即 (2c)， $R = 3h/(2\pi C m_s)$ ，和其修正公式(4d)， $R m_{ss} = h/(4\pi C) = 0.176 \times 10^{-37} cmg$ 。这是联合运用广义相对论(或牛顿力学)和黑洞理论以及热力学的公式结果。如果没有黑洞理论，公式(4d)的这一特殊解就找不出来。因此，如果没有霍金的黑洞理论，就不可能找到在黑洞视界半径 R_b 上的这些守恒公式，而正是这些守恒公式的存在才阻止了恒星级史瓦西黑洞内部的能量-物质塌缩成为奇点而使黑洞能以极长期的寿命而真实地存在于宇宙中。也正因有了霍金的黑洞理论，才有可能知道任何黑洞的寿命，才了解黑洞内部

与外界的能量是如何交换的。结果，黑洞从过去存在于自然界的死而不化的物体变成现在活的物体。可见，本文中运用霍金理论的公式才避免了广义相对论对“奇点”问题的危机。同样的情况其实早已发生过，正如原子中的电子必需依从量子力学的测不准原理才不致落到原子核内，而稳定在原子核的外层运动。这才使得我们人类能出现和存在于现今美妙的世界里。

H. 黑洞视界半径上的参数的单一性和唯一性：黑洞的所有物理状态参数 ($M_b, T_b, R_b, \rho_b, \tau_b, \dots$) 中, 只要有一个被确定, 比如说 M_b 被确定, 其它的所有参数都随着 M_b 的被确定而被唯一的确定了. 从这个观点来看, 黑洞又是自然界最简单的物体. 这也就是说, 同一个参数值的所有黑洞, 在其视界半径 R_b 上的各种参数值是完全一样的. 但其内部的状态可以不相同, 黑洞愈大, 其内部的状态的差异也就愈大愈复杂. 反之, 所有的 $M_{bm} \approx 10^{-5}g$ 的最小引力黑洞都只是由一个粒子组成, 而各种参数都一样, 因此, 只有所有的 $M_{bm} \approx 10^{-5}g$ 的最小引力黑洞内部状态才都是一样的, 而达到这一状态时即爆炸解体消失于普朗克量子领域。

I. 从第 III 节可知, 黑洞只有从外部吸取能量物质或与其它星体或黑洞碰撞才会膨胀增大尺寸, 而不停地向外所辐射的能量却极微, 1998 年由遥远的 Ia 型超新星的爆发而发现宇宙早期直到现在的加速膨胀。现在主流的科学学家们都认为在宇宙早期出现了具有负能量或者排斥力的暗能量造成了宇宙加速膨胀, 现在不少的科学家正努力想找到暗能量以求得到诺贝尔奖。作者曾指出, 由遥远的 Ia 型超新星的爆发而发现宇宙早期的加速膨胀是我们这个宇宙大黑洞在早期与另外一个宇宙大黑洞碰撞与合并所造成的结果。^[4]而这种合并似乎到现在尚未完全完成。因为合并一旦完成, 两大黑洞的质量就会相加而成为新黑洞的质量, 两个原来黑洞的视界半径就会相加而成为新黑洞的视界半径。这样, 新黑洞因无外界能量物质可以吞噬而会停止膨胀。作者的上述解释是合乎宇宙的观测实况的。因为只有两个宇宙黑洞在其早期碰撞而产生宇宙加速膨胀的上述解释才符合我们宇宙的平直性要求和当今较准确的观测值 ($\Omega=1.02\pm 0.02$)。有排斥力的暗能量和所有其它理论都可能成为找不到的幽灵, 因为它们都不符合此要求, 解释不了我们宇宙的平直性^[4]。

J. 两种不同的黑洞模式和两种不同的黑洞命运。

按照单独的广义相对论, 黑洞中心有一个奇点, 在视界半径与奇点之间的内部空间是真空。黑洞永远不向外辐射任何能量-物质, 在这样的条件下, 黑洞将永远地存在于自然界。这类黑洞会从外界吸收能量-物质或其它天体而增加自己的质量和尺寸, 但它永远是一个绝对的黑洞而不会消失, 因此, 在自然界已存在的黑洞和未来将出现的黑洞每一个都会有无限长的生命。这种可能性能存在吗? 它符合自然的根本规律吗? 有许多确凿的证据已经证实我们宇宙就是一个巨无霸黑洞。^[4]^[18]作者在本文的下篇已经作了有力的证明。^[18]在宇宙黑洞内, 各种物质物体和人类的存在证明宇宙空间并不是真空, 也没有观测到存在“奇点”的任何证据。而那些抱着广义相对论方程的极端的奇点结论不放的科学家们, 其实也说不清奇点究竟奇到什么程度。这是即不合理性也不符合宇宙的实际状况的。本文另开思路, 独创地综合运用几种经典理论的基本公式, 特别是应用霍金的黑洞辐射量子蒸发能量的公式, 证明每个黑洞与宇宙中其它任何物体或者系统一样, 都存在着对抗引力塌缩的机制, 都合乎生长衰亡的法则, 都是一个总熵增加的不可逆过程。在这种模式的大黑洞内部, 各处和区域依据其不同的动静平衡条件而可以组成极不相同

物体和系统。比如，在我们这个宇宙大黑洞内部，就可以在不同的地方存在着大小黑洞，恒星，行星，生物，人类和宇宙尘埃等等。但是，可以明确地定论，我们宇宙任何地方绝对不可能出现高于 10^{32}k 的高温，也绝对不可能出现小于 10^{-5}g 的黑洞，永远不会找到“奇点”或者“奇点的大爆炸”。

K. 关于人造黑洞：作者两年多前曾经论证过人类也许永远制造不出来任何大小的人造黑洞。请参看拙作“Mankind may be impossible to manufacture out any artificial real gravitational black holes forever”^[16]。其实道理很简单明白，因为要想以小于 10^{19}GeV 的能量制造出来小于 10^{-5}g 的史瓦西黑洞，必然的，其相对应的温度 $>10^{32}\text{k}$ ，视界半径 $<10^{-33}\text{cm}$ ，寿命 $<10^{-43}\text{s}$ 。这是不可能达到的。而且这种 $<10^{-5}\text{g}$ 的史瓦西黑洞已经深入到 Planck Era 的量子时代，在这种量子时代，而由广义相对论所得出的黑洞的概念和理论还能够存在和适用吗？而要想制造出 $>10^{-5}\text{g}$ 的史瓦西黑洞，就要求能制造出来大于 10^{19}GeV 的能量，这是人类能达到的能量吗？

XI. 作者最后的几句话：

老子曰：“大道至简”。本文独创的观点和论证方法是简单的，是违反以广义相对论为主流的学术界的观点的，但却是稍能圆满自洽的，也会经得起观测的检验的。这也许不会受到大部分科学家与学者们或读者们的认可，因为本文缺乏新理论和复杂的数学公式，而这些东西都正是物理学界的主流学者们终身引以为骄傲的。但本文中的新的观念，新的论证方法与计算都来源于现代可靠的经典理论的基本原理和公式并且和所有其它理论计算所得出的数据以及观测的数据相符合。而且容易被理解和接受。本文的重要贡献就是找出了所有黑洞的最后命运是塌缩分裂成为两个最小引力黑洞 $M_{\text{bm}} \approx 10^{-5}\text{g}$ 后而在普朗克领域强烈的爆炸中消亡。这是由于本文推导出了新的公式(4e)， $m_{\text{ss}} M = hC/8\pi G = 1.187 \times 10^{-10}\text{g}^2$ 和 (4d)， $Rm_{\text{ss}} = h/(4\pi C) = 0.176 \times 10^{-37}\text{cmg}$ ，而将视界半径 R 上的霍金量子辐射作为能量-物质粒子 m_{ss} ，而与其热动力和其引力的平衡联系起来。本文用简单的方法以解决复杂问题的思路也许可以作为引玉之抛砖供给未来者作另类思考。

====完====

参考文献：

- [1]. 约翰—皮尔卢考涅：“黑洞，”湖南科学技术出版社，2000
- [2]. 王永久：“黑洞物理学，”湖南科学技术出版社，2000，4
- [3]. 何香涛：“观测天文学，”科学出版社，2000，4
- [4]. 张洞生：对宇宙加速膨胀的最新解释:这是由于在宇宙早期所发生的宇宙黑洞间的碰撞所造成的
<http://www.sciencepub.net/academia/0101>。
<http://www.sciencepub.org/newyork/0102>
- [5]. 约翰. 格里宾：“大宇宙百科全书，”湖南出版社，2001，9
- [6]. 苏宜：“天文学新概论”，华中理工大学出版社，2000.
- [7]. 吴时敏：“广义相对论教程，”北京师范大学出版社，1998. 8

- [8]尼古拉·沙波什尼科夫： 期刊：《天体物理学杂志》 发布时间：2008-4-2 13:13:2
<http://www.sciencenet.cn/htmlpaper/2008421428593631704.html>
- [9]. 晚年的致密恒星阶段：www.yckjw.gov.cn 信息发布[2006-11-10 15:25:00]
- [10]. http://news.xinhuanet.com/tech/2008-05/29/content_8273876.htm
- [11], 英國教授稱銀河系可能有 20 多個黑洞
<http://popul.jqcq.com/big5/natural/2007-08/187918038.html>
- [12]. 天体物理学家找到解中子星内部结构的方法 <http://tech.163.com> 2004-09-16 07:18:48 来源: 网易科技报道
- [13]。致密星. <http://hometown.aol.com/lklstars8/15b.htm>
- [14]。天文学家发现迄今最大最古老黑洞, <http://tech.sina.com.cn/other/2004-06-30/0752381423.shtml>
- [15]。天文学家首次清晰观测到银河系中心黑洞(图) <http://www.enorth.com.cn> 2008-09-05 08:45
- [16]。Dongsheng Zhang: Mankind may be impossible to manufacture out any artificial real gravitational black holes forever". Nature and Science—0201.
<http://www.americanscience.org/journals/am-sci/0201>
- [17]。向义和：大学物理导论，下册 22.3.1，清华大学出版社 1999.7.
- [18]。张洞生：本文的下篇。对宇宙起源的新观念和新的完整论证：宇宙不可能诞生于奇点。

New York Science Journal

纽约科学杂志

ISSN 1554-0200

The international academic journal, “New York Science Journal” (ISSN: 1554-0200), is registered in the New York of the United States, and invites you to publish your papers.

Any valuable papers that describe natural phenomena and existence or any reports that convey scientific research and pursuit are welcome, including both natural and social sciences. Papers submitted could be reviews, objective descriptions, research reports, opinions/debates, news, letters, and other types of writings that are nature and science related. Manuscripts submitted will be peer-reviewed and the valuable papers will be considered for the publication after the peer review. There is no charge for the manuscript submissions.

If the authors (or others) need hard copy of the journal, it will be charged for US\$80/issue to cover the printing and mailing fee.

Here is a new avenue to publish your outstanding reports and ideas. Please also help spread this to your colleagues and friends and invite them to contribute papers to the journal. Let's work together to disseminate our research results and our opinions.

Papers in all fields are welcome, including articles of natural science and social science.

Please send your manuscript to: sciencepub@gmail.com

For more information, please visit:

<http://www.sciencepub.net>

<http://www.sciencepub.org>

<http://www.sciencepub.net/newyork>

<http://www.sciencepub.org/newyork>

New York Science Journal

525 Rockaway PKWY, #B44, Brooklyn, NY 11212, The United States,

Telephone: 347-321-7172

Email: sciencepub@gmail.com

Website: <http://www.sciencepub.net/newyork>

New York Science Journal

ISSN 1554-0200

Marsland Press

Brooklyn, New York, the United States

<http://www.sciencepub.net>

<http://www.sciencepub.org>

sciencepub@gmail.com

ISSN 1554-0200



9 771554 020066